Deterministic-Probabilistic Safety Analysis Methodology for Analysis of Core Degradation, Ex-vessel Steam Explosion and Debris Coolability

Pavel Kudinov[1]
Sergey Galushin[1]
Dmitry Grishchenko[1]
Sergey Yakush[1]
Yvonne Adolfsson[2]
Lisa Ranlöf[2]
Ola Bäckström[2]
Anders Enerholm[2]
Pavel Krcal[2]
Anna Tuvelid[2]

[1]Division of Nuclear Power Safety (NPS)
Royal Institute of Technology (KTH)
Sweden
[2]Lloyd's Register Consulting – Energy AB
Sweden

July 2015

Abstract

This reports summarizes the experience achieved within the NKS-DPSA project during 2014. The aim of the project is to develop the methodology for application of Integrated Deterministic-Probabilistic Safety Analysis (IDPSA) with PSA/DSA to the Nordic nuclear energy industry and regulatory needs. We further develop a Risk Oriented Accident Analysis Methodology (ROAAM) framework that demonstrates how dynamic behavior in NPPs can be better included in safety analyses. The methodology is developed and demonstrated through analysis of the relocation of the core melt to the lower plenum, as initial conditions for the melt-vessel structure interactions, melt release and ex-vessel steam explosion and debris bed coolability in Nordic BWRs. The influence of timing in PSA level 1 sequences and possible recovery actions on the amount and properties of the melt in the lower head are addressed. It is shown that IDPSA results can be used to refine and improve the PSA in several ways. One example is the analysis of recovery of core cooling, where IDPSA has provided usable information regarding the timing and possibility of core coolability (reflooding). This information can be used as a basis material for the HRA, to re-define the binning of plant damage states as well as provide probabilities for failure of coolability. The analysis performed for phenomena such as steam explosion shows interesting results that are relevant for the PSA-modelling. The analysis provides insights regarding under which conditions each phenomenon should be modelled and can therefore influence the sequences for which the phenomena is modelled. The results may also be used as one input to the quantification of phenomena. The analysis can be developed to further facilitate the use in PSA. Experiences from performed studies are summarized in the report as well as suggestions of areas which need further investigations.

Key words

Deterministic-Probabilistic Safety Analysis Methodology for Analysis of Core Degradation, Ex-vessel Steam Explosion and Debris Coolability

Final Report from the NKS-R DPSA activity

(Contract: NKS_R_2013_107)

Pavel Kudinov[1], Sergey Galushin[1], Dmitry Grishchenko[1], Sergey Yakush[1]
Yvonne Adolfsson[2], Lisa Ranlöf[2], Ola Bäckström[2],
Anders Enerholm[2], Pavel Krcal[2], Anna Tuvelid[2]

[1]Division of Nuclear Power Safety (NPS), Royal Institute of Technology (KTH)
[2]Lloyd's Register Consulting – Energy AB

June 2015

CONTENTS

List of Figures

List of Tables

Chapter 1. **Introduction**

This report summarizes the experience achieved within the project DSA/PSA Dynamic Probabilistic Methodology during 2014. The project is motivated by the discussions at the workshop "Proceeding of the IDPSA-2012 Integrated Deterministic-Probabilistic Safety Analysis Workshop"[1].

The overall aim of the project is to develop the methodology for application of IDPSA with PSA/DSA to the Nordic nuclear energy industry and regulatory needs. The project aims to:

- To develop a framework that demonstrates how dynamic behavior in NPPs can be better included in safety analyses.
- To address in-depth issues of risk importance for different severe accident scenarios.
- To suggest improved approaches to PSA-modelling considering information provided from IDPSA analysis.

The methodology aimed for by the project is developed and demonstrated through analysis of the following examples of severe accident scenarios and phenomena:

- Relocation of the core melt to the lower plenum, as initial conditions for the melt-vessel structure interactions, melt release and ex-vessel steam explosion and debris bed coolability in Nordic BWRs;
- The influence of timing in PSA level 1 sequences and possible recovery actions on the amount and properties of the melt in the lower head;
- The influence of timing on steam explosion and coolability risks in PSA

The first two cases are chosen to develop understanding and methods for the initial sequences in a PSA level 2 (following core melt) and the third is to gain understanding on how to treat scenarios following melt through.

The main benefits of the project are:
- Better understanding of the modelling pre-requisites in current PSA (level 1 input to level 2 and level 2 design).
- New methods for combined deterministic-probabilistic analysis and
- Practical experience in using them in combination with existing PSA models.

The project outcome will allow the end users to enhance understanding, completeness and consistency of safety analysis dealing with risk analysis in:
- management of severe accident issues;
- improved reliability analysis modelling methods for level 2 PSA;
- presentation of results in level 2 PSA, and related risk criteria;
- handling of modelling uncertainties;

Not being the main focus of the proposed project, but the methodology could also be used for (for example): identify safety vulnerabilities (scenarios of safety importance which

can threaten safety barriers) in active and passive safety systems.

Experiences from performed studies are summarized in the report as well as suggestions of areas which need further investigations.

Chapter 2. **State of the Art Review of the Probabilistic, Deterministic and Integrated Safety Analysis.**

Over the past decades, methods of Probabilistic Safety/Risk Analysis (PSA/PRA) have emerged as important tools to examine safety of complex, potentially hazardous, engineered systems such as Nuclear Power Plants (NPP). As safety requirements become increasingly stringent, requirements for quality and completeness of PSA models also increase. However further increase of the PSA models complexity is not necessarily an effective way to increase accuracy of PSA methods.

Deterministic analyses are the basis for construction of a nuclear power plant. The analyses are based on the single failure criterion and a number of conservative assumptions such as loss of offsite power and no credit for non-safety systems. The initiating events considered in the analyses are divided in different event categories, ranging from likely events (once or several times/year) down to residual risks. The more likely the event category is the higher the margins (conservatisms) against core damage must be. Thus, there are already some probabilistic considerations in the deterministic analyses.

The core damage frequency for both existing and advanced future plants is calculated to be in the range from 10^{-5}/reactor year to 10^{-8}/reactor year. However, the plant operation is sometimes hit by "improbable" (defined in PSA as very low probability) events, which can surprise, revealing a potential vulnerability in the complex plant system. We recognize that state of the art PSA methods provide numbers to quantify probability of what is already known as an "issue", but are not capable of revealing what, and to what extent, is not known (i.e. scenarios that are not prescribed in the PSA input). PSA is based on a set of assumptions about possible accident scenarios believed to be conservative. Such "decomposition" of a complex problem into a set of pre-defined sequences can be prone to false conservatism in the PSA or deterministic analysis, rendering possibility of potentially dangerous scenarios being missed or underestimated.

Standard PSA and deterministic approach has fundamental problems with resolving the dynamic nature of mutual interactions between (i) stochastic disturbances (e.g. failures of the equipment), (ii) deterministic response of the plant (i.e. transients), (iii) control logic and (iv) operator actions. Passive safety systems, severe accident and containment phenomena are examples of the cases when such dependencies of the accident progression on timing and order of events are especially important.

Since the late eighties, realistic deterministic-dynamic models, commonly referred to as best-estimate methods, received recognition as safety analysis tools. However, the best estimate codes are still used in a largely decoupled manner from the PSA. That hinders their application to risk analysis and identification of plant vulnerabilities.

In making predictions regarding the response of a system to disturbances, both the uncertainties arising from the stochastic nature of events (aleatory uncertainties) as well as those arising from lack of knowledge about the processes relevant to the system (epistemic uncertainties) have to be taken into account. Often, it is difficult to distinguish between epistemic and aleatory uncertainties [2]. Dynamic PSA methodologies allow a unified framework to account for the joint effects of both types of uncertainties

simultaneously in predicting the distribution of risk associated with the system response.

Dynamic PSA methodologies can be divided into three main categories [3]: (i) continuous-time methods, (ii) discrete-time methods, and (iii) methods with graphical interfaces. While the methods with graphical interfaces are also either continuous or discrete time methods, they are listed as a separate category because the availability of a graphical interface is usually regarded as rendering them more user friendly. IDPSA tools usually employ (i) system simulation codes and models with explicit consideration of the effect of timing on the interactions between epistemic (modeling) and aleatory (scenario) uncertainties, (ii) a method for exploration of the uncertainty space. A review of the IDPSA methods for nuclear power plant applications can be found in [3, 25]. The inputs for all dynamic methodologies are:

- a time-dependent system model (such as RELAP5 [4] or MELCOR [5] codes),
- possible normal and abnormal system configurations which may need to be determined using a failure-modes-and-effects (FMAE) analysis, and
- transition probabilities (or rates) among these configurations.

2.1.1 IDPSA methods and the decision making process

It was mentioned previously [1] that the readiness of a tool is difficult to determine if there are no clear criteria for success or goal for the analyses. In terms of decision making, quantification of consequences into figures of merit is necessary (i.e. to establish safety goals and success criteria).

IDPSA methods are capable of quantifying aleatory uncertainties in time dependent scenarios. It was emphasized (during the IDPSA meeting 2012 [1]) that this mostly had an effect within the context of academia whereas it did not do much for deployment into the industry. Therefore, focus must be directed towards what the decision makers need and what they regard as important.

Credibility, uncertainty quantification (robustness of decision), comprehensiveness (risk profile instead of one number) and understanding were outlined as important factors in terms of what kind of data to be provided for the decision makers. Consistency was also emphasized as important since different kinds of decisions (e.g. for industry or regulators) put different requirements on the data provided.

2.2 Risk Oriented Accident Analysis Methodology

The Risk Oriented Accident Analysis Methodology (ROAAM) [26], [27] can be considered as an example of a decision support method. The ROAAM marries probabilistic and deterministic approaches. This methodology developed by Professor Theofanous [26] has been applied to successfully resolve different severe accident issues in LWR plants, and severe accident treatments in ALWR designs e.g., [27].

The focus of ROAAM is upon reducing the uncertainty to the extent that a defense-in-depth is considered as achieved. When the whole community of experts in a given problem area is convinced that the demonstration is effected and regarded successful the problem may be considered solved (in a robust and final way). Eventually the complete reaching of all experts is effected by publication in the technical literature, with additional iterations thereof if necessary. ROAAM provides guidelines for development of framework for bounding of epistemic (modelling) and aleatory (scenario) uncertainties in a transparent and verifiable manner that enables convergence of experts opinions on the outcome of the analysis (not necessarily on the uncertainties in the input information).

ROAAM integrates risk assessment (analysis) and risk management (modifications in the design, procedures, etc.) in an effective manner in order to resolve safety issues.

When applied to the Nordic BWR plants, the tight coupling between severe accident threats (steam explosion and basemat melt-through due to debris un-coolability) and high sensitivity of the SAM effectiveness to timing of event (e.g., vessel failure) and characteristics (e.g., melt release conditions) present new challenges in decomposition, analysis and integration.

It is instructive to note that discussion of approaches to risk management regulatory framework has been initiated at US NRC [28]. Risk Management Task Force provided recommendation that NRC should implement a consistent process that includes both deterministic and probabilistic methods. It is acknowledged that Risk assessments provide valuable and realistic insights into potential exposure scenarios. In combination with other technical analyses, risk assessments can inform decisions about appropriate defense-in-depth measures.

ROAAM+ framework employs a two-level coarse-fine iterative analysis. First, fine-resolution but computationally expensive methods are used in order (i) to provide better understanding of key phenomena and their interdependencies, (ii) to identify transitions between qualitatively different regimes and failure modes, and (iii) to generate reference data. The fine-resolution codes are run independently, assuming wider possible ranges of the input parameters. Second, a set of coupled modular frameworks is developed connecting initial plant damage states with respective containment failure modes. Deterministic processes are treated using surrogate models based on the data obtained from the fine-resolution models. The surrogate models are computationally efficient and preserve the importance of scenario and timing. Systematic statistical analysis carried out with the complete frameworks helps to identify risk significant and unimportant regimes and scenarios, as well as ranges of the uncertain parameters where fine-resolution data is missing. This information is used in the next iteration of analysis with fine-resolution models, and then refinement of (i) overall structure of the frameworks, (ii) surrogate models, and (iii) their interconnections. Such iterative approach helps identify areas where additional data may significantly reduce uncertainty in the fine- and coarse-resolution methods, and increase confidence and transparency in the risk assessment results. The overall modular structure of the frameworks and the refinement process are discussed in the paper in detail [29].

2.3 Quantitative Definition of Risk and ROAAM Basics

According to quantitative definition of risk, proposed by Kaplan and Garrick [30], the risk R_i associated with specific scenario s_i can be characterized by its frequency f_i and consequences c_i. Consequences are obtained from predictions that are subject to epistemic uncertainty due to incomplete knowledge. The degree of uncertainty in the prediction of the future course of events can be quantified as "probability" P_i or "likelihood" of c_i. Such probability is evaluated by an expert based on the available evidences (i.e. data and/or experience with similar courses of action in the past). Therefore, two rational beings given the identical evidence must assess the probability identically [30]. "Frequency" is the outcome of an experiment involving repeated trials. Aleatory uncertainty is expressed in terms of frequency.

$$R_i = \{s_i, f_i, P_i(c_i)\} \tag{2.1}$$

Consequences c_i of scenario s_i can be presented as joint probability density function $\text{pdf}_{C_i L_i}(L_i, C_i)$, which accounts for the epistemic uncertainty and possible dependencies between the loads (L_i) on the system in question and its capacity (C_i) to withstand such loads. Thus, failure probability P_{Fi} for scenario s_i can be evaluated as

$$P_{Fi} = P(L_i \geq C_i) = P(C_i - L_i = Z_i \leq 0) = \iint_{Z_i \leq 0} \text{pdf}_{C_i L_i}(c, l) dc dl \qquad (2.2)$$

or, in case when load and capacity are independent

$$P_{Fi} = P(L_i \geq C_i) = \int_{-\infty}^{\infty} \int_{-\infty}^{l \geq c} \text{pdf}_{L_i}(l) \, \text{pdf}_{C_i}(c) dc \, dl = \int_{-\infty}^{\infty} \text{CDF}_{C_i}(l) \, \text{pdf}_{L_i}(l) dl \quad (2.3)$$

where CDF_{C_i} is the cumulative probability density function for the capacity. Unacceptability of containment failure is equivalent to requirement that all P_{Fi} should be below "physically unreasonable" level P_s.

The idea of characterizing risk as a set of triplets (scenario, its frequency, and probability of consequences) was further developed and practically applied to assessment of severe accident risks in ROAAM [27]. According to ROAAM, the use of Risk for effective management and regulation of rare, high-consequence hazards requires the simultaneous (coherent) consideration of (i) safety goal, (ii) assessment methodology, and (iii) application specifics. ROAAM provides guidelines for development of frameworks for bounding the epistemic (modeling), and aleatory (scenario) uncertainties in a transparent and verifiable manner that should enable convergence of experts' opinions in the review process.

Important premise of ROAAM is that safety goals can be defined only qualitatively when epistemic uncertainty is significant. The goal should effectively communicate the idea that the perceived hazard is "physically unreasonable" under "any circumstances" leading up to it in a "physically meaningful" context. More specifically, for severe accident analysis the safety goal can be defined as: "containment failure is a physically unreasonable event for any accident sequence that is not remote and speculative" [27].

In order to achieve the transparency and verifiability, ROAAM employs its principal ingredients: (i) identification, separate treatment, and maintenance of separation (to the end results) of aleatory and epistemic uncertainties; (ii) identification and bounding/conservative treatment of uncertainties (in parameters and scenarios, respectively) that are beyond the reach of any reasonably verifiable quantification; and (iii) the use of external experts in a review, rather than in a primary quantification capacity.

Separation of epistemic and aleatory uncertainties stems from the work of Kaplan and Garrick [30]. Separate treatment of screening frequency for aleatory, and the physically unreasonable concept for epistemic uncertainties is a must for clarity and consistency of the ROAAM result.

An arbitrary scale for probability is introduced which defines a physically unreasonable process as one involving the independent combination of an end-of-spectrum with one expected to be outside but cannot be positively excluded [27]:
- 1/10   Behavior is within known trends but obtainable only at the edge-of-spectrum parameters.
- 1/100   Behavior cannot be positively excluded, but it is outside the spectrum of reason.

- 1/1000 Behavior is physically unreasonable and violates well-known reality. Its occurrence can be argued against positively.

The starting point of ROAAM is an interest in the "likelihood" (L_j) of different containment failure modes (hazards H_k) given a set of initial plant damage states ($\{D_j\}$)

$$L_j(H_k) = G(p_1, p_2, \dots, p_l), \quad \text{given } \{D_j\} \tag{2.4}$$

where damage states have frequency higher than selected screening frequency f_s and lower than target frequency f_t achieved as the prevention goal, that is, $f_s < f_j(D_j) < f_t$.

The approach employed in ROAAM is not to realize a defensible approximation to function G, and seeking the likelihood L_j, but to establish that it is (or can be made by appropriate decisions) low enough as to regard the hazard H_k as physically unreasonable, avoiding excess conservatism while still remaining convincing [27].

A separation must be made between the aspects of systems response that can be stated as well-posed physical problems or "causal relations", and other aspects which are subject to inherently variable behavior and called "intangibles". The structure of separation synthesis is called "probabilistic framework". Each framework refers to a particular "scenario" s_i. The art in the decomposition is to envelop the behavior through the coherent use of "intangibles" and respective "scenarios" such that it will be understandable (and scrutable). Each "causal relation" requires an in-depth and demonstrable understanding of the controlling physics; "scenarios" and "intangibles" are to fill in the gaps whenever this is not possible. Uncertainty in causal relations can be reduced. Uncertainty in intangibles can only be qualitatively approached, but it can always be bounded. The adequacy of scenarios can be determined according to the completeness of the logical structures used in deriving them. The process of integration through the probabilistic framework is effected by introducing a scale for the temporary quantification of intangibles, and the results are rendered in qualitative terms by applying this scale in reverse.

The problem is decomposed into framework and stochastic scenarios $\{s_i\}$, such that:

$$L_{ji}(H_k) < P_{ji}(H_k), \quad P_{ji}(H_k) = F(d_1, d_2, \dots, i_1, i_2, \dots) \tag{2.5}$$

where $\{d_i\}$ is a set of "deterministic" parameters, $\{i_i\}$ is a set of "intangible" parameters, $P_{ji}(H_k)$ is based on arbitrary probability scale. The goal of analysis is to show that

$$P_{ji}(H_k) < P_s \text{ given } \{D_j\} \text{ for all } \{s_i\} \tag{2.6}$$

where P_s is the "physically unreasonable" level. The above structure separates out epistemic from aleatory uncertainty which is also motivated by the distinct approaches to judge residual risk: with screening frequency for aleatory, and with physically unreasonable concept for epistemic. Any stochastic behavior not already included in the definition of the severe accident window (the plant damage states to be considered) can be taken up in the definition of scenarios and intangibles, since they would be expected to dominate the uncertainty in any case. If necessary, however, stochastic parameters, or even processes, can appear explicitly in (2.5). A similar separation can be effected in this case, too, by simply finding the total probability in each frequency range, and applying the same criteria for judging the results – but now these frequencies should be combined

with the respective plant damage state frequencies [27].

2.4 Nordic BWR challenges for ROAAM

Severe accident management (SAM) in Nordic boiling water reactors (BWRs) relies on ex-vessel core debris coolability. In the case of core meltdown and vessel failure, melt is poured into a deep pool of water located under the reactor. The melt is expected to fragment, quench, and form a debris bed that is coolable by natural circulation of water. Success of the strategy is contingent upon melt release conditions from the vessel which determine (i) properties of the debris bed and thus if the bed is coolable or not, and (ii) potential for energetic interactions (steam explosion) between hot liquid melt and volatile coolant. Both non-coolable debris bed and steam explosion pose credible threats to containment integrity.

While conceptually simple, this strategy (i) involves extremely complex and often tightly coupled physical phenomena and processes, which are also (ii) sensitive to the conditions of transient accident scenarios. For instance, late recovery actions might affect core degradation and relocation processes, which can change formation of the in-vessel debris bed, reheating and re-melting of multi-component corium debris, thermo-mechanical interactions between melt and vessel structures and penetrations, vessel failure, melt release and jet fragmentation, debris solidification, energetic melt-coolant interactions, two-phase flow in porous media, spreading of debris in the pool, spreading of particulate debris bed, etc. (Figure 2.1). These phenomena have been a subject of extensive investigations in a large-scale research program on Melt-Structure-Water Interactions (MSWI) at the Royal Institute of Technology (KTH) over the past few decades.
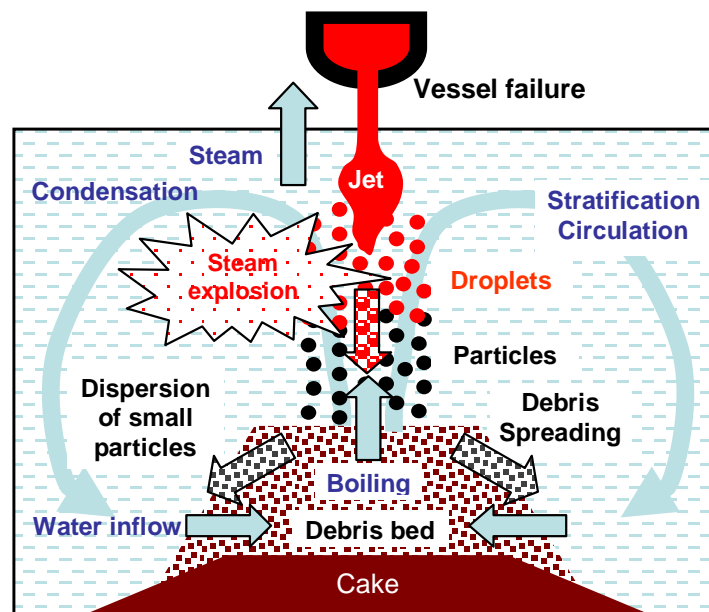
Figure 2.1. Severe accident phenomena in Nordic BWR.

While a significant progress has been made in understanding and predicting MSWI physical phenomena, complex interactions and feedbacks between (i) scenarios of accident progression, and (ii) phenomenological processes, have hampered a comprehensive assessment of SAM in the Nordic BWRs. Presently, the issues of ex-vessel debris coolability and steam explosion are considered as intractable by only probabilistic or only deterministic approaches.

Information about the initiating events and plant damage states is necessary input information for the IDPSA analysis and it can be provided from the PSA-L1. In Chapter 3 we provide an overview of PSA-L1 results which are used in this work.

Timing of events such as failure and recovery of safety systems determines in-vessel accident progression, core relocation process and properties of the debris in the lower head. The properties and configuration of the debris determine initial conditions for corium-structure interactions, vessel failure and melt release conditions. Therefore core degradation and relocation scenarios have significant impact on the ex-vessel accident progression and risks. For addressing the effect of timing of the events on the in-vessel and ex-vessel accident progression a set of initial plant damage states and possible further failures and recovery actions has to be provided. Such information is available from the PSA-L1. In the following section a discussion of the basic information from PSA-L1 which is necessary for IDPSA analysis and identification of specific topics of interest is provided.

2.4.1 Phenomenology and Scenarios

While ROAAM is logically sound and has been successfully applied in several practical cases to resolve severe accident issues, there are some challenges for application of ROAAM to Nordic BWR case. Typical phenomenological stages of severe accident progression in Nordic BWR are shown in Figure 2.2.

The multistage path from the initial plant damage state to the containment threats is an important source of complexity and uncertainty. Phenomena and scenarios including operator actions are tightly coupled in their mutual interactions and eventual impact on the possibility of different containment failure modes. Conditions created at the earlier stages can significantly affect configurations and problem statements at later stages. For instance, if there is no activation of lower drywell flooding, then steam explosion risk is eliminated, but hot corium melt will attack cable penetrations in the containment floor leading to almost immediate containment failure.

Timing of transition between different stages is also important. Different time-dependent trajectories of the accident scenarios with the same logical sequence of the stages can result in different outcomes. For instance, decay heat is decreasing with time providing much better chances for coolability of the debris bed if melt is released from the vessel later [31]. However, if melt is released from the vessel later, it will have higher temperature, which could increase the risk of debris agglomeration [32], [33], [34] hindering coolability of the debris bed [35], and creating a potential for an energetic steam explosion which can threaten containment integrity.

Combination of (at least) two threats (non-coolable debris and steam explosion) is another source of uncertainty. On one hand, there is a possibility that steam explosion might contribute to spreading of the debris over containment floor. On the other hand, even a mild steam explosion might lead to degradation of debris bed cooling function, e.g. by destroying protective covers for cable penetrations in the containment floor and exposing them to hot debris, or by creating a leak of coolant from the lower drywell, or by activating filtered containment venting, releasing fraction of nitrogen which can potentially lead to drop of containment pressure well below atmospheric level, etc.
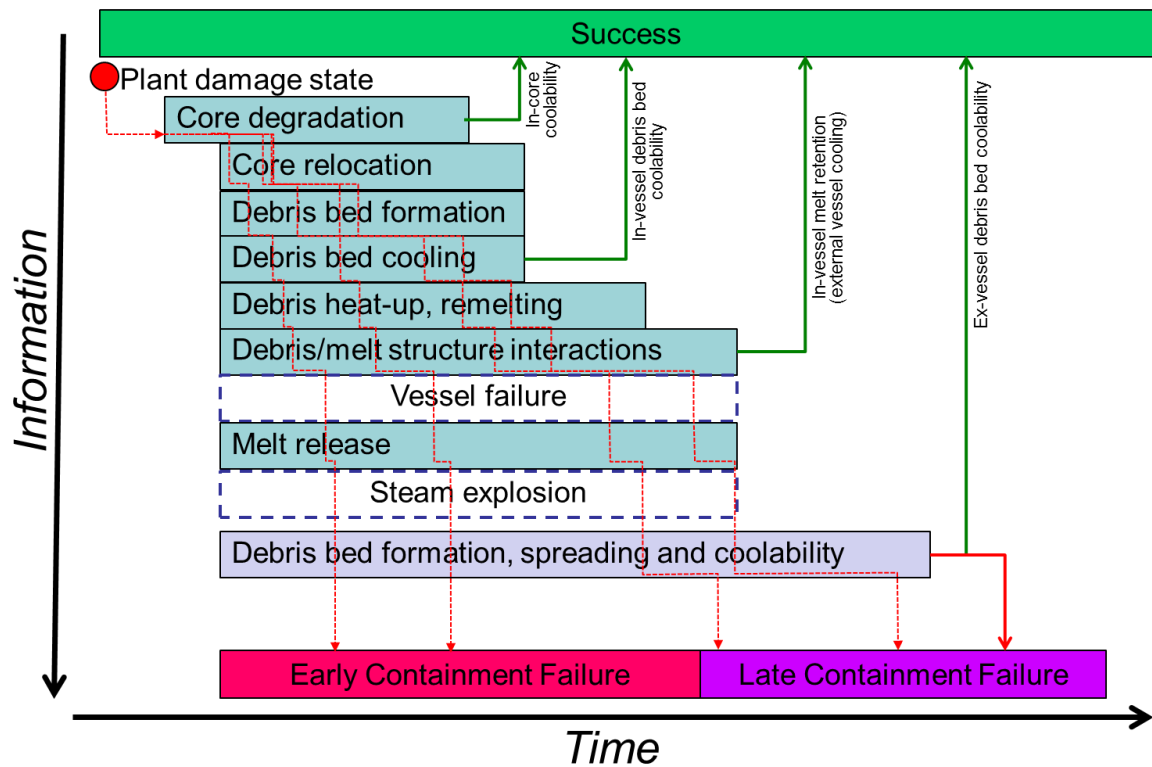
Figure 2.2. Severe accident progression in Nordic BWR.
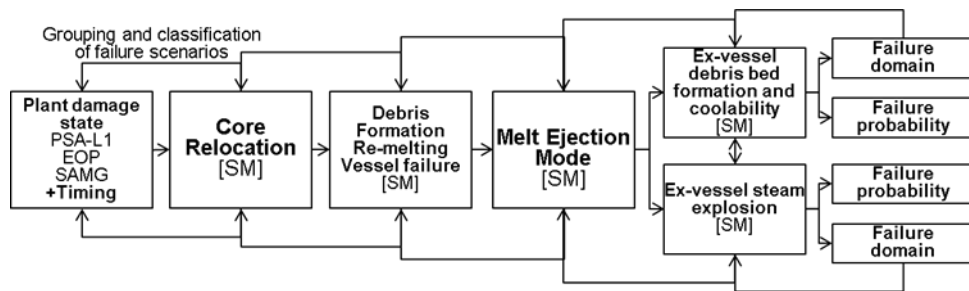
Figure 2.3. ROAAM+ Framework Nordic BWR.

The major challenge for application of ROAAM to Nordic BWR is the complexity of tightly coupled transient phenomena and scenarios which limit the effectiveness of heuristic approaches in (i) problem decomposition and (ii) a priori judgment about importance and impact of coupled and time dependent phenomena and scenarios on the accident progression and outcome.

2.4.2 Decision Making Context

Conditional containment failure probability is considered in this work as an indicator of severe accident management effectiveness for Nordic BWR. It is instructive to note that different modes of failure (assumed to be equivalent to loss of containment integrity) can potentially lead to quite different consequences in terms of radioactivity release. At this point we consider any failure mode as unacceptable for the sake of conservatism.

The ultimate goal of ROAAM process is to provide a scrutable background in order to achieve convergence of experts' opinions in decision making on the question: is

containment failure physically unreasonable, given existing SAM and current state-of-the-art knowledge? This question is driven by "concerns". If inherent safety margins are large, then the answer to the question is positive and can be demonstrated through consistent conservative treatment of uncertainties in risk assessment by improving necessary knowledge and data. Otherwise, improvement of the state-of-the-art knowledge is ineffective. Appropriate modifications of the system (e.g. safety design, SAMGs, etc.) should be undertaken in order to achieve the safety goal.

However, it is not always obvious that existing system cannot meet the safety goal even if further investments in development of new knowledge will be continued. Especially for complex systems, such as SAM of Nordic BWR, uncertainty can create a space for decision makers' "hope" that the system is safe due to some incompletely understood phenomena or interactions, and thus acquiring further knowledge about the system is justified. As such proposition is driven by the "hope", it is clear that conservative treatment of uncertainty would not be very helpful. For clarifying if such hope is reasonable, the assessment should be focused on the necessity of containment failure using "optimistic" treatment of uncertainty.

Thus, to be truly useful for decision making on the Nordic BWR SAM case, the risk assessment framework should be capable of providing assessments in support for both possible decisions: (i) current strategy is sufficiently reliable and no changes are necessary; (ii) strategy is not sufficiently reliable and changes are necessary.

A difficulty arises when neither failure nor success can be demonstrated with a sufficient confidence. For instance, bounding ("conservative" or "optimistic") approaches fail to characterize system risks when failure or success domains are positioned in the middle of the uncertainty space. In other words, only an "optimal" course of events can lead to success or to failure. This is often the case when there are competing phenomena or threats, when positive or negative effect of some parameters or events on the failure possibility changes depending on other parameters or events. For instance, in case of successful attempt of in-vessel debris cooling using control rode guide tube (CRGT) flow, melt release from the vessel can be prevented. However, if corium retention is not successful, CRGT cooling can lead to delay of vessel failure, formation of a larger melt pool with higher superheat. Melt release from the vessel with such conditions can significantly increase potential energetics of steam explosion and the risk of formation of agglomerated, non-coolable debris bed. Feasibility of using "best estimate" or "risk informed" approaches for decision making in this case is contingent on the system, data and knowledge. If dependencies are strong, risk quantification can be polluted with uncertainty to the point where "everything is possible" due to "combinatorial explosion of possibilities". Using "risk informed" approach in such case with large irreducible uncertainties can be at best inconclusive, and in the worst case misleading. If "everything is possible", it is a clear sign that the system is complex. In other words, understanding and control of the system is beyond our reach and changes in the system are necessary in order to make its behavior predictable with sufficient confidence.

Eventually decision has to include cost benefit analysis. If potential costs of improving the current state of knowledge are high then the decision to change the system in order to reduce its complexity would be the most reasonable. If the costs of knowledge improvement are acceptable, then extensive sensitivity and uncertainty analysis can be quite useful for identification of priorities for defining research goals and collection of new data. However, quantitative uncertainty in estimations of risks related to potential losses vs cost of necessary research is usually quite high.

Thus a structured process is needed for coherent (i) development of risk assessment framework, (ii) collection of necessary data, and (iii) development of necessary knowledge. This process should be guided by extensive sensitivity and uncertainty analysis and eventually result in a robust and scrutable assessment of either "possibility" or "necessity" of containment failure in order to support decision making.

The detailed description of the important aspects of development of such process for Nordic BWR SAM can be found in [24].

Chapter 3.   Sequence Modelling in PSA Level 2

3.1 Assumptions and Limitations in PSA

Probabilistic Safety Assessment (PSA) is used to systematically identify, evaluate and rank the sequence of events that can lead to core damage and radioactive release to the environment. Identification and hence opportunities for improvement in risk dominant feature of the facility is one of the overall objectives. The analysis is probabilistic, i.e. it is based on probability and reliability calculations and the result is an estimate of the frequency of detected events.

Some key assumptions and limitations in PSA L1 analysis are:
- Implemented deterministic analyses are correct.
- Blow-down paths and building structures can withstand emerging loads at rupture.
- Studied transient time is normally 1 day, i.e., objective function is required during this time (Level 1 analysis includes 24 hours from initiating event, sequences that have not led to the core overheating within this time are not considered as core damage sequences and excluded from Level 2 analysis).
- Aggravating manual interventions are not considered.
- Restricted modeling of manual interventions during transients (only when clear instructions are provided and there is sufficient time available).
- System requirements should be established either via thermal-hydraulic calculations or through references in the SAR.
- Timing within sequences is represented simplified (conservative)

3.2 Phases during severe accidents

The first phase of an accident is studied in PSA L1 and the result is a number of sequences ending with either success or core damage.

For those sequences ending with core damage the following accident progression is studied in PSA L2. The accident progression is normally divided in:

- **In-vessel** – Describes the heatup and meltdown of the core
- **Vessel melt through**– Describes the phenomena occurring at vessel melt through
- **Ex-vessel** – Describes the long term progression of the plant after melt through

There are interesting phenomena to study with deterministic methods both in PSA L1 and in the different phases of PSA L2.

3.2.1 Core Damage States in PSA L1

The simplest form of core damage states in PSA L1 is to just differ between core damage and success. Normally the core damage states are separated into different categories with respect to the cause of the core damage. Possible reasons to core damage can be:
- HS1: Failure to shut down the reactor.
- HS2: Failure to make up water to the reactor.
- HS3: Loss of residual heat removal.
- HS4: Overpressure of the primary system.

- Overpressure of the containment

Typically loss of core cooling or failure of residual heat removal give the major contributions to core damage, but this varies from plant to plant.

Failure to shut down the reactor normally gives a low contribution to the total core damage frequency. Reactivity control is a very complex process to model since an incomplete or delayed shutdown puts higher demands on the other functions such as higher demands for core cooling, increasing pressure in the primary system etc. It may therefore be interesting to study this in more detail since the core damage frequency due to failure of shutdown may be underestimated in the existing PSA studies. This is further described in section 3.3.1 below.

3.2.2 Plant Damage States Classification in PSA L2

In PSA L1 for Nordic BWR reference plant design the core damage states are grouped into 4 categories: HS1 (ATWS), HS2 (Loss of core cooling), HS3 (Failure to remove decay heat) and HS4 (Primary system overpressure). The categories (HS1, HS2, HS4) correspond to early core damage scenarios, HS3 – corresponds to late core damage.

In addressing ex-vessel behavior and consequences the following physical phenomena can challenge containment integrity: direct containment heating (DCH), ex-vessel steam explosions (EVE) and ex-vessel debris coolability (DECO).

A quantitative perspective on these matters should be derived from the Level 1 PSA. DCH scenario corresponds to high pressure (HP) accident scenario, steam explosion in the containment (EVE) corresponds to low pressure (LP) scenario and, finally, both consequences will lead to large amounts of core debris relocated to the lower drywell and it can challenge lower drywell floor and penetrations integrity, so the question of ex-vessel debris bed coolability is an all-pervasive issue.

Initial conditions and correspondent frequencies that will lead to different core degradation, in-vessel debris bed formation, vessel failure scenarios can be identified from PSA L1 data.

The core damage sequences, thus, can be grouped together based on the aforementioned challenges to the containment integrity as follows:
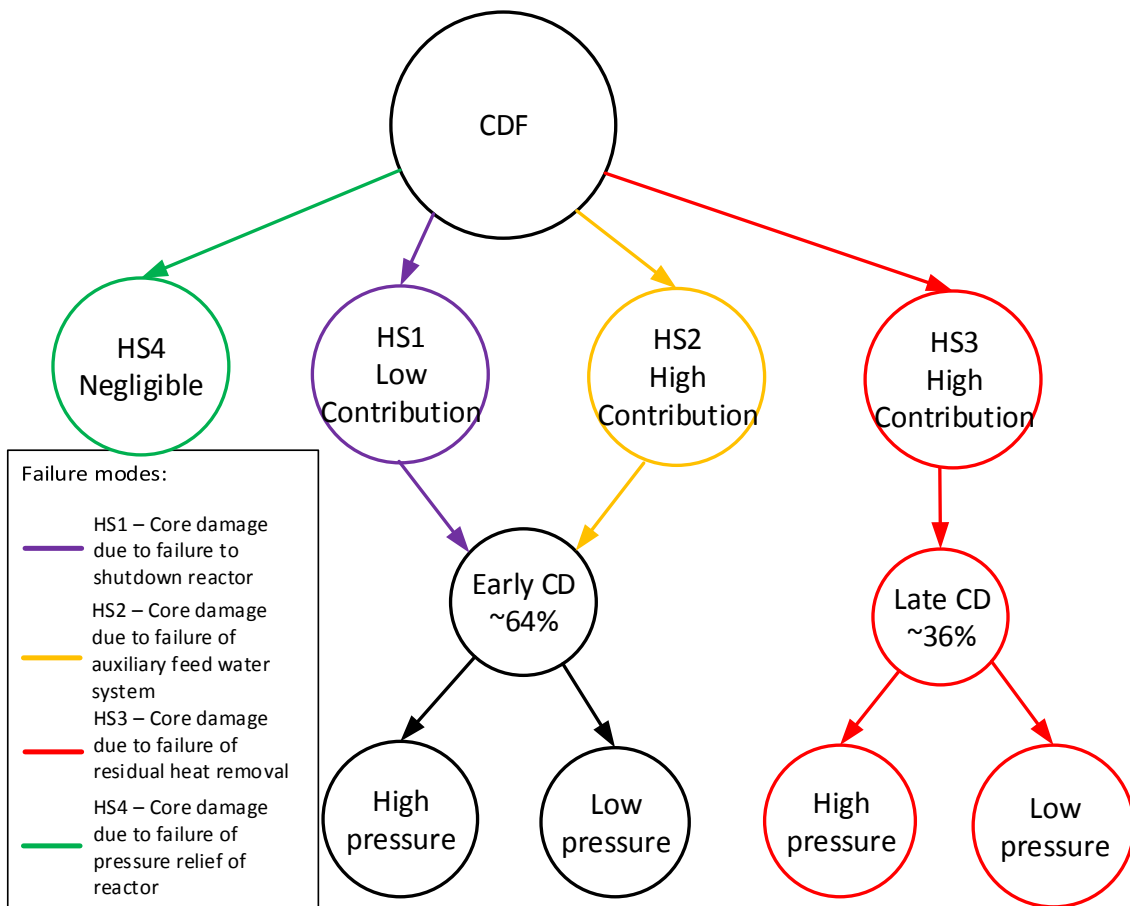
Figure 3.1. Core Damage States Classification

The phenomena during core meltdown and vessel melt through belong to PSA L2. The link between PSA L1 and L2 is the plant damage states. The plant damage states describe not only the core damage state but also the conditions in the primary system and the containment. This is further described in section 3.2.3.

3.2.3 Level 2 PSA

In a standard PSA, the output of PSA Level 1 is typically core damage (possibly separated in a few sub-categories). These core damage sequences are then divided into a number of sub-categories based on attributes, which shall be representing the important features for the Level 2 progression.

There is normally around 20-40 Plant Damage States (PDS) defined in the interface between Level 1 and 2. This interface is therefore reasonably crude.

For the plant studied there are 27 PDSs for power operation and low power operating modes. The attributes that are considered relevant to characterize the core melt for the continued process are:

- Core damage state (failure of shutdown, core cooling or residual heat removal)

- Initiating event (Transient or LOCA)

- Time point of the core melt (early, late)

- Reactor pressure (low, high)

- Containment atmosphere (inert, air)
- Can cooling with containment spray system be taken into account (Failed, Yes)?
- Activated containment pressure relief, 361 (activated, not activated)
- Activated filtered release, 362 (activated, not yet activated, failed)
- Bypass of containment (bypass, intact)
- Warm suppression pool (warm if pool cooling fails, else cool)

The events that are represented in a PSA Level 2 are the events that change the conditions for retaining of releases within the RPV or within the containment. Hence, if the coolability in the RPV is different in different scenarios – then this is vital information. If the sequences are affecting the phenomena that can occur, then this is also vital information.

For each of the PDS there is a containment event tree. The containment event tree (CET) defines the accident progression as analyzed in the PSA. The sequences in the CET end at the release categories (RC), and there are normally around 15-40 of such. The RCs can be defined in different ways, for example release size or defined by type of sequence. The normal approach is to use "by type of sequence", because then only a limited amount of verifying deterministic calculations are considered to be required. For the "by type of sequence" approach the characterization is based on, for example;

- Release path (containment bypass, containment rupture, filtered release, leakage)
- Timing of release (early, late)
- Initiator (pipe rupture, transient)
- Sprinkling of containment established (yes/no)

The feasibility study is aiming at studying, in a greater level of detail, the attributes that are of interest for the core relocation – and further on melt through of the reactor pressure vessel, RPV, and the following effects on phenomena.

The type of phenomena that are usually accounted for in a PSA are:

- Re-criticality (in the core, in lower plenum, in containment)
- Hydrogen burn (deflagration and detonation)
- In-vessel steam explosion
- Ex-vessel steam explosion
- Direct containment heating
- Rocket mode
- Melt concrete interaction (basemat penetration)
- Steam generator tube rupture (only for PWR)

The effect of the phenomena can be:

- Containment rupture
- Different type of bypass

- Activation of filter

The consequence most focused on is of course containment rupture.

Chapter 4.   **Methodology for Connecting IDPSA and PSA Analysis**

4.1 Improvement of Sequence Modelling with IDPSA Methodology

From the initial sequences in the PSA Level 1, all events that are leading to a certain PDS are then treated in the same manner in the continued sequence (however, dependencies are treated logically correct if the failure should affect systems in PSA Level 2). It is however obvious that it will be different scenarios from a deterministic stand point if there is an initial loss of offsite power and no start of the diesels, compared to a scenario where the diesels would stop after some hours.

The purpose with the improved integrated link between the PSA and deterministic analyses is hence to be able to judge if, for example, these scenarios need to be treated differently in the PSA context.

The approach chosen in this report was to identify some sequences from the PSA Level 1 and to use the DPSA methodology to evaluate the progress of these sequences. The first phase of the project focused on the mechanisms for core relocation, since this is an important factor for the continued sequence. By identifying the mechanisms that contribute to the core relocation, the analysis was also expected to provide information on efficient measures, non-efficient measure or contra-productive measures to avoid core relocation. The second phase of the project has also studied further phenomena in the sequence.

Eventually, it is expected that the IDPSA integration will give a clearer answers to:

- Can the core melt process/relocation be stopped and how?

- Are there actions that must not be taken during a sequence?

- How will the conditions for phenomena be affected, and thereby give guidance on how to treat these in the PSA?

- Based on the above information, it will also feedback requirements on definition of plant damage states.

The PSA scenarios chosen for analysis of recovery were:

- High pressure loss of core cooling scenarios

- Recovery of core cooling in different combinations
    - Different time points for depressurization of the RPV
    - Different time points for start of the ECCS
    - Different mass flows from the ECCS

4.2 Application of Decision Trees for Characterization of the Failure Domains in IDPSA Results

Detailed exploration of the uncertainty space usually results in huge amount of the data generated by the deterministic codes. Therefore, one of the main problems for application of IDPSA methods is data post-processing and communication of the analysis results. Extracted information should be suitable for decision making and risk-informed characterization and eventually improvement of safety and performance of the system. Scenario grouping and classification approach with application of decision trees [36] has been developed for post-processing and visualization of the results generated by IDPSA tools.

| Scenario Grouping | → | PCA Analysis Variable Analysis & Data Transformation | → | Scenario Clustering Classification of scenarios in the failure domain | → | Decision Tree is built per each failure mode |
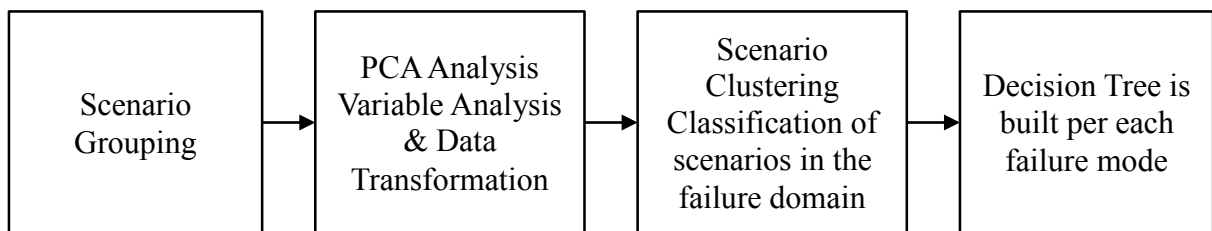
Figure 4.1. Grouping and Classification approach

The main steps of this approach are:
- Scenario grouping is performed. The main idea of this step is to focus the analysis on the sequences intractable in classical PSA. Thus, scenarios where the order and timing of events are not important are grouped first and excluded from further considerations as directly amenable to PSA analysis. Then scenarios where the order of events is important but not their timing are grouped. Remaining group of scenarios contains sequences where the outcome depends on the order and timing of the events.
- Next, Principal Component Analysis (PCA) is carried out in order to identify and quantify a group of principal components which have the largest influence on the system response [38].
- Then, based on the PCA results the clustering analysis is performed using Adaptive Mesh Refinement (AMR) method [37].
- In the final step a decision tree is built for each failure mode using clustering results data. Decision tree is used for data representation that explains failure domain-cluster structure. The structure is easy to visualize and interpret in the decision-making process [39], [40].
- Finally, information of the leaf nodes is used for failure domain probability calculation. Decision tree classification algorithm performs orthogonal partitioning of the search space using data impurity measure as a splitting criterion [36].

4.2.1 Application of Decision Trees

A grid based clustering algorithm performs orthogonal partitioning of the uncertainty space, similarly to the partitioning of learning data set in the decision tree. Therefore, complexity of the decision trees can be significantly reduced when using clustering results data rather than row scenario data.

26

A decision tree is a classification and data-mining tool for extraction of useful information contained in large data sets. An instance is classified by starting at the root node of the tree, testing the attribute specified by this node, then moving down the tree branch corresponding to the value of the attribute in the given example. This process is then repeated recursively for the sub-tree rooted at the new nodes until no further branching in the tree can be made, or some stopping pre-set conditions are met [40], [42]. A flow-chart like structure is generated in which internal nodes represent test on an attribute, each branch represents outcome of test and each leaf node represents class label (decision taken after computing all attributes). Decision trees can be used as a powerful visual and analytical decision support tool, especially in case of multidimensional data -visualization of results in the original space is non-trivial. Decision tree can be constructed using different data impurity measures (e.g. Gini impurity measure, information gain measure) to select the best split among the candidate attributes at each step while growing the tree [42]. Decision trees also can be used as a predictive model which maps observations about an item to conclusions about the item's target value.

Classification and Regression Decision Trees

Most algorithms that have been developed for learning decision trees are variations on a core algorithm that employs a top-down, greedy search through the space of possible decision trees [40], [41]. The best split is identified by a splitting criterion that use different data impurity measures (e.g. Gini impurity, Information gain measure). In this work we use Classification and Regression Tree (CART) with Gini criterion. CART $-$ is a non-parametric decision tree learning technique that produces either classification or regression trees, depending on whether the dependent variable is categorical or numeric, respectively [43].

The *Gini* impurity index (commonly used in CART) at node t is defined as

$$GINI(t) = \sum_{j \neq i} p(j|t)p(i|t) \tag{4.1}$$

where i and j are the categories of the target variable, $p(j,t)$ and $p(i,t)$ – proportion of cases in node t with attribute i and j respectively. Thus, when the cases in a node are evenly distributed across the target categories, the *Gini* index takes its maximum value *1-1/k*, where k is the number of categories for the target variable. The minimum value is zero and it occurs when all the data at a node belongs to one target category.

The *Gini* criterion for split at s at a node t is defined as:

$$GINI_{split}(s,t) = GINI(t) - p_L GINI(t_L) - p_R GINI(t_R) \tag{4.2}$$

where p_L is the proportion of cases in t sent to the left child node and p_R is the proportion of cases in t sent to the right child node. $s \in S$ - refers to a particular generic split among all possible sets of splits S.

The split s is chosen to maximize the value of $GINI_{split}(s,t)$. Since *GINI(t)* is constant for any split s on node t, it can be alternately said that the split s is to be chosen such that the quantity

$$Gain(s,t) = p_L GINI(t_L) + p_R GINI(t_R) \tag{4.3}$$

is minimized [43].

Probability estimation using Decision Trees

The failure domain is represented by agglomerations (clusters) of non-overlapping cells (grids) in the uncertainty space. If all points in the uncertainty space are equally probable then the probability of the failure domain is the ration of the volume of the failure domain to the total volume of the uncertainty space.

Decision tree represents the failure domain by final nodes in the tree and respective classification rules that lead to these nodes. The probability of each cell can be obtained as average probability of scenarios contained in correspondent cell:

$$\bar{p}_k = \left. \Sigma_{i=1}^{N_{scen}} p_i \middle/ N_{scen} \right. \tag{4.4}$$

and the probability of a failure mode i is

$$p_i = \sum_{j=1}^{N} \sum_{k=1}^{M_j} \bar{p}_k \xi^n \tag{4.5}$$

where n – dimensionality, ξ^n- cell volume, $\bar{p}_k$- is average probability of scenarios contained in cell k, M_j- cells contained in the final failure node (leaf) j and N – total amount of failure nodes (leafs). Depending on the values $\bar{p}_k$ it is possible to assign weights per each cell when building a tree, so the scenarios (cells) with higher probability are likely to be classified into the same final node.

Chapter 5.   Core Relocation Analysis

In chapter 5, 6 and 7 core relocation, steam explosion and bed coolability are studied as example cases to develop the IDPSA methodology.

5.1 Description of the simulated Transient

The MELCOR code is used for analysis of the core degradation transients starting from selected plant damage states. The station blackout (SBO) scenarios (with different timing of power recovery) are chosen as the major contributor to the CDF according to PSA-L1.

- **Complete station blackout scenario:**
  This includes battery-powered half-passive systems like the ADS-Valves (System 314) and the Water-Valves (System VX105). The realism of this assumption is open to discussion, but should not be considered entirely out of the realm of possibility considering the Forsmark 2006 Incident [16], in which an overvoltage incident in the 400 kV switchyard caused the failure of 2 (out of 4) of the so called Uninterruptable Power Supply (UPS), including their 220 V batteries. The failure of all 4 was a distinct possibility.

The timing of the safety systems recovery is as part of the accident scenario space. For instance, we consider a delay in activation of Reactor Pressure Vessel (RPV) depressurization systems which includes battery-powered ADS-Valves (System 314) and Water-Valves (System VX105, FL314 & FL330). Overpressure protection system (FL314) is spring-operated will open stepwise, starting at slightly above 70 bar and opening completely at 75 bar to protect the RPV from failure. The auxiliary Feedwater System (System 327, FL327) is considered non-functional. Other system like the Control Rod Guide Tube (CRGT) Cooling or the Residual Heat Removal (RHR) Systems are also considered non-functional. The capacity and timing of activation of the Emergency Core Cooling System (ECCS System 323, FL323) is another element of the scenario. Necessary condition for activation of the ECCS is low pressure in the RPV. Mass flow begins at pressure difference of 12.5 bars between down comer (DC) and wet well (WW) and will reach its maximum value at 2 bars above the wetwell pressure.

5.2 Nordic BWR Reference Plant Design

The current MELCOR model of Nordic BWR reference plant design with a thermal power output of 3900 MW thermal. We assume 700 fuel assemblies, all of type SVEA-96 Optima2 with an active length of 3.68 meters and Uranium Dioxide density of 10460 kg/m^3.

The original input file is split in 14 cells in the z-direction, 1 to5 for the lower plenum, 6 and 7 for the core support plate and the inactive inlet zone, 8 to 13 for the active core zone and 14 for the core exit below the core grid. In radial direction the input file has 6 cells for an inner radius of 2.4075 meters for the RPV. The outermost radius also contains the downcomer.
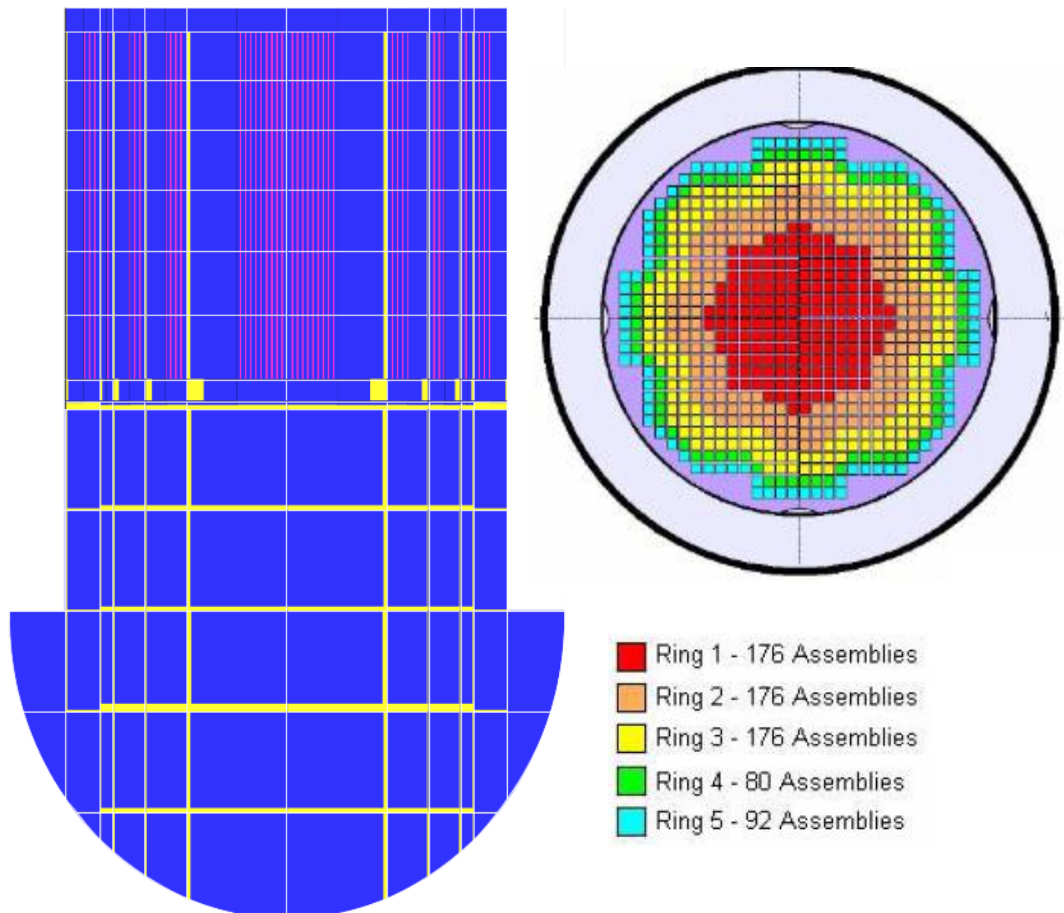
Figure 5.1. Nordic BWR MELCOR Model Core Nodalization
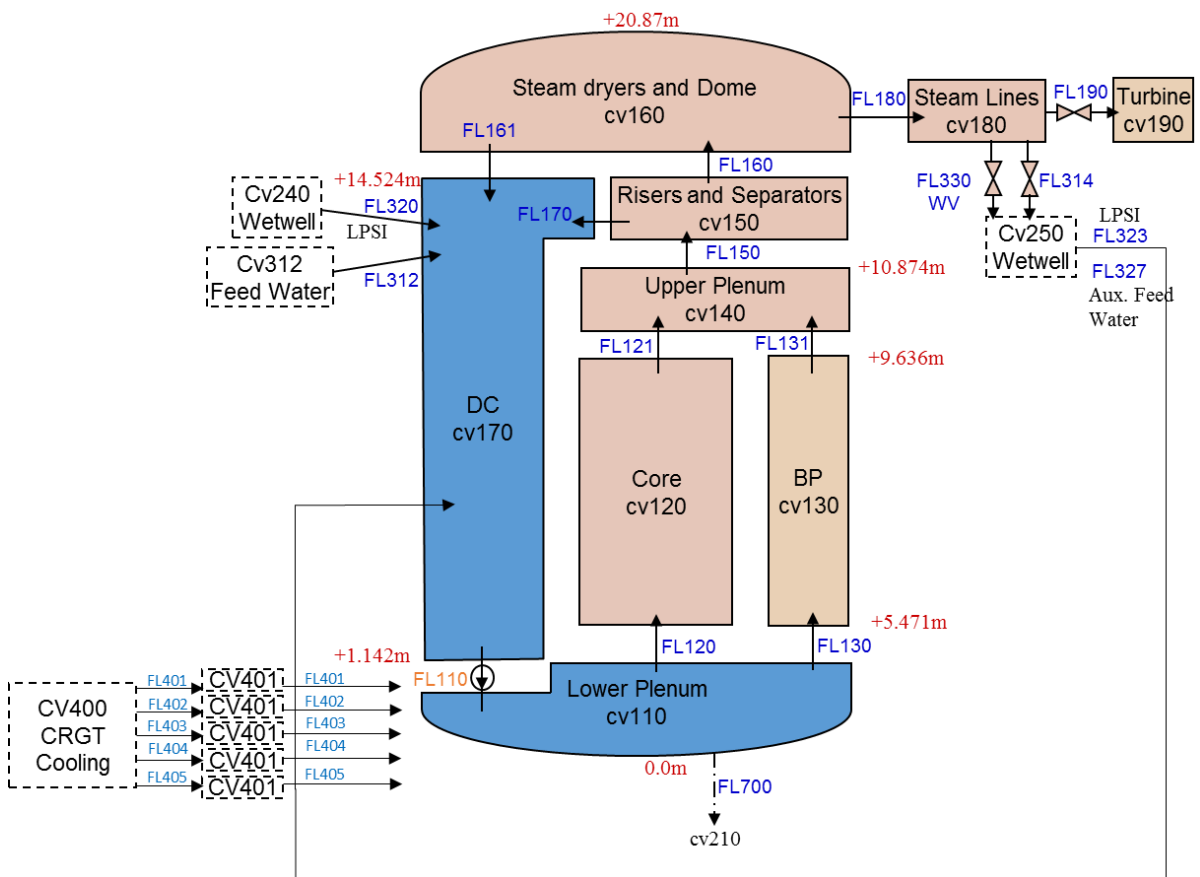
Figure 5.2. Nordic BWR MELCOR Model Vessel Nodalization
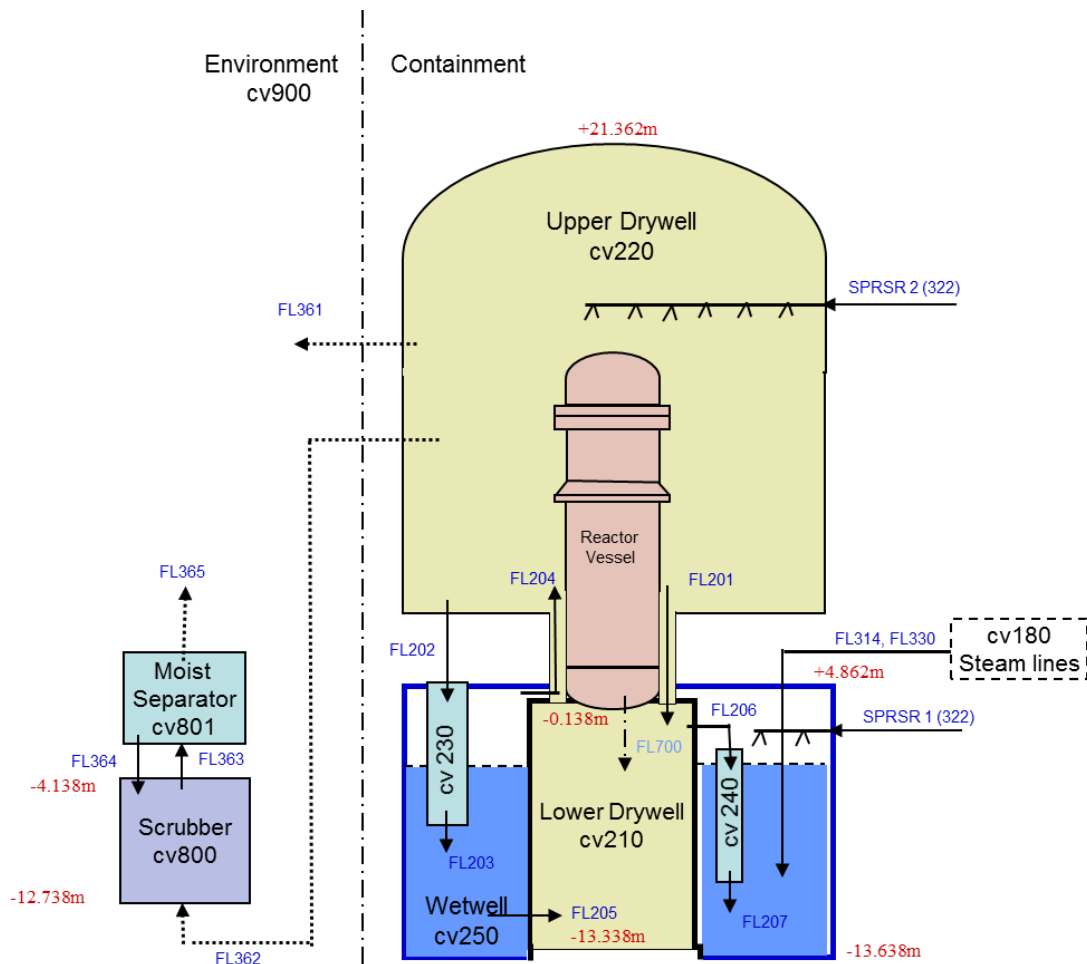
Figure 5.3. Nordic BWR MELCOR Model Containment Nodalization

Description of safety systems used in Analysis:
- System 354: Scram, the hydraulic actuating power shut-off system gives fully insertion of all control rods within a few seconds after initiation. This rather complicated control rod system is not modeled in MELCOR. Instead fission power is decreased (during 3.5 s) by a tabular function and scram condition, in this case loss of power, is applied as a control function.

  - Active

- System 314: Pressure control and relief system has several functionalities and is able to operate with only battery backups. Opening of SRV's (system 314TA function) provides instant depressurization of the primary system to a designed operation pressure. The ADS (system 314TB function includes VX105 Motor operated valves) is initiated on low water level (1m below the core top) discharging steam to WW to a level sufficient for the low pressure injection sources (ECCS) to be activated. In current Nordic BWR MELCOR model ADS valves reclose on low pressure, motor operated vales VX105 stay opened.
  - (314 TA) Function. The spring-operated part of the overpressure protection system is still operating to specifications and will open valves stepwise, starting at slightly above 70 bar and opening completely at 75 bar, to discharge steam to the containment and protect the Reactor Pressure Vessel (RPV) from explosive failure.

31

- (314 TB) Function will be recovered after a time-period imposed by the IDPSA tool

- System 323: The low pressure coolant injection (LPCI) is part of the emergency core cooling system (ECCS), which provides water injection into the down comer to facilitate reflooding in the bottom of the core.

    - Function will be recovered after a time-period imposed by the IDPSA tool, with mass flow between 0 and 100% capacity – imposed by the IDPSA tool.

- System 358: Water transfer from WW to DW is initiated in an early phase of the accident to fill the cavity and provide debris cooling when vessel breach occurs.

    - Active

- System 361: Containment venting system (CVS) via atmosphere is the ultimate pressure relief directly to the ambient surrounding when the internal containment pressure rises above the containment failure limit.

    - Active

- System 362: Containment venting with multi venturi scrubbing system (CVS MVVS) provides a controlled filtered release that suppress the amount of radioactive aerosols that escaped to the environment below the failure limit of the containment.

5.3 Core Relocation Analysis Results

We employ the GA-IDPSA [10] coupled with MELCOR code (see Appendix B for details) to search the space of scenario parameters such as (i) activation time delay of the depressurization of the Reactor Pressure Vessel (affected: Systems 314 and VX105) from 0 to 15 000 seconds; (ii) activation time delay of the low-pressure coolant injection (affected: System 323) from 0 to 15 000 seconds; (iii) maximum mass flowrate delivered by System 323, when working, between 0 and 1120 kg/s (fraction from 0.0 to 1.0 of full ECCS capacity) in order to find combinations which provide specific values of selected fitness function, e.g. mass of the relocated debris. The vessel breach condition was not implemented in the analysis.

It was previously found that there is a transition region between the regions of small and large relocations [25]. Detailed analysis of the effect of the timing of activation of ADS system (Systems 314 and VX105 – activation time varied between 0 – 10000sec) and ECCS (system 323 – activation time varied between 0 – 10000sec, full capacity) has been performed using grid based sampling methodology. The vessel breach condition was not implemented in the analysis.

Figure 5.4 - Figure 5.6 present summary of obtained results.
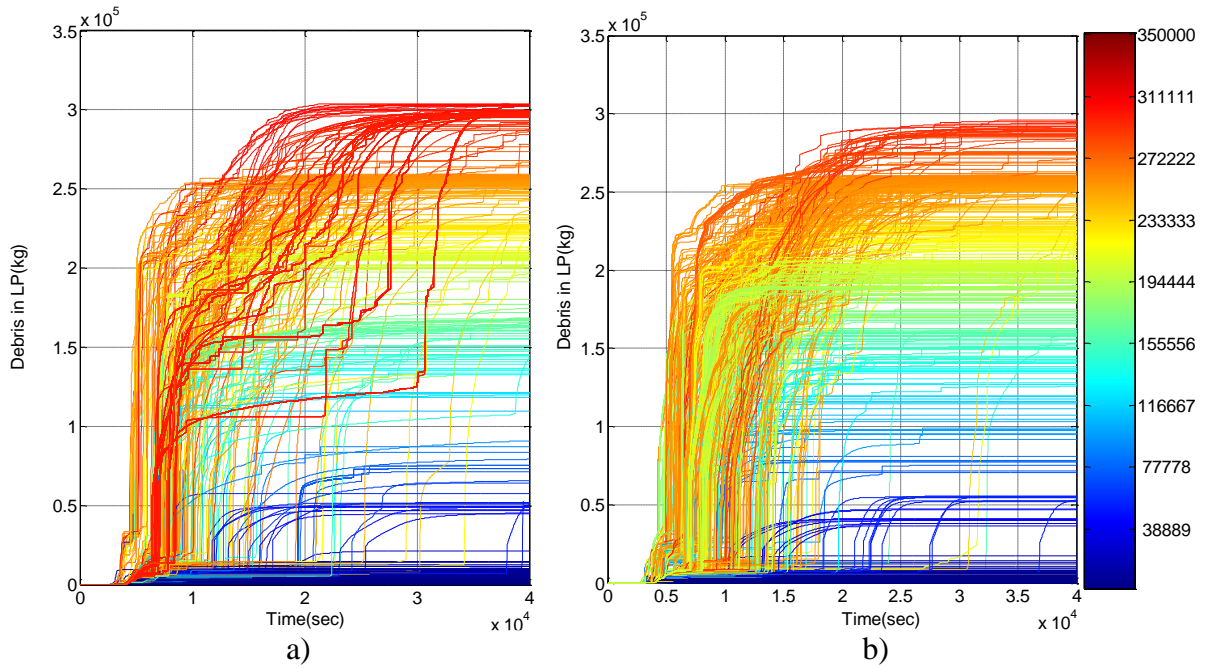
Figure 5.4. Relocated debris mass over time as a function of a) $ADS_{\Delta T}, ECCS_{\Delta T}, ECCS_A$, and b) $ADS_{\Delta T}, ECCS_{\Delta T}$, with full ECCS capacity.
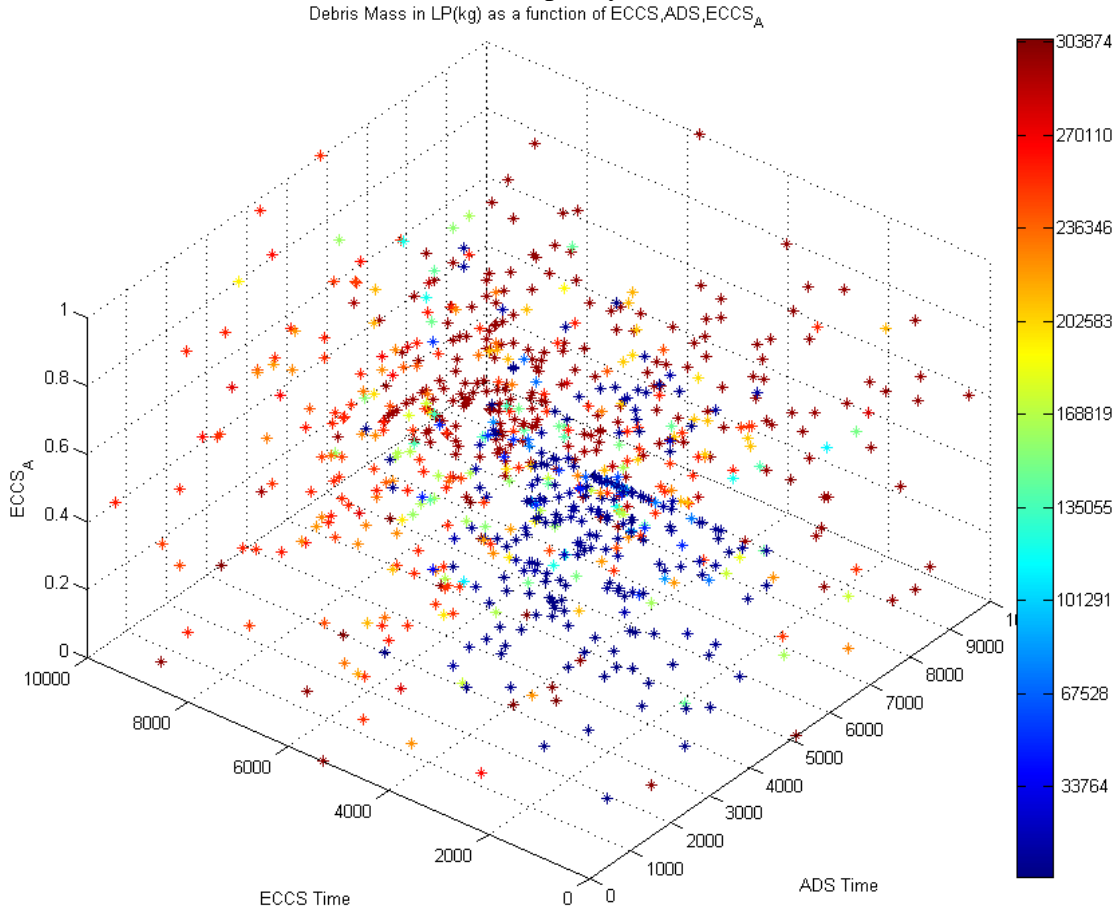
Figure 5.5. Relocated debris mass over time as a function of $ADS_{\Delta T}, ECCS_{\Delta T}, ECCS_A$.
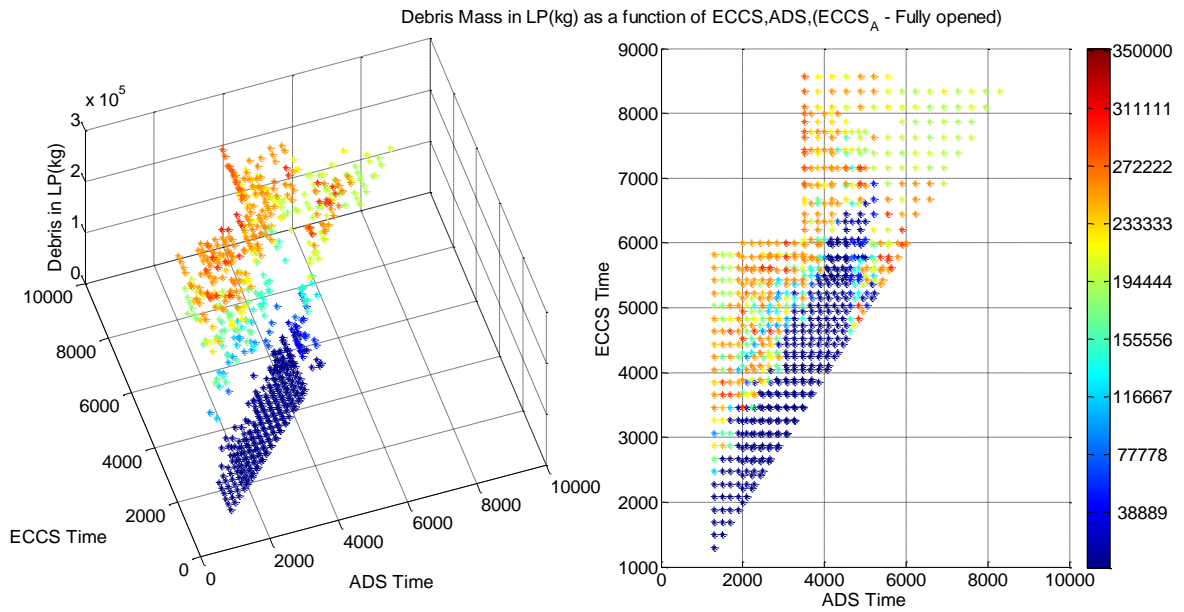
Figure 5.6. Relocated debris mass map depending on recovery time of $ADS_{\Delta T}, ECCS_{\Delta T}$ with full capacity of ECCS.

5.4 Analysis of the Results

For the analysis of the results classification and clustering analysis was used in order to group different transients into clusters, whose members have similar characteristics determined by the user.
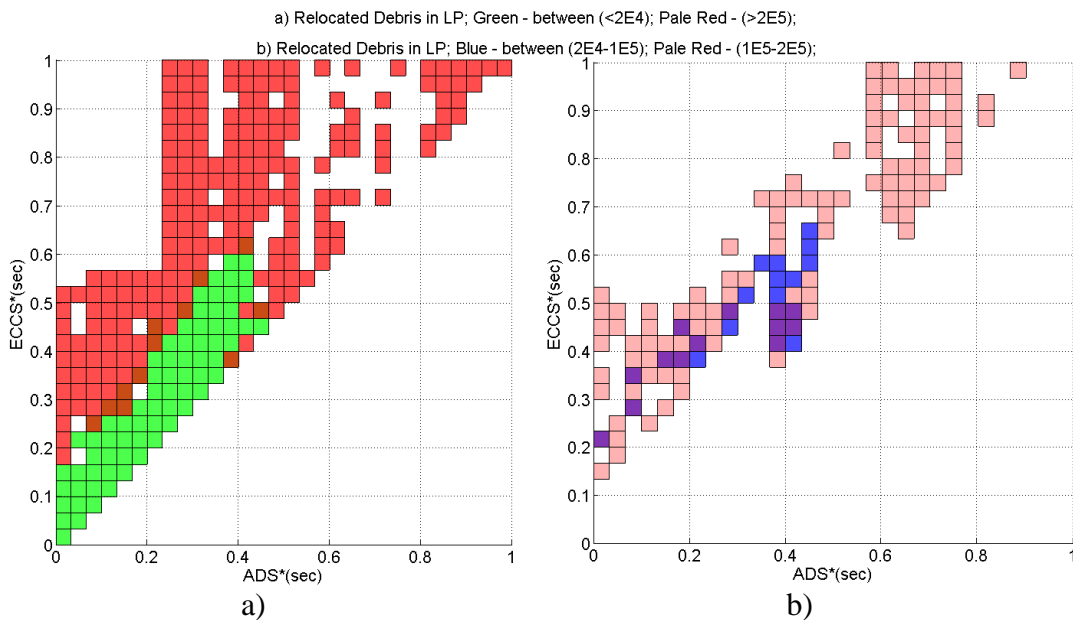
Figure 5.7. Clustering analysis results for the mass of relocated debris.

In Figure 5.7 the clustering analysis results based on the amount of relocated debris to the lower plenum indicates two characteristic domains of the scenarios space. Green and red domains represent scenarios with small relocations (between 0 and 10 tons) and very large relocations (over 200 tons). The shape of the domains suggests that the activation of ECCS is effective in preventing core relocation only within certain time window. If activation is delayed, then large mass of relocated debris is expected with high likelihood. It is instructive to note that domains of scenarios with intermediate (10-100 tons) and

large (100-200 tons) relocation masses are rather small (Figure 5.7b). The figure shows that the domains of very large, large and intermediate relocations may overlap, especially for the late ADS activation where decay heat is lower. In the overlap domain relatively large variation of the masses of relocated debris (from 10-200 tons) can be obtained with relatively small variations of the input parameters.

Figure 5.4 illustrates the amount of relocated debris over time for different scenarios (with different timing of $ADS_{\Delta T}, ECCS_{\Delta T}$). To analyze typical scenario behavior we employ pattern analysis, to identify possible relocation patterns and the effect of timing of $ADS_{\Delta T}, ECCS_{\Delta T}$ on the relocation pattern (for detailed description of the approach see Appendix C).

For the analysis we took 837 scenarios generated with MELCOR code with full ECCS injection capacity. Since we are interested in the relocation patterns for scenarios that can threaten vessel integrity, in pattern analysis we consider only scenarios that exceed 20 tons of relocated debris in LP (570 scenarios).

Using pattern analysis approach it was found that the major part of the scenario space can be represented by a limited amount of patters, see Figure 5.8.
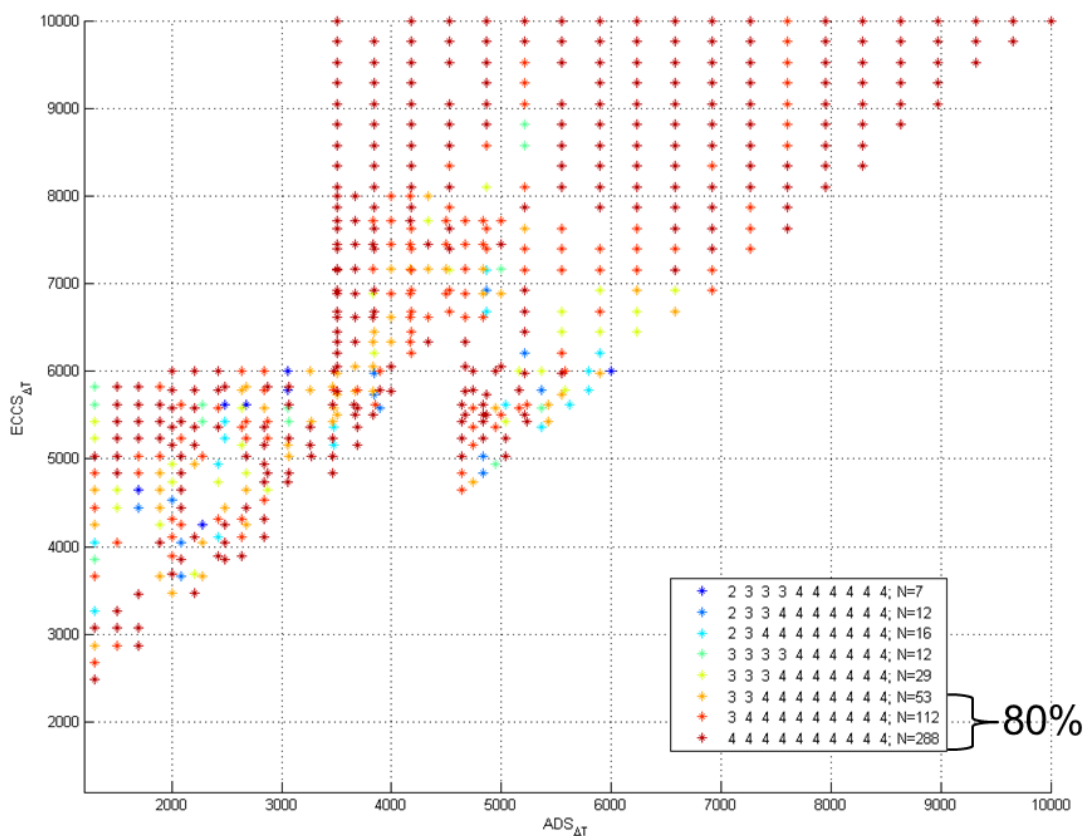
Figure 5.8. Pattern analysis results.

In most of the cases we observe over 75% relocation within 30-90 minutes after reference time (time when 20 tons relocation mass is reached).
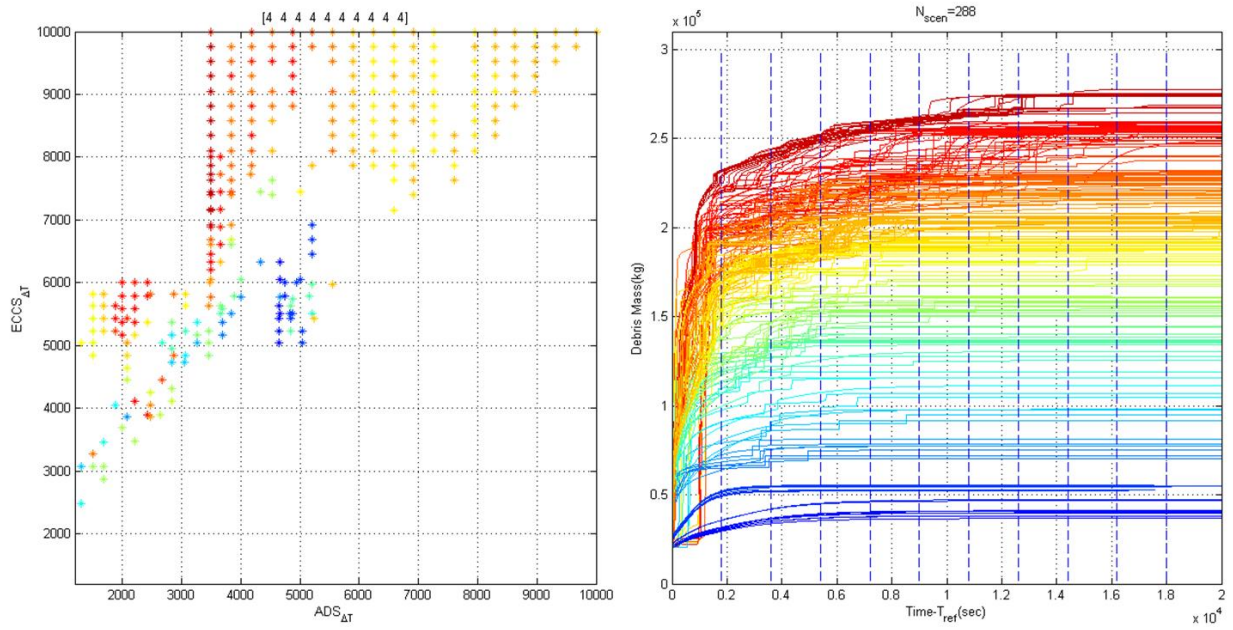
Figure 5.9. Pattern analysis results. Pattern 1.

The results also indicate that in most of the cases the differences between relocation masses at 30, 60, 90min after reference time are within 20-30 tons and the typical relocation pattern can be considered as 1-2 step relocation.

Chapter 6.   **Steam Explosion**

For the assessment of the conditional (i.e. scenario / plant damage state wise) containment failure probability due to ex-vessel steam explosion the SEIM (Steam Explosion Impact Map) framework is used. The framework links (see Figure 6.1) melt ejection mode and pool characteristics with resulting explosion loads and containment structural fragility.
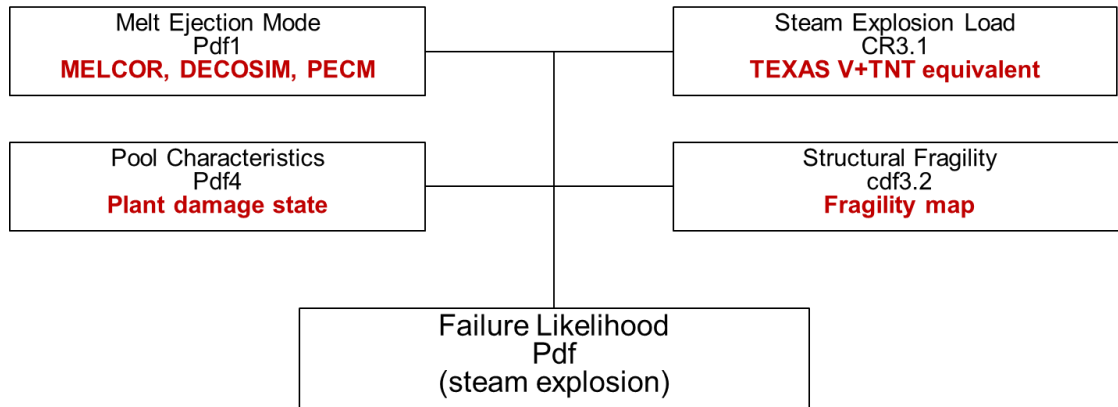
Figure 6.1. SEIM framework

Melt Ejection Mode is defined as a number of vessel failure scenarios each characterized by a specific set of modelled and stochastic parameters such as melt thermal properties, release rate, effective jet diameter, etc. Pool Characteristics are determined by the accident scenario progression and plant damage states (PDS). Steam Explosion Load analysis is performed using NRC approved 1D code TEXAS-V complemented when required by MC3D 2D calculations for resolving 2D spatial effects.

SEIM combines deterministic analysis with Monte Carlo based sampling to provide values of failure frequency which are then used to estimate conditional containment failure probabilities and failure domains as a function of model input parameters.

Description of the Melt Ejection Mode and Pool Characteristic sub-frameworks is beyond the scope of the current report. In the following, we only review the Causal Relation 3.1 used to predict containment loads in case of a steam explosion.

6.1 SEIM framework: steam explosion module

Steam explosion loads are estimated using the computationally fast polynomial model that was developed for the analysis of steam explosion in Nordic BWRs. The model combines two modules: one for the estimation of the energetics of a steam explosion and the other one for calculation of actual loads. Loads are computed using TNT-equivalent method that propagates impulses predicted in the epicenter of a steam explosion towards sensitive locations in the containment: hatch door, containment wall, and the center of the containment base.

The list and supported ranges of the model input parameters are provided in the Table 6.1. The fragility limits for structural elements in the containment were taken as constant thresholds:
- 80 kPa·s for the failure of the containment base or wall,
- 50 kPa·s for the failure of the reinforced hatch door and
- 20 kPa·s for the failure of the non-reinforced hatch door.

These values are subject to ongoing verification and yet to be confirmed. More detailed analysis of the structural fragility could be required if outcome of the risk analysis of early containment failure will turn to be sensitive to small variations in fragility thresholds.

Table 6.1: Ranges of input parameters used for generation of the database of FM solutions

#	Parameter	Units	Range		Explanation
			min	max	
1	XPW	m	5	9	Water level
2	PO	Bar	1	4	System pressure
3	TLO	K	288	368	Water temperature
4	RPARN	m	0.035	0.3	Initial jet radius
5	CP	J/kg·K	350	650	Fuel heat capacity
6	RHOP	kg/m3	7500	8500	Fuel density
7	PHEAT	J/kg	260 000	400 000	Fuel thermal conductivity
8	TMELT	K	1600	2800	Fuel melting point
9	TPIN	K	1620	3150	Melt superheat
10	UPIN	m/s	-8	-1	Melt release velocity
11	KFUEL	W/m·K	2	42	Fuel thermal conductivity
12	CFR	-	0.002	0.0027	Proportionality constant of fine fragmentation rate
13	TFRAGLIMT	ms	0.5	2.5	Fragmentation time

The model for the calculations of the explosion loads is derived from the TEXAS-V code and reproduces TEXAS-V solutions. Specifically, a model of reference Nordic BWR was implemented in TEXAS-V and used to generate an extensive database of solutions for steam explosion. This database was then used to train an Artificial Neural Network (ANN) to closely reproduce TEXAS-V predicted explosive impulses given 13 input parameters (see Table 6.1). The details of the approach, as well as, assessment of the discrepancy between TEXAS-V and the ANN can be found in [54].

Note that ANN returns a set of explosion impulses and a respective set of confidence levels that the actual impulse will not exceed the given value.

6.2 SEIM failure domain

The failure domain is constructed in the space of pre-defined input parameters (input space). Input space is partitioned into a finite number of cell, where every cell is characterized by a unique combination of input parameters ranges. Every cell is then sampled equal number of times varying deterministic and intangible parameters. The framework compares load against capacity and renders every computed case to a failure or success. Number of failed and successful cases is counted in every cell weighted by corresponding pdfs of deterministic and intangible parameters and normalized to provide the respective conditional failure frequency. The conditional failure frequency is then compared to the screening frequency to provide the outcome of the mitigation strategy for each cell. Then, cells where conditional failure frequency exceeds screening frequency are grouped into failure domain. Subdomains (cells) are color marked: green color identifies safe subdomains, i.e. those for which failure frequency is smaller than screening frequency, red signifies the opposite. Note that all data presented here is obtained

assuming 0.001 as the screening frequency unless otherwise stated.

Three modes of melt release have been addressed: 70 mm jet diameter, 140 mm jet diameter and 300 mm jet diameter. Data is provided for 3.5 bar system pressure. The failure domain is determined in the space of SEIM SM input parameters: xlo – water pool depth, UPIN – melt jet release velocity; tlo – water pool temperature.

Failure domains for 70 mm jet diameter are demonstrated in Figure 8.1.. The results suggest that given ~98% confidence level failure of the reinforced hatch door (50 kPa·s) is physically unreasonable regardless of the choice for distribution of the intangible parameters, i.e. optimistic or pessimistic.
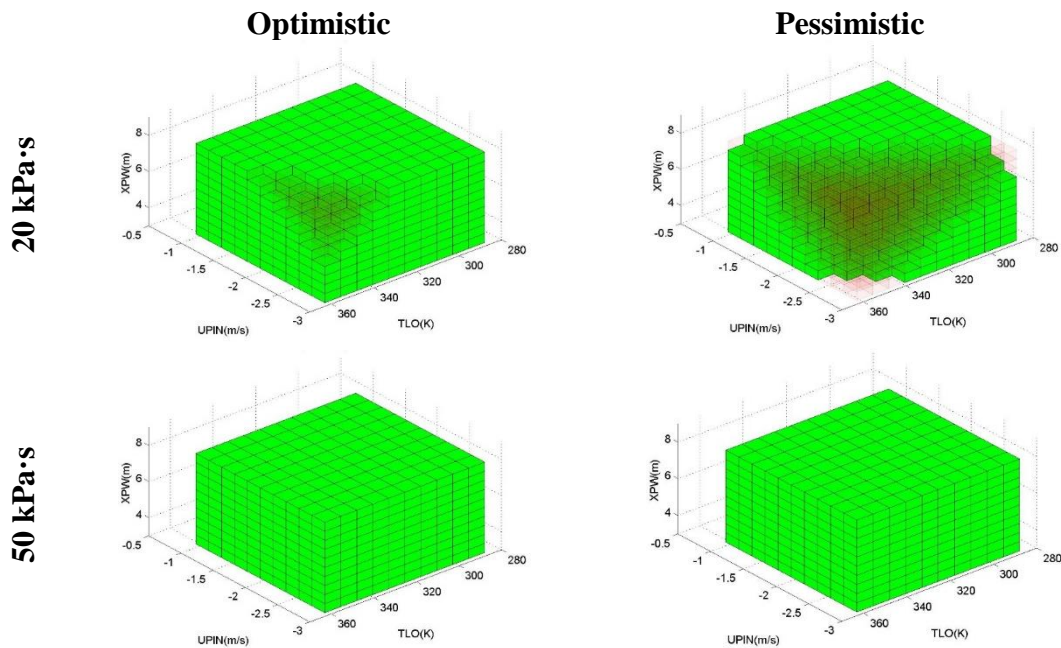
Figure 6.2. SEIM failure domain in terms of SEIM input space parameters: 70 mm jet diameter - 98% confidence level – 0.001 screening frequency – 3.5 bar system pressure.

On the other hand, failure domain of the non-reinforced hatch door (20 kPas·s) constitutes around 5-50% of the input space depending on the distribution set of the intangible The analysis suggests that for jets ≤∅70 mm failure of the Nordic BWR containment with reinforced hatch door due to steam explosion is physically unreasonable, i.e. less than 1 case out of 1000 results in explosion loads exceeding fragility limits.

Failure domains for 140 mm jet diameter are demonstrated in Figure 6.3. The results are provided given the same ~98% confidence level. According to the obtained maps only in case of optimistic considerations there is a small fraction of the input space (<10%) where frequency of failed cases stays below physically unreasonable level. In case of pessimistic assessments, this fraction is zero.

The failure domain of the reinforced hatch door occupies around 30-60% of the input space depending on the distributions of the intangible parameters. This indicates that variation of intangible parameters distribution will not resolve the associated risk but instead transition of the accident scenarios from 70 mm jets to 140 mm jets can be the key point in the SEIM risk assessments.

On the other hand, the failure domain of the pedestal is sensitive to the distribution of the intangible parameters as the fraction of the failure domain changes from almost 0 to about 20% between optimistic and pessimistic assessments. This implies that careful analysis of the distributions of the intangible parameters can help to resolve the failure of the reinforced hatch door in case of 140 mm jet diameters.
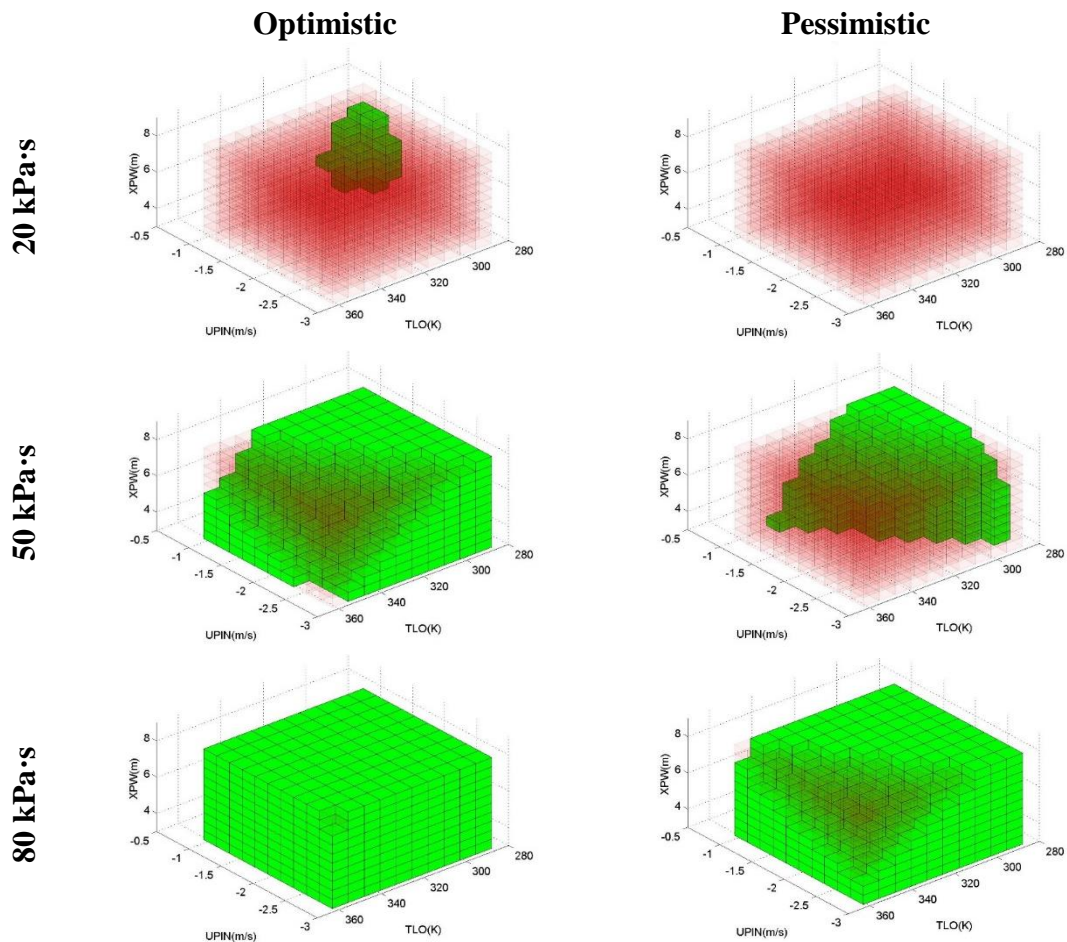
Figure 6.3. SEIM failure domain in terms of SEIM input space parameters: 140 mm jet diameter - 98% confidence level – 0.001 screening frequency – 3.5 bar system pressure.

Further investigation of the SEIM failure domain with 300 mm jet diameters has revealed that given decreased ~84% confidence level failure domain still dominates the input space. In the Figure 6.4 one can see that assuming 0.990 screening frequency the failure of the pedestal is imminent for the major part of the input space regardless assumed distributions for the intangible parameters. Resolution of scenarios with melt jets 300 mm or more is not possible and only forward analysis using complete framework can demonstrate whether these scenarios are likely to occur or not.
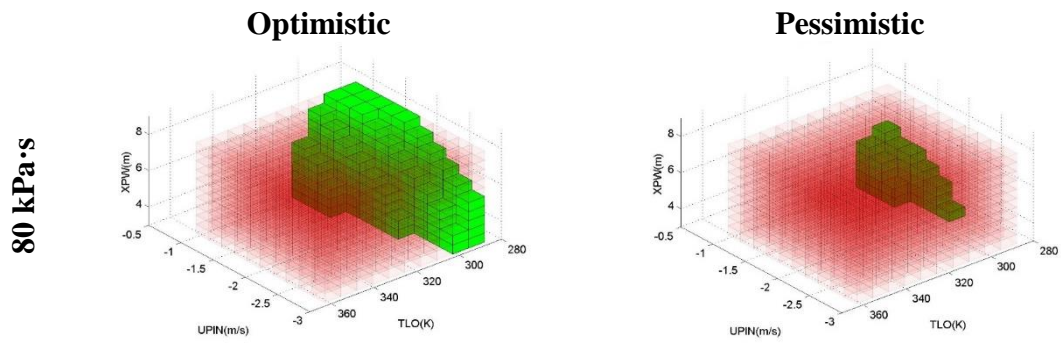
Figure 6.4. SEIM failure domain in terms of SEIM input space parameters: 300 mm jet diameter - 84% confidence level – 0.990 screening frequency – 3.5 bar system pressure.

Chapter 7.   **Ex-vessel Debris Bed Coolability**

Phenomenology of ex-vessel debris bed formation and coolability is quite complex, it includes (i) jet breakup, (ii) melt droplet sedimentation and interaction with water pool; (iii) debris agglomeration; (iv) particle spreading by pool flows; (v) debris bed self-levelling by vapor flows; (vi) debris bed coolability; (vii) post-dryout behavior with possible remelting, etc. The physical phenomena involved are closely coupled and interconnected. Debris bed cooling is provided by heat transfer to the water that enters the porous bed interior by filtration from the pool. Steam generated inside the debris bed is escaping predominantly upwards, generating two-phase convection flows in the pool and changing conditions for FCI. In turn, FCI phenomena affect particle properties (size distribution and morphology). Particle properties, packing, agglomeration and lateral redistribution affect the debris bed coolability phenomena. The large-scale circulation in the pool can spread effectively the falling corium particles over the basemat floor, distributing the sedimentation flux beyond the projection area of particle source (e.g., size of reactor vessel). Debris is gradually spread under the influence of steam production in the bed, resulting in self-leveling of the settled portion of the debris and changing the shape of debris bed with time. This can serve as an additional physical mechanism that prevents formation of tall non-coolable debris bed.

Relevant phenomena have been extensively studied in the past. Experiments (Figure 7.1.) on debris bed and particle properties (DEFOR-S) [46] debris agglomeration (DEFOR-A) [32], porous media coolability (POMECO) [47], particulate debris spreading (PDS) [48] have been carried out. A set of full and surrogate model has been developed and validated against produced experimental data for the debris formation [49], agglomeration ([50], [34]), coolability ([31]) and spreading [51] of the debris (Figure 7.1.).
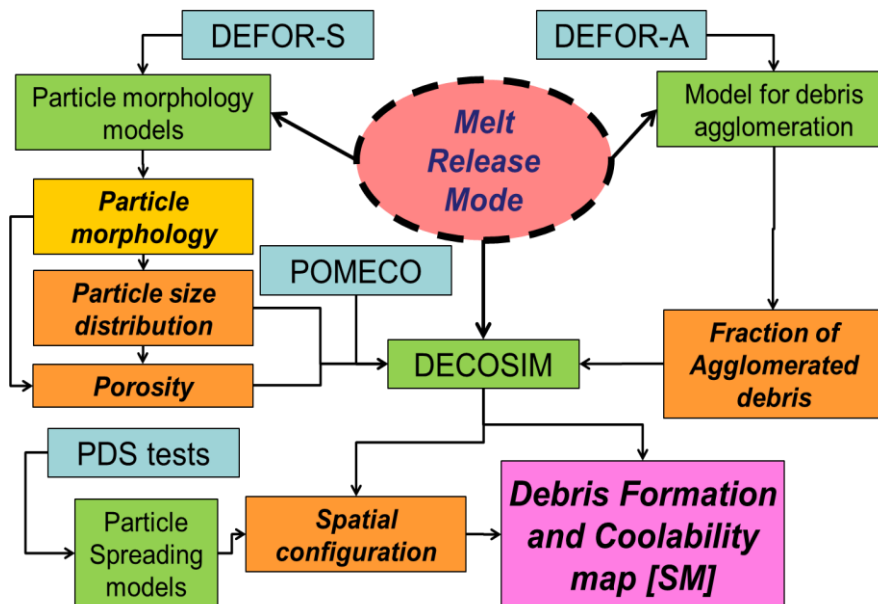
Figure 7.1. Ex-vessel debris bed formation and coolability phenomenology, experiments and code development.
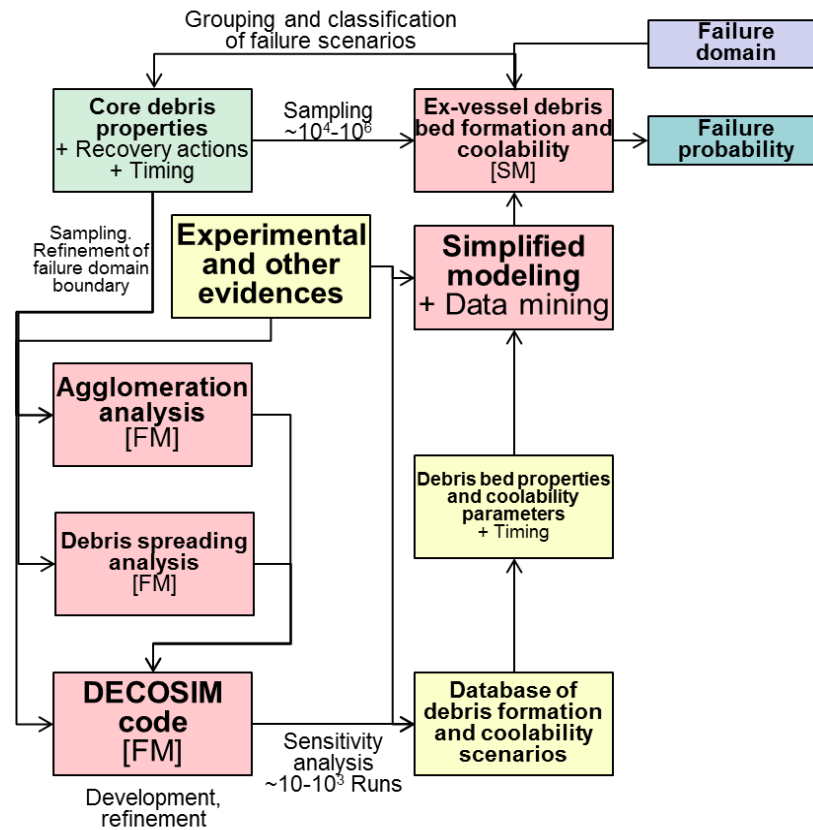
Figure 7.2. Ex-vessel debris bed formation and coolability surrogate model.

Influence of severe accident scenarios is very important for the debris bed coolability. The most important factors for coolability are scenarios of:

- Melt ejection mode (MEM):
  - Total melt mass,
  - Timing of vessel failure,
  - Duration of melt release,
  - Melt composition,
  - Melt superheat,
  - Melt jet diameter,
- Pool conditions during melt release (dependent on the operator actions):
  - Pool depth (water inventory) at time of melt release,
  - Lower drywell pool initial temperature,
  - Pool temperature in the wetwell,
  - Connection between lower drywell and wetwell.

Melt ejection mode and pool state determine the properties of the debris bed:
  - Porosity,
  - Particle size distribution,
  - Mass fraction of agglomerated debris,
  - Spatial configuration of the bed.
  –

All parameters can be assessed based on deterministic models and experimental evidences for specific melt pouring conditions.

Debris particle formation determines particle morphology (porosity) and size distribution. Both factors are very important for coolability. Debris particle formation has been addressed in DEFOR-S experiment and analytical models have been developed for prediction of particle morphology. Confirmatory tests with other binary-oxidic simulant

materials also have been carried out to confirm how sensitive experimental results are to the material properties. Data produced in the DEFOR tests can be used for validation of the models and extrapolation of the results to plant conditions.

The influence of the reference plant design specific condition (e.g. melt free fall height) on the size of the debris has to be further investigated. E.g. high speed of the melt jet at the entrance to the pool can decrease size of the debris and thus negatively affect coolability. Experiments with higher initial velocity of the jet have been carried out in DEFOR facility to clarify these concerns. No significant effect of the initial jet velocity (starting from few meters per second) was found. Therefore, no need for further development of jet breakup modeling approaches was identified.

Debris bed formation phenomena include particle packing, avalanching, and agglomeration, which, together with the distribution of mass flux of particles falling onto the pool basemat determine the shape of debris bed, an important factor for coolability. DECOSIM code has been developed for analysis of debris spreading by large scale recirculation flows in the pool and debris bed formation in the case of gradual melt release. Systematic parametric studies are necessary to build a debris bed shape map. Another factor that affects debris bed shape is "self-leveling" (self-spreading) of the debris under the influence of steam escaping the debris bed. PDS (particulate debris spreading) experimental and analytical activities are ongoing, with the aim to quantify the time scale of debris bed self-spreading and to compare it with the characteristic times for reaching dryout, temperature escalation and, possibly, remelting of the debris in the cases where vapor cooling is insufficient to stabilize the dry zone temperature.

Agglomeration of the debris has been demonstrated in analysis and experiments as a negative factor for coolability. Confirmatory DEFOR-A tests with different simulant materials have been carried out for validation of methods and tools developed for prediction of agglomeration.

Prediction of the debris bed coolability is the ultimate goal. Experimental data has been produced for validation of the codes and models against following phenomena: (i) effect of the debris bed spatial configuration on the debris bed coolability; (ii) effect of the prototypical debris bed morphology and size distribution on the pressure drop and dryout heat flux. DECOSIM code is used to quantify debris bed coolability in different debris bed configurations and scenarios, and to create a surrogate model for the bed coolability map, taking into account uncertainties in: (i) properties of the debris bed; (ii) modeling uncertainties in the porous media flow models [20].

Chapter 8.   Preliminary Analysis Results using ROAAM+ Framework

8.1 Preliminary Analysis Results using ROAAM+ Framework

The goal of this section is to illustrate comprehensive uncertainty analysis for identification and clarification of (i) main contributors to the uncertainty and risk; (ii) importance of the dependencies between different accident stages in different accident progression scenarios; (iii) the needs for further refinement of the knowledge and tools (models, experimental data, etc.)

We discuss key elements of the reverse analysis with the failure domain (FD) identification and forward analysis with estimation of failure probability (FP) for ex-vessel steam explosion and coolability.

8.1.1 Description of the framework

The surrogate models implemented in the framework (see Figure 2.3) and their role is detailed in the Table 8.1. Four techniques were used for implementation of the SMs: (i) mapping (based on mapping of the FM solution to a grid in the space of the input parameters); (ii) polynomial (scaling analysis and data fitting); (iii) physics based uses simplified modelling of the phenomena; (iv) Artificial Neural Networks (ANN is based on complex regression analysis). Failure criteria are determined for SEIM and DECO.

Table 8.1: Surrogate models of the ROAAM+ framework

SM	Type	Role
CORE	Mapping	Given timings of ADS and ECCS recovery provides time, composition and mass of core relocation and conditions in the lower drywall: pressure, pool temperature and depth
Vessel failure	Polynomial	Given mass and composition of the debris in the lower head computes timings of the IGT, CRGT and vessel failures and corresponding mass and composition of liquid melt available for release
Melt release	Physics based	Given timings and mode of lower head failure computes conditions of melt release, i.e. ablation of the breach, rate and duration of the release, thermal properties of the melt
SEIM	ANN	Given conditions of melt release and LDW characteristics, returns three explosion impulses and three values of containment capacity
DECO	Physics based	Given conditions of melt release and LDW characteristics, returns dryout heat flux and max debris bed heat flux

At given melt release conditions SEIM surrogate model estimates characterizes loads by mean and standard deviation of the explosion impulses predicted by TEXAS-V for different triggering times. Different confidence levels are used: mean value (in ~50% cases the impulse will be lower); mean plus standard deviation (in ~84% cases the impulse will be lower); mean plus two standard deviations (in ~98% cases the impulse will be lower). The SEIM failure domain is determined for three fragility limits: 20, 50 and 80

kPa·s. These roughly correspond to the order of magnitudes of fragility limits for non-reinforced hatch door, reinforced hatch door and reactor vessel pedestal respectively. Current implementation of DECO is a combination of two surrogate models: (i) spreading of particles during sedimentation in the pool which estimates the slope angle of the formed debris bed; (ii) debris bed coolability (returning actual and critical heat flux for given debris bed configuration).

Forward and reverse analysis (see Figure 2.3, Chapter 2.2) is currently performed by considering two distributions (optimistic and pessimistic) for the intangible parameters. Optimistic distribution is determined such that it decreases the probability of high loads. Pessimistic distribution decreases probability of low loads.

The failure domain is constructed in the space of the input parameters (input space) partitioned into a finite number of cells. Every cell is characterized by a unique combination of the input parameters ranges. The output of the SM is sampled in each cell (by varying deterministic and intangible parameters). The framework compares loads against capacity and renders every computed case to a failure or success. The number of "fail" and "success" cases is counted in each cell, weighted by corresponding probability density functions of deterministic and intangible parameters and normalized to provide conditional failure probability which is compared to the screening probability. The cells where conditional failure probability exceed screening level are grouped into a "failure domain" indicating conditions at which the mitigation strategy fails. For visualization green color identifies "safe" domain and red signifies the opposite. Note that all data presented here is obtained assuming 0.001 as the screening probability unless otherwise is explicitly stated.

8.1.2 Reverse Analysis for Steam Explosion using SEIM Surrogate Model

Three scenarios of melt release have been considered: 70, 140 and 300 mm jet diameters. System pressure was fixed to 3.5 bar. The failure domain is determined in the space of the SEIM input parameters: xlo – water pool depth, UPIN – melt jet release velocity; tlo – water pool temperature. The results for 70 mm jet diameter suggest that reaching to 50 kPa·s load, equivalent to failure of the reinforced hatch door and stronger containment structures is physically unreasonable with ~98% confidence regardless of the choice of the intangible parameters distributions. The failure domain for 20 kPa·s (non-reinforced hatch door) constitutes around 5-50% of the input space depending on the pessimistic/optimistic distributions of the intangible parameters (Figure 8.1.).

Failure domains for 140 mm jet diameter are presented in Figure 8.2.. The results are provided for ~98% confidence level and suggest that only in case of optimistic assumptions there is a small fraction of the input space (<10%) where probability of failure at 20 kPa·s is below physically unreasonable level. In case of pessimistic assumptions, this fraction is zero. The failure domain for 50 kPa·s criterion (reinforced door) occupies around 30-60% of the input space depending on the distributions of the intangible parameters. This indicates that transition form 70 to 140 mm jets is more important for the failure probability than different distributions of the intangible parameters.

<div align="center">

Optimistic   **Pessimistic**

</div>
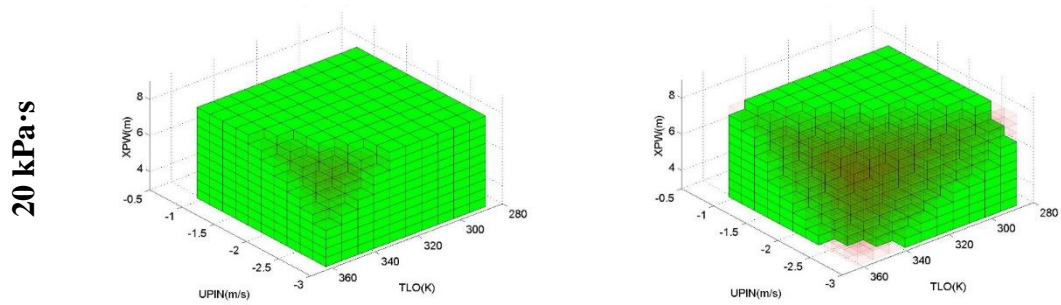
Figure 8.1. Failure domain for 20 kPa·s in the SEIM input space parameters. Jet diameter 70 mm; confidence 98%; screening probability 0.001.
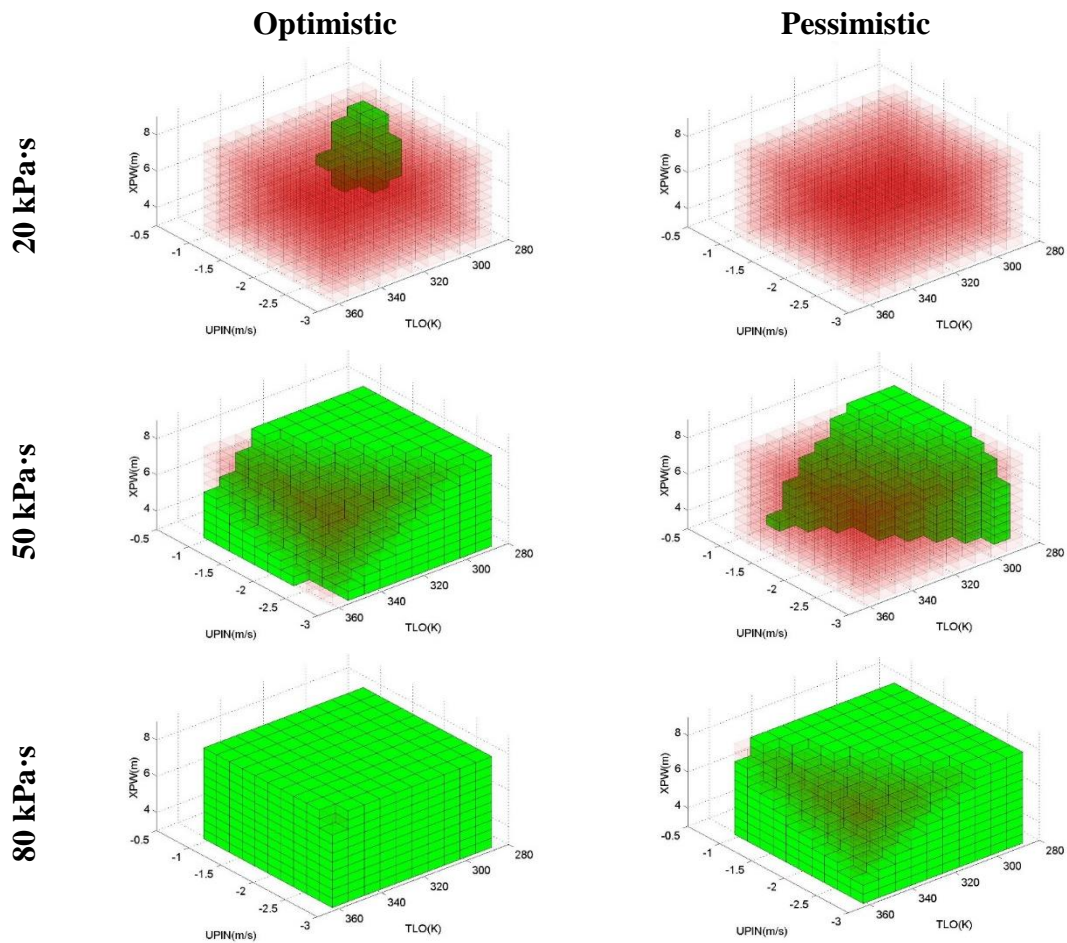
Figure 8.2. Failure domain in the SEIM input parameter space. Jet diameter 140 mm; confidence level 98%; screening probability 0.001.

The failure domain at 80 kPa·s (pedestal) is more sensitive to the distribution of the intangible parameters (optimistic/pessimistic) and can change from almost 0 to about 20%. Thus obtaining knowledge on the distributions of the intangible parameters can help to reduce uncertainty in the pedestal failure in scenarios with 140 mm diameter jet. It is instructive to note that for 0.99 screening probability (almost imminent failure) the failure domain of the reinforced hatch door (Figure 8.3.) still occupies about 20% of the input space.

Pessimistic
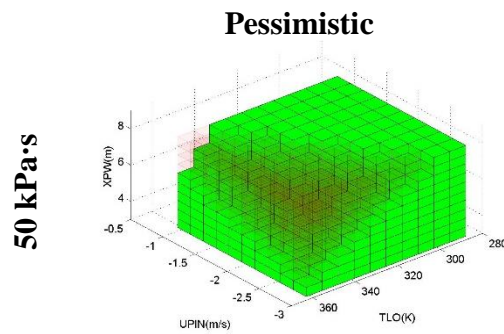
Figure 8.3. SEIM failure domain in terms of SEIM input space parameters. Jet diameter 140 mm; confidence level 98%; screening probability 0.99.

For 300 mm jet diameter, the failure of the pedestal is imminent for the major part of the input space regardless of the assumptions about distributions for the intangible parameters even with decreased (~84%) confidence level (Figure 8.4.). This means that forward analysis using complete framework is necessary in order to assess whether such scenarios of melt release are possible.

In general the failure domain is growing if the jet diameter, water pool depth, or water temperature or the jet release velocity are increased. The major effect is still due to the jet diameter.

Optimistic **Pessimistic**
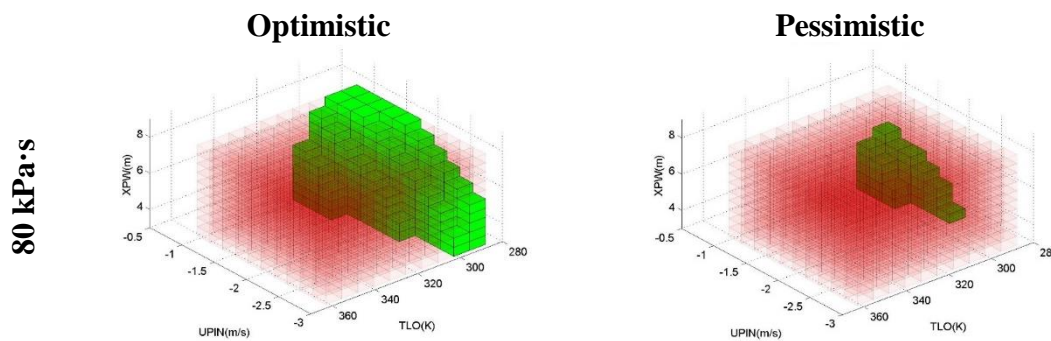
Figure 8.4. SEIM failure domain in terms of SEIM input space parameters. Jet diameter 300 mm; confidence level 84%; screening probability 0.99.

8.1.3 Reverse Analysis for Steam Explosion using the Whole Framework

The failure domain was determined in the space of CORE SM input parameters, i.e. ADS and ECCS activation times. The results are provided in the Figure 8.5.

Clearly the failure domain is large and only a small safety domain exists. The first reason is that LDW conditions are dominated by deep (>6.6 m) water pools (see Figure 8.6.). The water pool depth can be changed in the mitigation strategy. However, reduction of the pool depth will lead to increased risk of agglomeration. The second reason is scenarios of melt release are dominated by cases with melt velocities exceeding 5 m/s. This shifts the input space of SEIM parameters towards SEIM failure domain leaving only jet diameter as a parameter that defines the failure domain in the input space of CORE SM (Figure 8.7.).
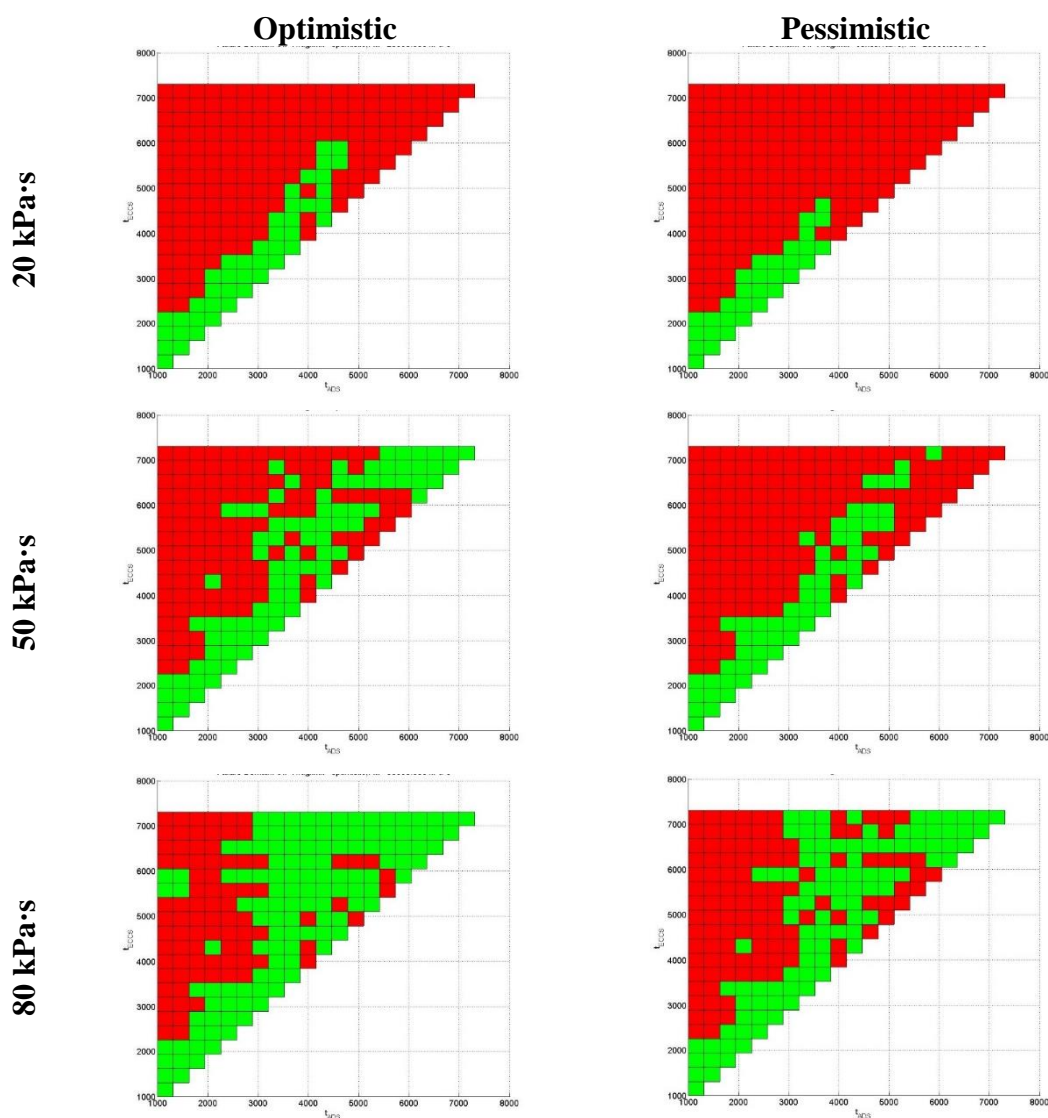
Figure 8.5. SEIM failure domain in terms of CORE input space parameters (ADS,ECCS recovery time(sec)). Confidence level 98%; screening probability 0.001.

Water level, m   Water temperature, K   LDW pressure, Bar
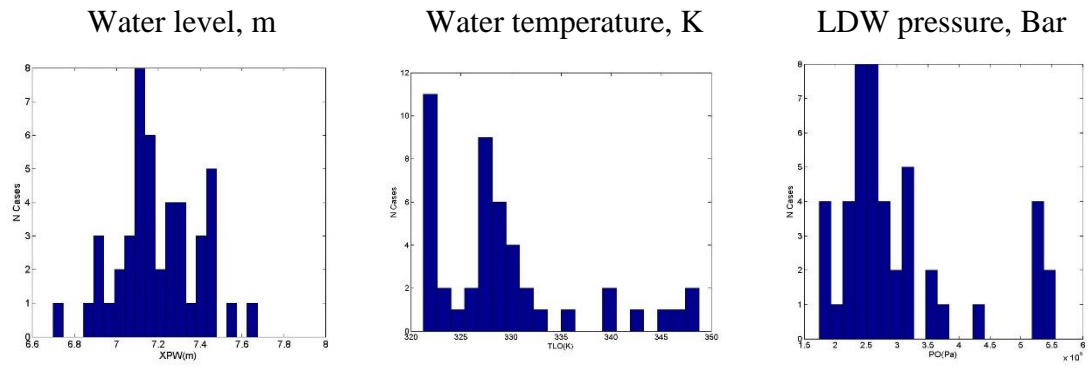
Figure 8.6. LDW pool characteristics.

Jet radius, m   Melt release velocity, m/s
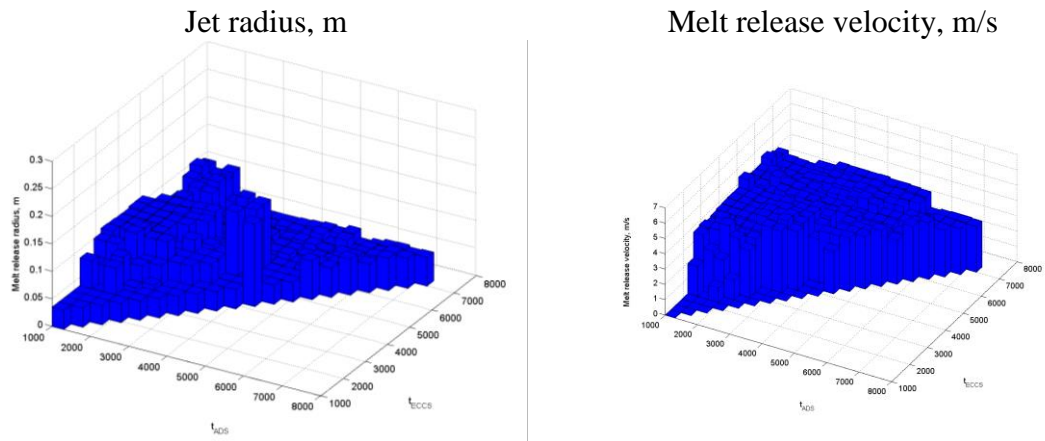
Figure 8.7. Melt jet release characteristics.

8.1.4 Revere and Forward analysis for Debris Bed Coolability with and without Consideration of the Particle Spreading in the Pool

The DECO failure probability was determined using following assumptions: constant debris bed porosity 40%; two distributions for the debris bed particles: "pessimistic" (1-1.5 mm) and optimistic (1-3 mm); and two ranges with uniform distribution of the initial debris bed angle: 0-35°, 0-20°. It was identified that failure domain is sensitive to the debris bed angle and particle size distribution (Figure 8.8.).
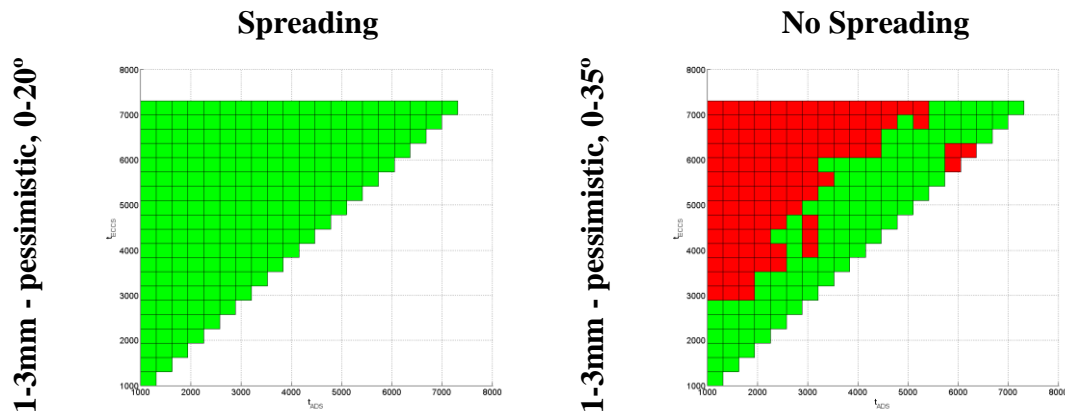
Figure 8.8. DECO failure domain in terms of CORE input space parameters (ADS, ECCS recovery time (sec)). screening probability 0.001.

A surrogate model for debris bed formation in the gradual melt release mode was developed and verified against DECOSIM simulations. Significant (1-2 order of magnitude) reduction in dryout probability was demonstrated (see Table 8.2 and Figure 8.8.) when particle spreading in the process of debris bed formation is taken into account. Reason for that is demonstrated in Figure 8.9.. Specifically, tall debris beds cannot be formed with small particles. DECO SM with integrated model of particle spreading predicts very small failure domain and failure probabilities. Further validation of particle spreading model is necessary against PDS-P experiments and DECOSIM simulations. In addition, extension of the debris bed formation model to subcooled water pool (delayed onset of boiling, less efficient particle spreading) and massive releases (short interaction time, collective effects due to high concentration of particles) are necessary.

Table 8.2: Effect of particle convective spreading on the dryout probability

Slope angle distribution	Pool depth, [m]	Conditional dryout probability, [%]
Uniform, 0°-35°	8	19.3
Surrogate model	8	0.13
Uniform, 0°-20°	5	7.1
Surrogate model	5	0.33
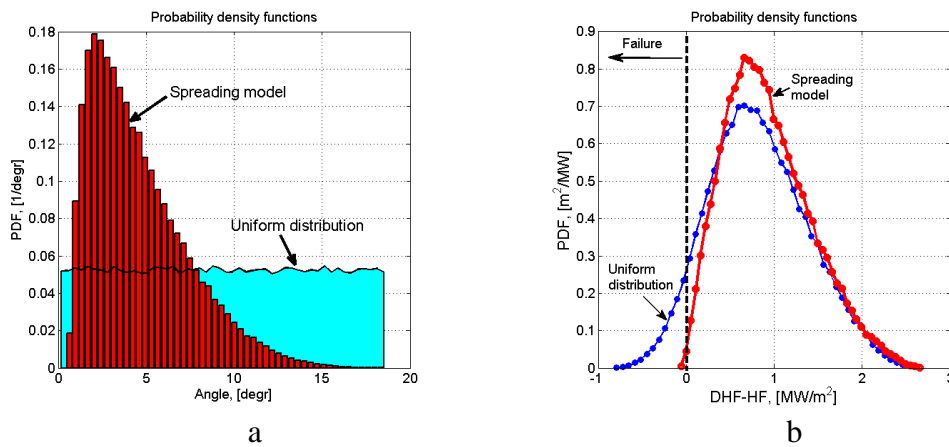
Figure 8.9. Probability density functions of the debris slope angle (a) and capacity minus load for debris coolability (b).

8.1.5 Summary of the Preliminary Risk Analysis Results

The main purpose of the preliminary results is to demonstrate how ROAAM+ approach can help to understand the importance of different factors based on simultaneous consideration of scenario (aleatory) and epistemic (modeling) uncertainties. ROAAM+ framework can clarify importance of different (optimistic/pessimistic) assumptions and models from risk perspective and suggest areas were research efforts would provide most effective reduction of the uncertainty. For instance, steam explosion failure domain is determined mostly by two parameters of melt release: jet diameter and initial velocity. This means that a better knowledge is necessary for the vessel failure and melt release phenomena, such as remelting of multi-component debris, filtration of liquid melt through porous debris bed and ablation/plugging of the vessel breach.

Debris bed coolability analysis demonstrated that convective spreading of particles in the pool is one of the most influential limiting mechanisms against formation of a tall non-coolable debris bed. Therefore, improved modelling of convective particle spreading in the pool is necessary to carry out robust risk analysis. Another important issue of the debris bed coolability, yet, to be included in the framework is debris agglomeration.
Current version of the surrogate models (SM) have different degrees of maturity need further verification and validation based on the in-depth evaluation of the preliminary results. Quantitative preliminary data might change in the iterative process of model refinement. Further development of ROAAM+ framework and tools for post-processing and presenting results of the risk analysis are necessary.

8.2 Data Post Processing and Characterization of Failure Domains in ROAAM+ framework

In chapter 0 it has been mentioned that decision tree approach can be used for characterization of the failure domains and visualization of the results similar to decision making process [36].

In this section we illustrate how proposed methodology can be applied in presentation of ROAAM + framework results.

8.2.1 Characterization of the failure domain for Debris Bed Coolability (DECO)

To illustrate failure domain characterization using decision tree approach for debris bed coolability we considered the following case:

- DECO SM with no spreading

- Uniform distribution of debris bed angle between 0 and 30 degrees.

- Uniform distribution of particle size between 1 and 3.5mm.
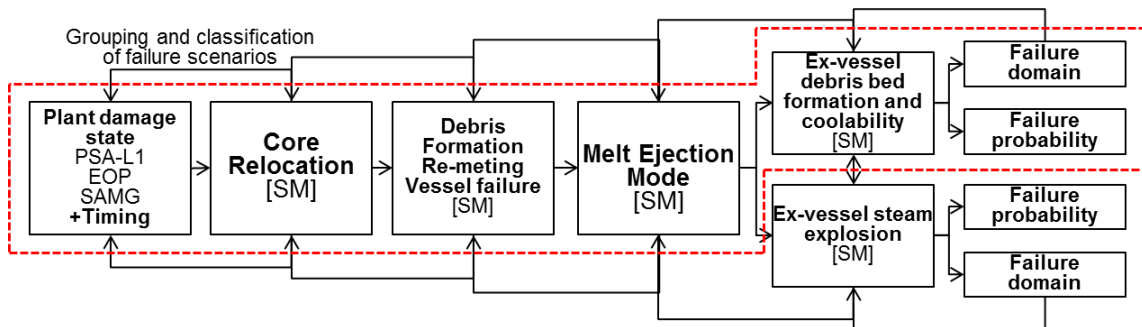
Figure 8.10. ROAAM+ Framework Nordic BWR (DECO Failure domain)
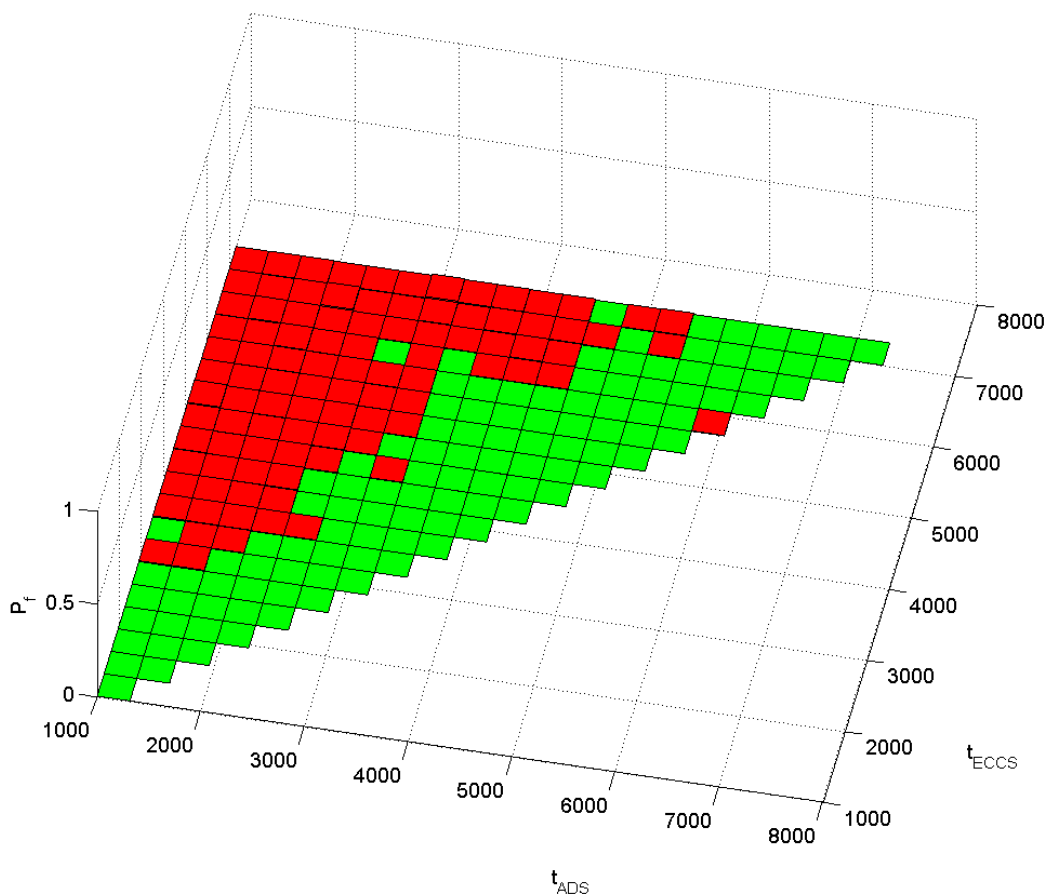
Figure 8.11. DECO failure domain in terms of CORE input space parameters (ADS,ECCS recovery time (sec)). screening probability 0.001.

ROAAM+ framework analysis gives the following failure domain as a function of CORE SM input parameters (see Figure 8.10): ADS (system 314) time delay, ECCS (system

53

323) time delay – which form accident scenario space.

Failure domain in Figure 8.11 can be represented in form of decision tree as a set of final nodes and decision rules that lead to these nodes.

Each final node in decision tree (see Figure 8.12) represents some specific area of scenario space and it is characterized by a set of decision rules that lead to this space. For example in Figure 8.13 – node j = 1 represent the area of input space where ADS and ECCS activation time is below 2890 seconds (which represents first decision rule (cut) in decision tree "ECCS<2890"), scenarios located in this area represent 10% of the total scenario space for selected PDS.
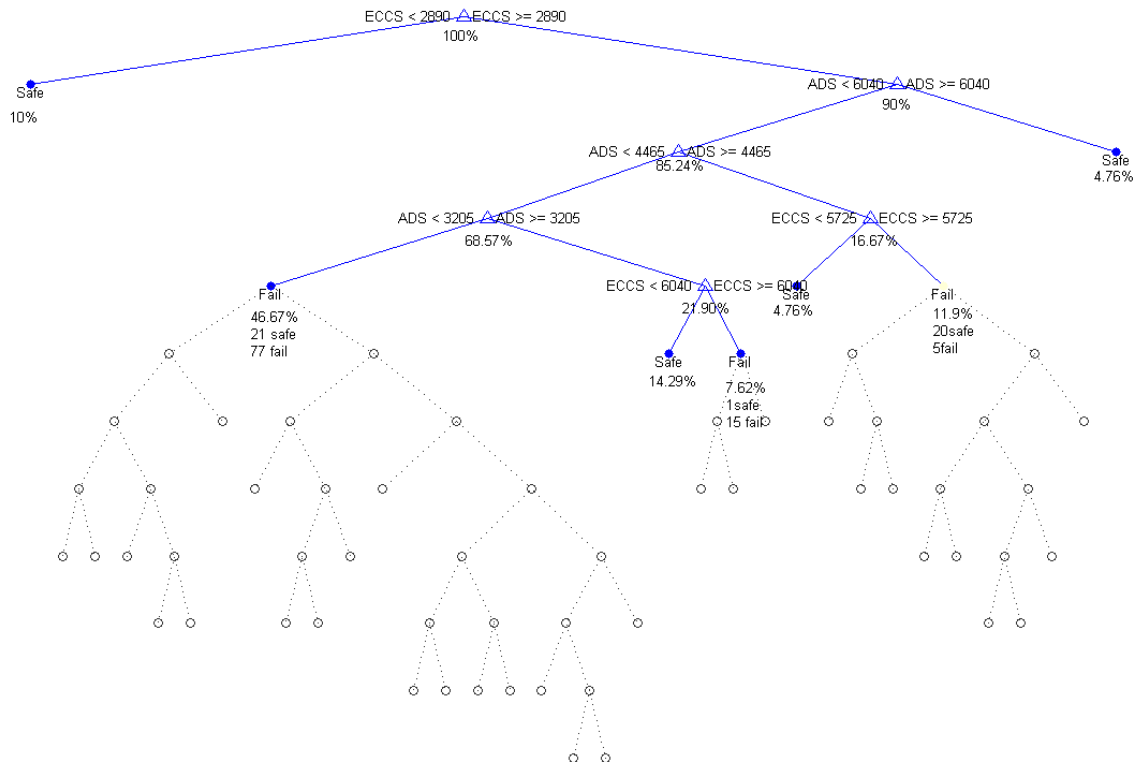
Figure 8.12. DECO failure domain in terms of CORE input space parameters (ADS, ECCS recovery time (sec)). Decision Tree representation.

The conditional containment failure probability for each node can be obtained as follows

$$P_{f(node)} = \sum_{i=1}^{k_j} p_{f_i} \xi_i \qquad (8.1)$$

where p_{f_i} - is probability of failure of cell i in node j, ξ_i - probability of cell (scenario) i in node j, k_j - total amount of cells in node j.
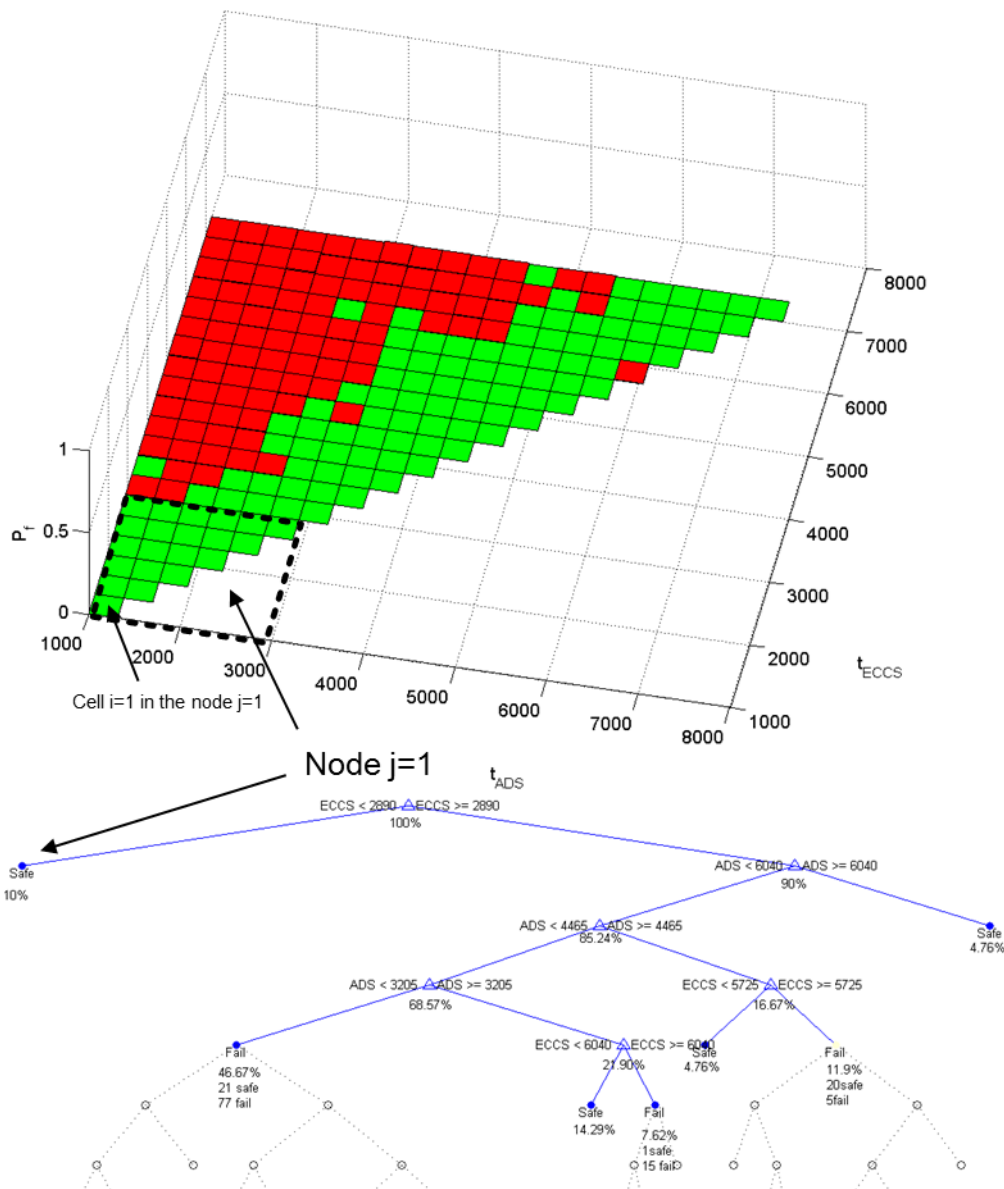
Figure 8.13. DECO failure domain in terms of CORE input space parameters (ADS,ECCS recovery time (sec)). Decision Tree representation.

If we assume uniform distribution of scenarios in our scenario space it is possible to obtain conditional containment failure probability for each node in the decision tree (Table 8.3). The results presented in the Table 8.3 indicate that total conditional containment failure probability due to debris bed coolability for selected PDS, assuming uniform distribution of scenarios in scenario space (i.e. recovery time of ADS and ECCS is uniformly distributed between $0 - 7300$ sec) equals $P_f = 2.277264e - 3$. We can also observe that the highest contribution to conditional containment failure probability is given by scenarios with early ADS activation and late ECCS water injection. Table 8.3 can be represented in form of block diagram to provide better understanding of the results.

Table 8.3: DECO Failure domain characterization

ADS(sec)	ECCS(sec)	%data	$P_{f(node)}$	FLAG
[0,2890]	[0,2890]	0,1	0	safe
[0,1945]	[2890,3520]	0,028571	7.3852e-5	fail
[1945,3205]	[2890,3520]	0,038095	0	safe
[0,3205]	[3520,7300]	0,4	1.80471e-3	fail
[3205,4465]	[2890,6040]	0,142857	0	safe
[3205,4465]	[6040,7300]	0,07619	3.19099e-4	fail
[4465,6040]	[2890,5725]	0,047619	0	safe
[4465,5725]	[5725,6670]	0,057143	0	safe
[5725,6040]	[5725,6670]	0,014286	1.1521e-5	fail
[4465,5410]	[6670,7300]	0,028571	6.8072e-5	fail
[5410,6040]	[6670,7300]	0,019048	0	safe
[6040,7300]	[6040,7300]	0,047619	0	safe
TOTAL			2.277264e-3	
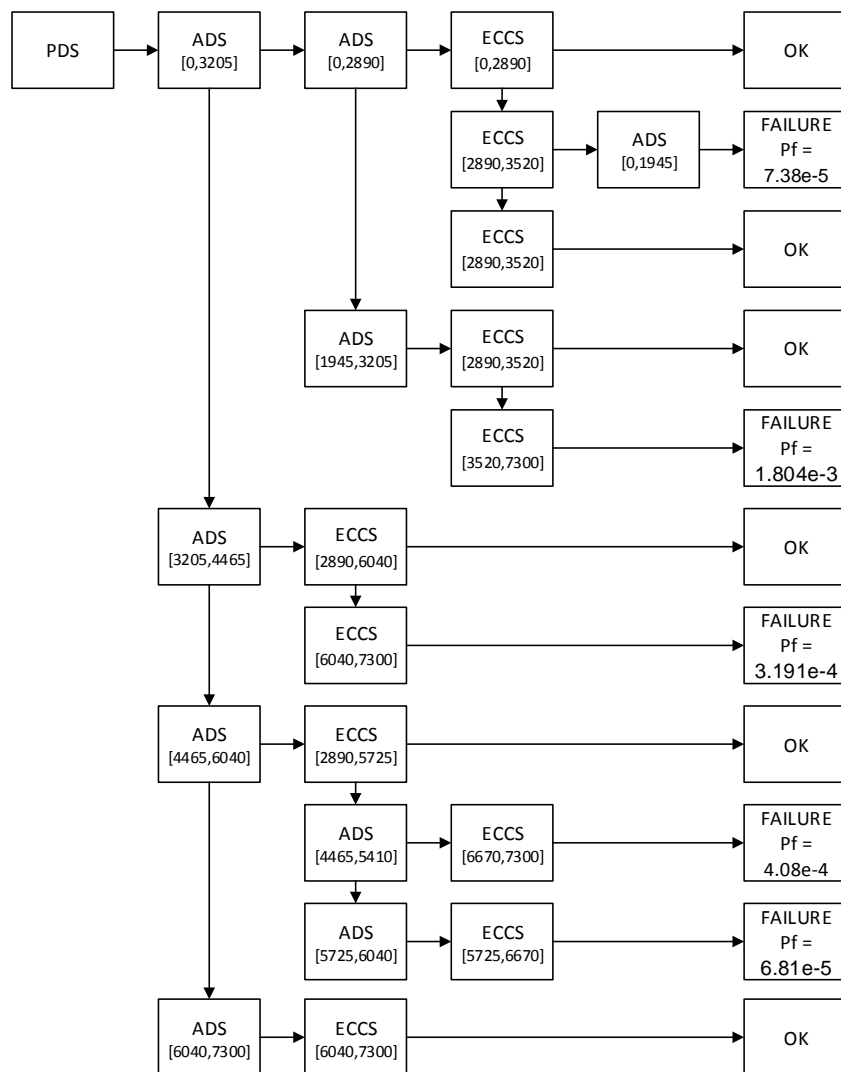
Figure 8.14. DECO failure domain in terms of CORE input space parameters (ADS, ECCS recovery time (sec)). Block-Diagram representation.

8.2.2 Characterization of the failure domain for Ex-Vessel Steam Explosion (SEIM)

Decision tree approach has been also used for characterization of SEIM failure domain in terms of CORE SM input space parameters (see Figure 8.15).
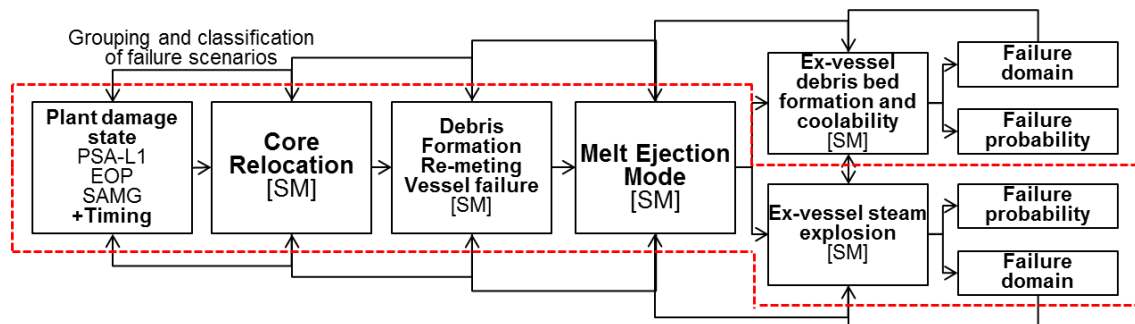
Figure 8.15. ROAAM+ Framework Nordic BWR (SEIM Failure domain)

We considered failure domain for reinforced hatch door that can withstand 50kPa impulse for the analysis (see Chapter 6 for details):
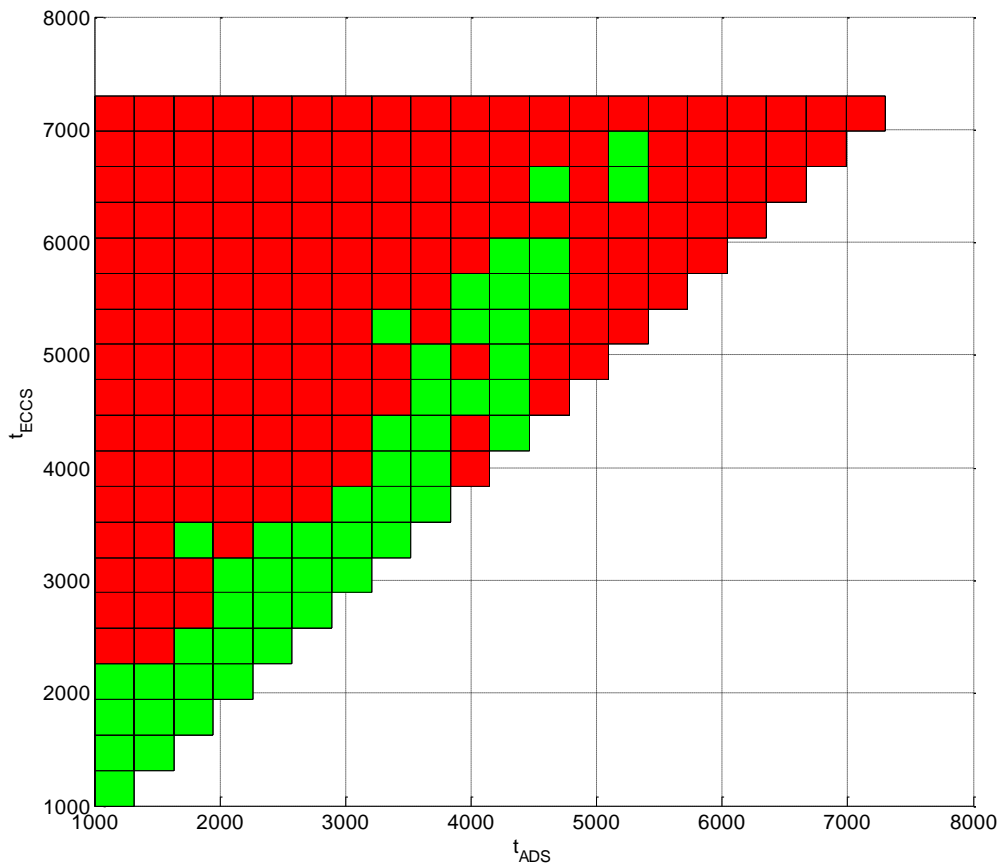
Figure 8.16. SEIM failure domain in terms of CORE input space parameters (ADS,ECCS recovery time(sec)). Confidence level 98%; screening probability 0.001.

Figure 8.17 represents decision tree representation of the failure domain represented in the Figure 8.16.
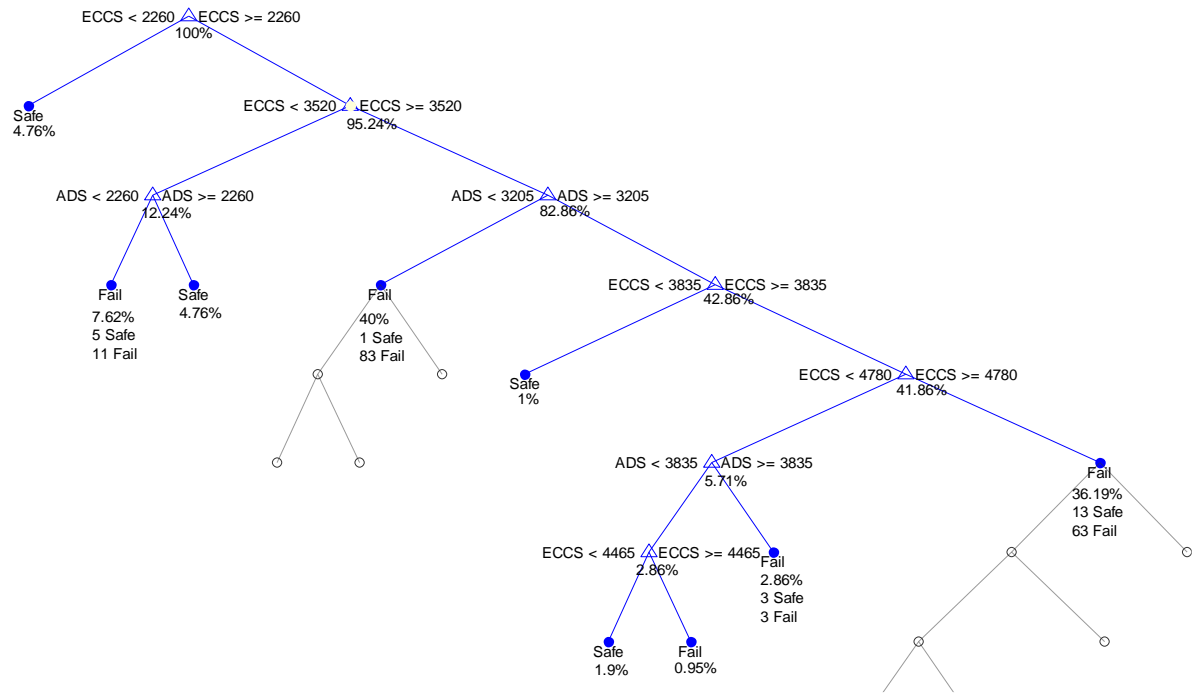
Figure 8.17. SEIM failure domain in terms of CORE input space parameters (ADS, ECCS recovery time (sec)). Decision Tree representation.

The conditional containment failure probability for each node has been calculated using equation (8.1), assuming uniform distribution of scenarios in our scenario space. The results of these calculations together with nodes information extracted from decision trees are presented in Table 8.4.

Table 8.4: SEIM Failure domain characterization

ADS(sec)	ECCS(sec)	%data	$P_{f(node)}$	FLAG
[0,2260]	[0,2260]	0.0476	0	safe
[0,2260]	[2260,3520]	0.0762	0.0517	fail
[2260,3520]	[3205,3835]	0.0476	0	safe
[0,3205]	[3520,3835]	0.4	0.395	fail
[3205,4465]	[2890,6040]	0.01	0	safe
[3205,3835]	[4462,4780]	0.0095	7.02801e-4	fail
[3835,7300]	[3835,4780]	0.0286	0.0142	fail
[3205,7300]	[4780,7300]	0.3619	0.295	fail
TOTAL			0.757	

Results presented in Table 8.4 indicate the highest contribution to conditional containment failure probability is given by early ADS and late ECCS scenarios. The total cumulative conditional containment failure probability for selected PDS equals $P_f = 0.757$.

Chapter 9. PSA-L2 Modifications based on IDPSA results.

9.1 Methodological enhancement – DSA and PSA integration

The results from the study are very interesting from a methodological point of view. It has been shown that a decision tree is a viable way of presenting the output of the DSA analysis. The question is; how can this data be used in a PSA context?

The gains in the PSA using the information from the IDPSA are at least;
- Improved sequence definitions when phenomena can be relevant (improved PDS definitions and the sequences in the containment event tree)
- Estimation of probabilities for phenomena
- Improved knowledge of timing in sequences (see also bullet 1 above) which can be the base for better PSA quantification

9.1.1 Improved Sequence Definitions

The binning of accident sequences from PSA level 1 into plant damage states as well as the modelling of accident progression scenarios in PSA level 2 are based on factors such as type of initiating event, time from initiating event and pressure in the reactor. These factors, attributes, are normally based on a finite amount of analyses, where engineering judgements are necessary. An IDPSA approach can provide valuable information regarding these factors and influence the definition of sequences in PSA, since the IDPSA approach is informed by significantly more calculations. Several key elements in the level 2 sequences and phenomena handling and their boundaries can be analyzed at each stage of the modelling of accident progression via for example a reverse analysis in the ROAAM+.

One example that have been studied with reverse analysis in the ROAAM+ approach is recovery of emergency cooling system (ECCS) and ADS. These safety systems have, for some reason, failed during PSA level 1 and a possibility of system recovery to avoid more severe consequences is modelled in PSA level 2. A successful recovery early in the sequence would allow the core to be arrested in the reactor pressure vessel (RPV) and hence provide the best possibility to limit the releases.

To arrest the core in the RPV based on the assumption that coolability is <u>possible</u> given successful recovery of the ECCS and ADS. Low pressure scenarios with activated re-flooding can for example be considered successful if it is activated within three hours after core melt. This modelling is supported by a few MAAP analyses.

The human reliability analysis regarding recovery actions is based on the available time for the operator action. It can be noted that the dominating sequences for loss of feedwater from PSA level 1 are due to loss of external power supply and failure of back-up power systems. The time for possibility of manual recovery of back-up power systems and the time for possibility of return of of-site power are therefore very important for the quantitative results.

The result of the reverse analysis using the ROAAM+ approach is graphically shown in the decision tree indicates the "safe" timespans, i.e. recovery of ECCS and ADS leads to coolability of the debris, and "failed" timespans, i.e. even with recovery there is a

possibility that the debris may not be coolable. The reverse analysis using the ROAAM+ approach indicates that the current assumptions regarding available time for recovery needs to be updated, since the successful states in the IDPSA indicates that the systems needs to be activated earlier to ensure a successful cooling.

It can be noticed that the "safe" state in the decision tree is given based on a threshold. Safe means, in the ROAAM+ approach, that the conditional failure probability for debris coolability is lower than 1E-3, which indicates in the arbitrary scale of probability a "physically unreasonable" level of likelihood (see Section 2.3).

When likelihoods used in ROAAM+ are translated into PSA probabilities, the arbitrary scale of probability should be applied in reverse in order to achieve the same meaning between "physically unreasonable" level in ROAAM and screening frequency in PSA. For instance, it should be evaluated in a continued project if 1E-3 probability threshold in ROAAM+ should be translated into PSA as 1E-4 of conditional frequency. The reason is that a threshold should preferably be set so that the conditional probability would be insignificant with regard to the target value (frequency of <1E-7 for releases).

The target value for PSA Level 1 is often set as 1E-5. A conditional failure probability for level 2 less than 1E-4 would hence fulfil the condition to be insignificant (two orders of magnitude below the acceptable threshold). This means that all "safe" scenarios can be disregarded in the PSA if 1E-4 is used as a threshold value in the analysis. This is identified as a future update and development of the connection between reverse analysis and PSA.

The studied example provides a possibility to identify how timing of the recoveries affects the possibility to obtain coolability. The results can be used to improve sequence definition in several ways:

- Give more accurate and refined definition of available times for different operating actions and thus provide a better basis material for the HRA.

- Identify the sequences where the debris may not be coolable after re-flooding.

- Provide failure probabilities for the identified sequences. Coolability may need to be modelled with a failure probability that is dependent on the timing of the sequence. Time dependent failure probabilities can be considered since the plant damage states are binned with time after initiating event as one factor. The binning of the plant damage states may therefore be updated with regards to the findings from the deterministic analysis.

The inverse ROAAM+ approach has, in addition to the coolability, also provided very interesting preliminary results for the treatment of phenomena in the sequence following melt through. To make full use of the results, more understanding is needed on the factors that is causing the situations that are described by the inverse analysis, for example: What type of sequences (from start) are causing a melt through above a certain size? This is an area where further work is needed.

9.1.2 Estimation of Probabilities of Phenomena and Consequences

In addition to a better understanding of the sequences and their causes, it has to be recognized that we will neither have full understanding nor the possibility to represent all possible realistic situations in a risk analysis. Hence it will also be of vital importance that, in addition to a better representation of the sequences, we improve our ability to estimate the probability that a certain phenomenon with risk significant consequences can

occur.

The analysis of physical phenomena requires extensive understanding of complex interactions and feedbacks between scenarios of accident progression and phenomenological processes. Physical phenomena are of high importance for the PSA level 2 results since they influence the severity of the consequences.

The analysis includes identification of relevant phenomena, identification of relevant sequences where phenomena can occur as well as estimating the probability of the phenomena. The available data for phenomena is often based on scarce data, which typically leads to conservative assumptions. Better support and basis material for the analysis of probabilities for phenomena, given conditions of scenario, would therefore increase the level of accuracy and credibility substantially.

The backwards analysis with ROAAM+ provides insights regarding under what conditions each phenomenon is relevant. The backward analysis regarding steam explosion, for instance, provides information regarding at what conditions a steam explosion can give consequences of risk significance. This may be used as one input to the quantification of probabilities of phenomena with certain consequences since the ratio of "failed" sequences may be used.

The estimation of other level 2 related failure probabilities such as recovery actions can also be refined by the results of the reverse analysis, see discussion in section 9.1.1.

9.1.3 Improved Knowledge of Timing in Sequences

From the PSA, cut set lists are produced (or rather minimal cut set lists). In most PSA tools, like RiskSpectrum® PSA, the same approach is used also for PSA Level 2. There are other methods to perform the PSA Level 2 calculations, which e.g. is the situation in FinPSA. The discussion in this section is focusing on the MCS approach, as used in RiskSpectrum PSA, and how this can be improved by including information from the decision trees developed within the DSA.

Let us assume that we have an MCS list. This list will include basic events representing phenomena (as well as component failures and human actions – but these are not of interest in this context). These phenomena are treated as individual events – and there is no information on timing. Now, let us assume that we have the decision tree as presented in section 4.2.

The combination of the MCS list, and the information in the decision tree could be merged. Figure 9.1 is presenting the conceptual idea, assuming that the event in the MCS list can have different probability (different mission time) in different sequences driven by the decision tree.

Top Event frequency F = 5,558E-03

No	Probability	%	Event 1	Event 2	Event 3	Event 4	Event 5
1	5.00E-03	89.97	nE-LMFW	DPS-MAN--H			
2	6.04E-05	01.09	nE-LMFW	CCF-SWS-PM---A-ALL			
3	6.04E-05	01.09	nE-LMFW	CCF-CCW-PM---A-ALL			
4	5.04E-05	00.91	nE-LMFW	CCF-SWS-PM---D-ALL			
5	3.61E-05	00.65	nE-LOOP	ACP-GT01-M	RHR-TR01-M		
6	2.10E-05	00.38	nE-LMFW	CCF-DPS-VS---A-ALL			
7	1.72E-05	00.31	nE-LOOP	ACP-GT01-M	RHR-PM01-D		
8	1.47E-05	00.26	nE-LOOP	ACP-DG01-A	ACP-GT01-M		
9	1.26E-05	00.23	nE-LMFW	CCF-DPS-VS---A-24			
10	1.26E-05	00.23	nE-LMFW	CCF-DPS-VS---A-23			
11	1.26E-05	00.23	nE-LMFW	CCF-DPS-VS---A-36			
12	1.26E-05	00.23	nE-LMFW	CCF-DPS-VS---A-12			
13	1.26E-05	00.23	nE-LMFW	CCF-DPS-VS---A-25			
14	1.26E-05	00.23	nE-LMFW	CCF-DPS-VS---A-13			
15	1.26E-05	00.23	nE-LMFW	CCF-DPS-VS---A-35			
16	1.26E-05	00.23	nE-LMFW	CCF-DPS-VS---A-34			
17	1.26E-05	00.23	nE-LMFW	CCF-DPS-VS---A-46			
18	1.26E-05	00.23	nE-LMFW	CCF-DPS-VS---A-16			
19	1.26E-05	00.23	nE-LMFW	CCF-DPS-VS---A-14			
20	1.26E-05	00.23	nE-LMFW	CCF-DPS-VS---A-56			
21	1.26E-05	00.23	nE-LMFW	CCF-DPS-VS---A-45			
22	1.26E-05	00.23	nE-LMFW	CCF-DPS-VS---A-15			
23	1.26E-05	00.23	nE-LMFW	CCF-DPS-VS---A-26			
24	6.00E-06	00.11	nE-LMFW	CCF-CCW-PM---D-ALL			
25	5.73E-06	00.10	nE-LOOP	ACP-GT01-M	RI		
26	5.01E-06	00.09	nE-LMFW	CCF-RHR-PM---D-ALL	FE		
27	4.23E-06	00.08	nE-LOOP	ACP-GT01-A	Ci		
28	3.63E-06	00.07	nE-LOOP	ACP-GT01-A	Ci		
29	2.60E-06	00.05	nE-LOOP	ACP-GT01-M	RI		
30	2.41E-06	00.04	nE-LOOP	ACP-DG01-M	AC		
31	2.07E-06	00.04	nE-LOOP	ACP-GT01-M	S\		

Figure 9.1. The conceptual idea of having the decision tree as input for the quantification of an MCS list. The figure is intended to illustrate that one event may have different failure probability in different cases.

This would mean that each individual combination of failure events, leading to a particular release, could be quantified for the possible alternatives of combinations in the decision tree.

The idea behind the merge of the decision tree and the MCS list would be to capture the good features of the MCS approach, but also to, in a condensed way, utilize all the relevant information from the deterministic calculations – including timing. An obvious strength of the concept would be to not simplify the very complicated scenarios by equations, but instead use the thresholds that are of interest.

Quantification and representation

Given that the information in the MCS list is available, and given that we have a decision tree capturing all relevant information, the quantification will not be a trivial task since additional information will be required. Timing is a very important part, and it is also expected that some events in the MCS list could be obsolete in some scenarios. Obsolete events should preferably, from PSA stand point, be represented separately in the PSA logic – and thereby be represented by separate MCSs.

To some extent the timing information could be considered being already part of the basic events, through the reliability model "mission time". This reliability model is represented by following formula:

$$Q(t) = q + (1 - q)\left(1 - e^{-\lambda Tm}\right) = 1 - (1 - q)e^{-\lambda Tm}$$

where:
Q(t) is the failure probability of the component; q is mission time independent failure probability for the component; λ is failure rate, mission time dependent failure probability; Tm is the mission time.

This reliability model is used for most components in the PSA model, which have a

mission time. However, this mission time is not referring to a specific time point, but rather specifying the time the component is required to operate. There is no way, in the PSA tool today, to specify an origo, for example, at the time core melt begins. In many cases the same events are used in the sequences prior to core damage, and hence they cannot be set zero in the PSA Level 2. This issue needs to be resolved, for example by assuming that the mission time in PSA Level 2 is in addition to the specified mission time (which would then be for PSA Level 1).
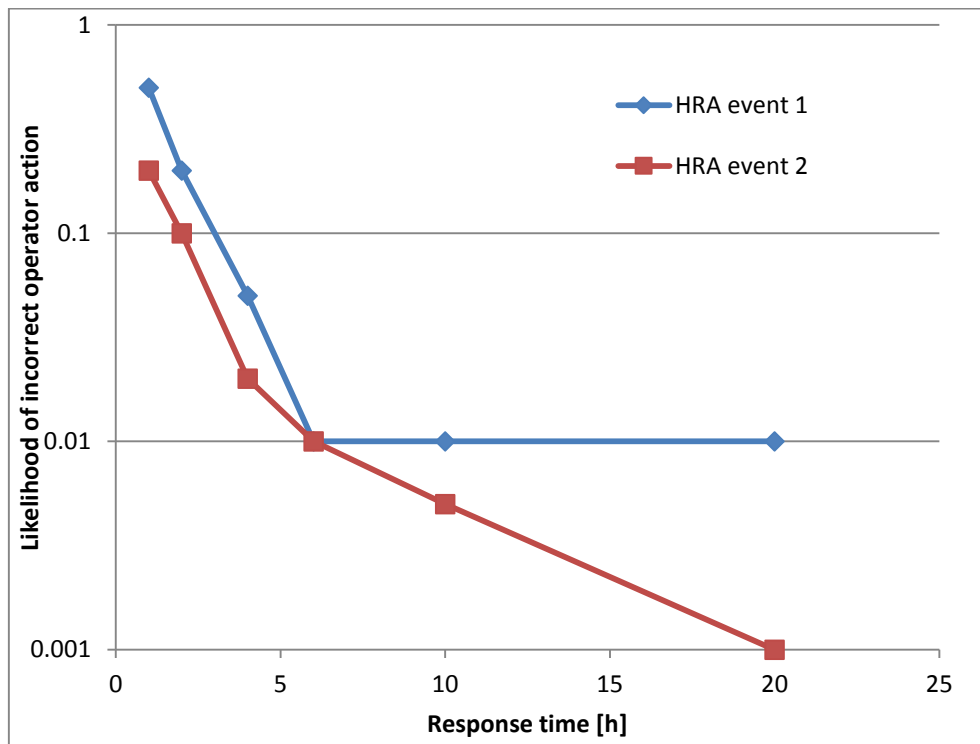
Figure 9.2. An example of two HRA events depending on required response

Other type of events that could be affected by different timing is for example phenomena and operator actions that could be dependent on available response time. The type of data for the operator response would need to have some time dependent model, like THERP, or to have some other method for inclusion of such data. It could also be a very simple reliability model, in which you specify the failure probability for some time points. Example is given in the graph below.

Regarding phenomena and their likelihood; the idea would be to identify the type of scenarios that could result in a specific type of phenomena, and scenarios where the phenomena could be ruled out. Therefore, a first hypothesis could be to have a few probabilities for phenomena – and select the most representative one for each scenario.

A challenging part will be to identify which events that should be referred to as affected. The decision tree will be on a high level – but the results for the MCS are on a very detailed level. It should be reasonably easy to, for example, allocate basic events to systems. But, there are support systems that affect more than one front line system, for example diesels, and it will be a challenge to define the appropriate timing for these events.

Assuming that these data are available and that we have been able to connect all basic events with their relevant node in the decision tree, we could calculate the MCS

conditional the decision tree. It is likely that there may be several combinations of timing of events that may cause the MCS. Some sort of convolution approach will then be needed to encompass all scenarios.

It should also be mentioned that how the quantification of the MCS list shall actually be performed is also a subject for research. Some possible methods could be:

- BBN, Bayesian belief networks, to be able to quantify events depending on other events
- Automata, to be able to include states and time into the analysis

The main focus of this phase of the project has been to study the possibility to improve the modelled sequences and phenomena, see section 9.1.1 and 9.1.2. The issued discussed in these chapters should preferably be resolved before using the results of the analysis in the way described in this chapter. No example of this type of analysis has therefore been performed during this phase of the project.

Chapter 10.   **Conclusions and Suggestions**

The results from the IDPSA show that an increased number of thermohydraulic calculations, performed according to an intelligent algorithm, can improve the understanding of the sequences and therefore input to the PSA or to the deterministic safety analyses.

The forward and reverse analysis with the ROAAM+ approach has successfully been used in the project. The evaluation of the results shows that using the results leads to clear benefits for both deterministic as well as probabilistic analysis regarding quality and verification of severe accident progression scenarios.

IDPSA can for both deterministic analysis and PSA be used to refine and improve the analysis in several ways.

The initiating events included in deterministic safety analysis are traditionally divided into a limited number of event classes which have specified analysis assumptions and acceptance criteria. The sequences have to be known when performing the deterministic analysis and the parametric studies are normally limited to one or two parameters. The large strength using IDPSA is its possibility to analyze a large number of combinations of system functions and manual operations which has been shown successfully with ROAAM+ approach. If there are exceedance of the acceptance criteria for certain sequences the results shows the excellence in using IDPSA to improve the understanding which conditions leads to the exceedance and also to provide basis for determining the probability of these sequences. By this the IDPSA results are excellent to use when there is a need for risk evaluation when for example the deterministic analysis shows that an analyzed sequence leads to exceedance of the acceptance criteria. It is in these cases possible to identify the conditions for the exceedance and thereby to either improve analysis or to make judgements if these conditions are acceptable. For sequences analyzed which involves manual operation or activation of non-safety systems the outcome of the IDPSA analysis is also important from an operational perspective as well as operator training to prevent those sequences which leads to exceedance of acceptance criteria.

IDPSA results can be used to refine and improve the PSA in several ways. One example is the analysis of recovery of core cooling, where IDPSA has provided usable information regarding the timing and possibility of core coolability (re-flooding). This information can be used as a basis material for the HRA, to re-define the binning of plant damage states as well as provide probabilities for failure of coolability.

The analysis performed for phenomena such as steam explosion shows interesting results that are relevant for the PSA-modelling. The analysis provides insights regarding under which conditions each phenomenon should be modelled and can therefore influence the sequences for which the phenomena is modelled. The results may also be used as one input to the quantification of phenomena. The analysis can be developed to further facilitate the use in PSA.

From the PSA stand point, the vision would be to continue the sequences from the core melting and vessel failure to study the impact on phenomena that could potentially challenge the containment. For each phenomena the key factors of importance should be identified, for example timing of vessel melt through, pressure in vessel at melt through, containment pressure at melt through etc. This would allow for an improved representation of phenomena, and also to represent the uncertainties in phenomena with

their contributing factors.

The IDPSA approach has not yet met this goal, but the analyses performed within this report have shown that this is not an unreachable goal. Significant progress has been made in just a couple of years. There is a good potential for development of a mathematical model to represent the IDPSA results in form of a decision tree as input for the quantification of the PSA Level 2 structure. This approach deserves a further evaluation in the future.

Acknowledgement

Disclaimer

The views expressed in this document remain the responsibility of the author(s) and do not necessarily reflect those of NKS. In particular, neither NKS nor any other organization or body supporting NKS activities can be held responsible for the material presented in this report.

References

[1]   VTT Research Report VTT-R-08589-12 Proceedings of the IDPSA-2012 Integrated Deterministic-Probabilistic Safety Analysis Workshop. November 2012.

[2]   M. Belhadj, M. Hassan, and T. Aldemir, *On the need for dynamic methodologies in risk and reliability studies.* Reliability Engineering and System Safety, 1992. **38**: p. pp.219-236.

[3]   T. Aldemir, et al., *NUREG/CR- 6942, Dynamic Reliability Modeling of Digital Instrumentation and Control Systems for Nuclear Reactor Probabilistic Risk Assessments.* 2007b, US Nuclear Regulatory Commission, Washington, DC.

[4]   C.D. Fletcher, and R.R. Schultz, *RELAP5/MOD3 User Guidelines. NUREG/CR-5535.* 1992, US Nuclear Regulatory Commission, Washington, DC.

[5]   R.O. Gauntt, et al., *MELCOR Computer Code Manuals. NUREG/CR-6119/SAND 2005-5713.* 2005, US Nuclear Regulatory Commission, Washington, DC.

[6]   A. Hakobyan, et al., *Dynamic generation of accident progression event trees.* Nuclear Engineering and Design, 2008. **238(12)**: p. 3457–3467.

[7]   U. Catalyurek, et al., *Development of a code-agnostic computational infrastructure for the dynamic generation of accident progression event trees.* Reliability Engineering and System Safety, 2010. **95**: p. 278–304.

[8]   T. Aldemir, *A survey of dynamic methodologies for probabilistic safety assessment of nuclear power plants.* Annals of Nuclear Energy, 2013. **52**: p. 113-124.

[9]   M. Kloos, and J. Peschke, *MCDET Approach for Considering Epistemic and Aleatory Uncertainties in Accident Simulations*, in *The 9th International Topical Meeting on Nuclear Thermal-Hydraulics, Operation and Safety (NUTHOS-9).* 2012: Kaohsiung, Taiwan.

[10]   Y. Vorobyov and T.N. Dinh. *A Genetic Algorithm-Based Approach to Dynamic PRA Simulation*. in *ANS PSA 2008 Topical Meeting - Challenges to PSA during the nuclear renaissance.* 2008. Knoxville, Tennessee: American Nuclear Society, LaGrange Park, IL.

[11]   Y.H. Chang, and A. Mosleh, *Dynamic PRA using ADS with RELAP5 code as its thermal hydraulic module.* PSAM 4. Springer-Verlag, New York, 1998: p. pp. 2468–2473.

[12]   S. Guarro, A. Milici, and R. Mulvehill, *Extending the Dynamic Flowgraph Methodology (DFM) to Model Human Performance and Team Effects NUREGCR/6710.* 2001, US Nuclear Regulatory Commission, Washington, DC.

[13]   T. Matsuoka, and M. Kobayashi, *GO-FLOW: a new reliability analysis methodology.* Nuclear Science and Engineering 1988. **98**: p. 64-78.

[14]   T. Matsuoka, and M. Kobayashi, *An analysis of a dynamic system by the GO-FLOW methodology. .* In: Cacciabue, P.C., Papazoglou, I.A. (Eds.), Probabilisitic Safety Assessment and Management. Elsevier, New York, pp. 1436-1547, 1991.

[15]   J.M. Izquierdo, et al., *Automatic generation of dynamic event trees: a tool for integrated safety assessment.* Reliability and Safety Assessment of Dynamic Process Systems, NATO ASI Series F, vol. 120. Springer-Verlag, Heidelberg, pp. 135–150., 1994.

[16] S.E. Yakush and P. Kudinov, *"A Model for Prediction of Maximum Post-Dryout Temperature in Decay-Heated Debris Bed,"* Proceedings of the 2014 22nd International Conference on Nuclear Engineering, ICONE22, July 7-11, Prague, Czech Republic, ICONE22-31214, (2014).

[17] P. Kudinov, A. Karbojian, C.-T. Tran, W. Villanueva, *"Experimental Data on Fraction of Agglomerated Debris Obtained in the DEFOR-A Melt-Coolant Interaction Tests with High Melting Temperature Simulant Materials,"* Nuclear Engineering and Design, 263, Pages 284-295, (2013).

[18] P. Kudinov and M.V. Davydov, *"Development and validation of conservative-mechanistic and best estimate approaches to quantifying mass fractions of agglomerated debris,"* Nuclear Engineering and Design, 262, pp. 452-461, (2013).

[19] P. Kudinov and M. Davydov, *"Development of Surrogate Model for Prediction of Corium Debris Agglomeration,"* In Proceedings of ICAPP-2014, Charlotte, USA, April 6-9, Paper 14366, (2014).

[20] S. Yakush and P. Kudinov, *"Simulation of Ex-Vessel Debris Bed Formation and Coolability in a LWR Severe Accident,"* Proceedings of ISAMM-2009, Böttstein, Switzerland, October 26 - 28, (2009).

[21] T. Silvonen, *Steam explosion case study using IDPSA methodology.* VTT Research Report VTT-R-05974-13, 2013

[22] CEA/NERA, Working Group on Operating Experience; "Status of OECD/NEA Country Regulatory Responses to the Forsmark-1 Event of 25 July 2006 and NEA/CSNI DiDELSYS Task Group Report Recommendations" (2010)

[23] R.O. Gauntt, R.K.C., C.M. Erickson, R.G. Gido, R-D. Gasser, and M.F.Y. S.B. Rodriguez, S. Ashbaugh, M. Leonard, A. Hill, *MELCOR Computer Code Manuals Demonstration Problems* 2001, Sandia National Laboratories: U.S. Nuclear Regulatory Commission Washington, DC 20555-0001.

[24] P. Kudinov, S. Galushin, W. Villanueva, S. Yakush, D. Grishenko, Development of Risk Oriented Approach for Assessment of Severe Accident Management Effectiveness in Nordic BWR, PSAM12, June 2014, Hawaii, USA.

[25] P. Kudinov, S. Galushin, S. Raub, V.-P. Phung, K. Kööp, I. Karanta, T. Silvonen, Y. Adolfsson, O. Bäckström, A. Enerholm, P. Krcal, K. Sunnevik, "Feasibility Study for Connection Between IDPSA and conventional PSA Approach to Analysis of Nordic type BWR's" NKS-R DPSA, Report NKS-315, 65p., 2014.

[26] T.G. Theofanous, "On Proper Formulation of Safety Goals and Assessment of Safety Margins for Rare and High-Consequence Hazards," Reliability Engineering and System Safety, 54, pp.243-257, 1996

[27] T.G. Theofanous and T.-N. Dinh, "Integration of multiphase Science and Technology with Risk management In Nuclear Power reactors: Application of the Risk-Oriented Accident Analysis Methodology to the Economic, Simplified Boiling Water Reactor Design," Multiphase Science and Technology, V20(2), pp.81-211, 2008.

[28] Apostolakis G., Cunningham M., Lui C., Pangburn G., Reckley W., "A Proposed Risk Management Regulatory Framework," U.S. Nuclear Regulatory Commission, NUREG-2150, Washington, DC, April 2012.

[29] Kudinov P., Galushin S., Yakush S., Villanueva W., Phung V.-A., Grishchenko D., Dinh N., "A Framework for Assessment of Severe Accident Management Effectiveness in Nordic BWR Plants," Probabilistic Safety Assessment and Management PSAM 12, June 22-27, 2014, Honolulu, Hawaii, Paper 154, 2014.

[30] S. Kaplan and B. J. Garrick, *"On The Quantitative Definition of Risk,"* Risk Analysis, 1: pp.11–27, (1981).

[31] Yakush S. and Kudinov P., "A Model for Prediction of Maximum Post-Dryout Temperature in Decay-Heated Debris Bed," Proceedings of the 2014 22nd International Conference on Nuclear Engineering, ICONE22, July 7-11, Prague, Czech Republic, ICONE22-31214. 2014.

[32] Kudinov, P., Karbojian, A., Tran, C.-T., and Villanueva, W., "The DEFOR-A Experiment on Fraction of Agglomerated Debris as a Function of Water Pool Depth," The 8th International Topical Meeting on Nuclear Thermal-Hydraulics, Operation and Safety (NUTHOS-8), Shanghai, China, October 10-14, N8P0296, 2010.

[33] Kudinov, P. and Davydov, M., "Development and Validation of the Approach to Prediction of Mass Fraction of Agglomerated Debris," The 8th International Topical Meeting on Nuclear Thermal-Hydraulics, Operation and Safety (NUTHOS-8), Shanghai, China, October 10-14, N8P0298, 2010

[34] Kudinov, P. and Davydov M., "Development of Surrogate Model for Prediction of Corium Debris Agglomeration," In Proceedings of ICAPP-2014, Charlotte, USA, April 6-9, Paper 14366, 2014.

[35] Yakush, S. and Kudinov, P., "Simulation of Ex-Vessel Debris Bed Formation and Coolability in a LWR Severe Accident," Proceedings of ISAMM-2009, Böttstein, Switzerland, October 26 - 28, 2009.

[36] Galushin, S. and Kudinov, P., "Scenario Grouping and Classification Methodology for Post Processing of Data Generated by Integrated Deterministic-Probabilistic Safety Analysis", Science and Technology of Nuclear Installations, Special Issue on Integrated Deterministic and Probabilistic Safety Analysis for Safety Assessment of Nuclear Power Plants" – In Press, June, 2015.

[37] Ilango and V. Mohan, A Survey of Grid Based Clustering Algorithms. International Journal of Engineering Science and Technology, (2010). Vol. 2(8).

[38] Jolliffe I. T., Principal Component Analysis. 2nd ed. (2002), New York, NY, USA: Springer.

[39] Maimon, O.Z. and L. Rokach, Data mining and knowledge discovery handbook. (2005), New York, Springer.

[40] Tuffery, S., Data Mining and Statistics for Decision Making. Wiley Series in Computational Statistics. (2011), Chichester, West Sussex ; Hoboken, NJ.: John Wiley & Sons, Ltd.

[41] L. Rokach and O. Maimon, Top-down induction of decision trees classifiers - a survey. IEEE Transactions of Systems, Man and Cybernetics, Part C, (2005). 35(4): p. 476-487.

[42] Mitchell, T.M., Machine Learning. McGraw-Hill series in computer science. (1997), New York: McGraw-Hill. xvii, 414 p

[43] K.P. Soman, S. Diwakar, and V. Ajay, Data Mining Theory and Practice. (2006), New Delhi: PHI Learning Pvt. Ltd.

[44] Bishop, Christopher M. (2006). *Pattern Recognition and Machine Learning*. Springer. p. vii.

[45] Han, H. Cheng, D. Xin, X. Yan, Frequent pattern mining: Current status and future directions. Data Mining and Knowledge Discovery, (2007), vol.15 (1) pp. 55–86

[46] Kudinov, P., Karbojian, A., Ma, W.M., Davydov, M., and Dinh, T.-N., "A Study of Ex-Vessel Debris Formation in a LWR Severe Accident", Proceedings of ICAPP 2007, Nice, France, May 13-18, 2007, Paper 7512.

[47] Lakehal D., "On the Modelling of Multiphase Turbulent Flows for Environmental and Hydrodynamic Applications," Int. J. Multiphase Flow, 28, pp. 823-863 (2002).

[48] Asmolov, V. V., Abalin, S. S., Merzliakov, A. V., Zagryazkin, V. N., Astakhova, Ye. V., Daragan, I. D., Daragan, V. D., D'yakov, Ye. K., Kotov, A. Yu., Maskaev, A. S., Rakitskaja, Ye. M., Repnikov, V. M., Vishnevsky, V. Yu., Volko, V. V., Popkov, A. G., Strizhov, V. F., "RASPLAV Final Report: Properties Studies: Methodology and Results," Kurchatov Institute, Moscow, 2000.

[49] Kudinov, P., Ma, W.M., Tran, C.-T., Hansson, R., Karbojian, A., and Dinh, T.-N. "Multiscale Phenomena of Severe Accident," NKS-R and NKS-B Joint Summary Seminar, Armémuseum, Stockholm, 26th - 27th March 2009.

[50] Kudinov, P. and Davydov, M., "Development and Validation of the Approach to Prediction of Mass Fraction of Agglomerated Debris," The 8th International Topical Meeting on Nuclear Thermal-Hydraulics, Operation and Safety (NUTHOS-8), Shanghai, China, October 10-14, N8P0298, 2010.

[51] Basso S., Konovalenko A. and Kudinov P., "Sensitivity and Uncertainty Analysis for Predication of Particulate Debris Bed Self-Leveling in Prototypic SA conditions", In Proceedings of ICAPP-2014, Charlotte NC, USA, April 6-9, paper 14329, 2014.

[52] Kudinov, P. and Davydov, M., "Development and Validation of the Approach to Prediction of Mass Fraction of Agglomerated Debris," The 8th International Topical Meeting on Nuclear Thermal-Hydraulics, Operation and Safety (NUTHOS-8), Shanghai, China, October 10-14, N8P0298, 2010.

[53] Wang, S.K., Blomquist, C.A., Spencer, B.W., McUmber, L.M., Schneider, Y.P., "Experimental Study of the Fragmentation and Quench Behavior of Corium Melts in Water, ANS Proceedings of the 25th National Heat Transfer Conference, HTC3, Houston, TX, 1988. pp. 120–153.

[54] Grishchenko D., Basso S., Kudinov P., "Development of TEXAS-V code surrogate model for assessment of steam explosion impact in Nordic BWR", NURETH-16, Chicago 2015, Paper 13937

[55] I. Lindholm, K. H. (1997). On Core Debris Behaviour in the Pressure Vessel Lower Head of Nordic Boiling Water Reactors. NKS.

[56] Nilsson, L. (2006). Development of an Input Model to MELCOR 1.8.5 for Oskarshamn 3 BWR. SKI Report 2007:05.

[57] R.O Gauntt, J. C. (2005). MELCOR Computer Code Manual Vol.2 Reference Manual Version 1.8.6. Albuquerque: Sandia National Laboratories.

[58] R.O Gauntt, J. C. (2005). MELCOR Computer Code Manuals Vol. 1 Primer and User's Guide Version 1.8.6 . Albuquerque : Sandia National Laboratories .

[59] Sunnevik, K. (2014). Comparison of MAAP and MELCOR and Evaluation of MELCOR as a deterministic tool within RASTEP.

[60] R. Wachowiak, "Modular Accident Analysis Program (MAAP) – MELCOR Crosswalk", EPRI Report, 2014.

Appendix A. Comparison of MAAP – MELCOR calculations of core degradation and relocation phenomena in Nordic BWR

In the section below the discovered discrepancies in input of MELCOR BWR 75 and MAAP are discussed. Thereafter the results obtained from the simulations of the selected SBO scenario are compared. In addition the impact of the maximum time step is evaluated and parameter studies of the discovered discrepancies are performed.

Discrepancies in nodalization and input parameters

When the input desk of the MELCOR BWR 75 model was compared to available data in MAAP, several differences were discovered both in nodalization and input parameters, which are discussed in the section below

1.1. Core nodalization

In Figure A.1, a schematic sketch of the axial nodalization in MELCOR respective MAAP is presented. No MAAP data was available to confirm the thickness of the core support plate, therefore two different interpretations of the nodalization could be made, either (a) or (b). In terms of axial heights, interpretation (a) agrees well with the nodalization applied in MELCOR. Interpretation (b) on the other hand, is based on the available core mass distribution in MAAP. Nodes in the lowest axial level 1 contains only steel, which therefore logically should represent the core plate and not the inactive fuel inlet (representing canister made of Zircaloy) assumed in (a). However, the thickness of the plate is significantly larger in interpretation (b) but contradictory, the amount of steel is considerably less compare to the mass assumed in the current MELCOR model where a thickness of 8.5 cm is applied. The core support plate and its interface to control rods and fuel assembly is a complex structure and simplification may therefore been made differently in MELCOR and MAAP. Thus, no conclusion could at this point be drawn whether interpretation (a) or (b) is more correct than another. If the thickness is larger than the value in MELCOR (8.5 cm) the timing of relocation to lower plenum will be affected assuming similar failure criteria.
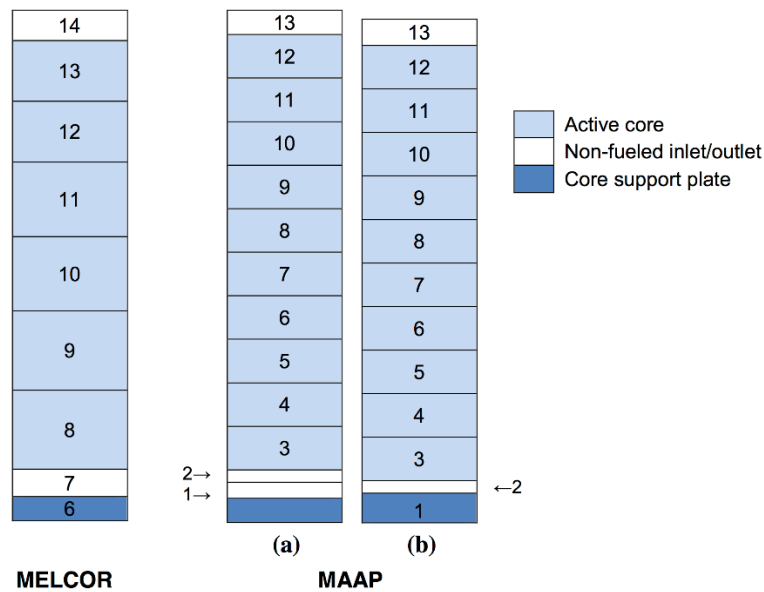
Figure A.1. Axial nodalization in core region. From available MAAP data two different interpretations (a) and (b) are possible.

Despite difference in core support plate thickness, the active core comprises 10 axial level in MAAP compared to 6 levels in MELCOR i.e. MAAP has a finer axial nodalization. Since modeling in MELCOR applies certain conditions and failure criteria to each cell, a finer nodalization could have an impact on the relocation progression. Due to the design of the SVEA-96 Optima2 fuel, MELCOR applies an average value of 3.68 m for the heated length [56] while the longest dimension is taken into consideration in available MAAP data. Moreover the axial levels in the active part of the core assumed to be evenly distributed in MAAP since no other information about the division was available, but are unevenly distributed in MELCOR.

As displayed in Table A.1, core elevations are 1-2 % less in MELCOR. Due to these differences, the whole core region is shifted approximately 0.1 m upwards in MAAP. Consequently, the initiation criteria for those safety systems that depend on the water level above/below top of active fuel (TOAF) e.g. the ADS will be activated on different heights in MELCOR and MAAP. In addition, the reference point for elevations within the reactor building in MAAP is way below the actual plant (probably at sea level) and not at the bottom of the vessel as in MELCOR. The relation found to be used when comparing elevations between the codes differs from the one given in Nilsson's report [56]. This difference can be the reason for deviations in core elevation but no such indication was seen.

Table A.1. Normalized elevations in core region

Parameter	MELCOR
TOAF [m]	0.99
Height of active core [m]	0.98
Elevation bottom of core support plate [m]	0.98

1.2. Initial core masses

By comparing core cross-sections in MELCOR and MAAP it is seen that the radii division among the five radial rings differs significantly, according to Figure A.2. In MAAP the radial distance from the center increases constantly for each ring, a correlation which is not applied in MELCOR BWR 75 model. Subsequently the fuel distribution among the rings is expected to differ considerably.
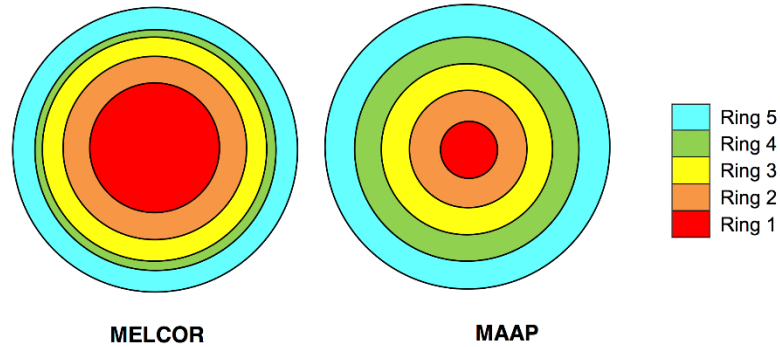
Figure A.2. Radial rings division in core

From Figure A.3 it can be deduced that all axial levels within one ring contains the same amount of fuel in MAAP (constant mass in each ring). Due to the coherent radii division the fuel mass increases stepwise towards the outer ring. On the opposite, the masses varies axially in MELCOR (small steps within each ring representing masses in axial level 8-13) and the three innermost rings contains twice the mass compared to the two outer, also defined in Table A.2.
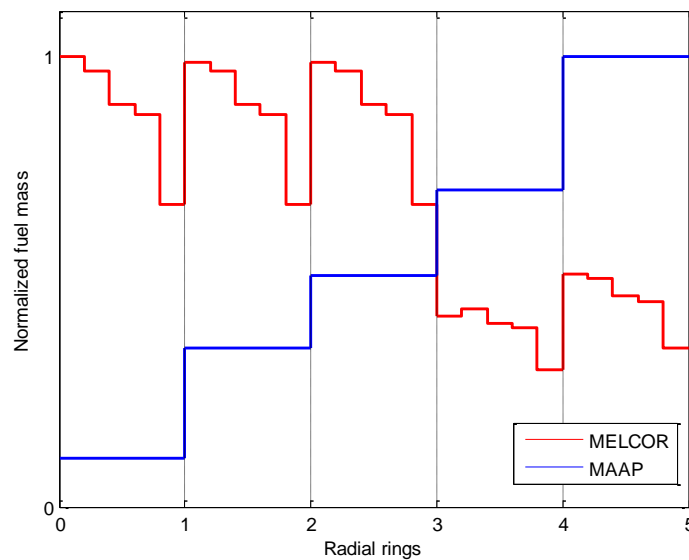
Figure A.3. Normalized fuel distribution for the axial levels of each ring

Moreover it was discovered that the total fuel mass deviates by approximately 5% i.e. MELCOR BWR 75 contains more UO_2 than MAAP, as seen in Table A.2.

Table A.2. Normalized initial fuel distribution among the rings

Ring #	1	2	3	4	5	Total
MELCOR	0.26	0.26	0.26	0.12	0.14	1.05
MAAP	0.04	0.13	0.19	0.26	0.37	1

Since the fuel mass differs by 5 % it is expected to see an adjustment in cladding material (Zircaloy) proportionally. By comparing initial core masses in MELCOR BWR 75 model not only to MAAP but also to the original MELCOR input created by Nilsson, insight was given to what extent modifications have been made. According to Table A.3 the total amount of Zircaloy has been kept constant independently of the UO_2 increase. The amount of Inconel and B_4C is also identical to the original input, but this is on the other hand more reasonable than the unchanged cladding mass. The mass of steel in the control blades and in the inlet part has been increased 3.9 tons and 2.4 tons respectively compared to Nilsson's input. The reason for this is unknown and since the only data available in MAAP is total mass of Zircaloy, the steel mass could not be compared. However, the total Zircaloy mass in the core (canister and cladding) is approximately 15 % larger than the amount given in MELCOR BWR 75 and Nilsson's input. A possible reason for the missing Zircaloy mass is the water channel since no input parameter defines the Zircaloy comprising the water channel structure. Assuming dimensions according to the assembly cross-section, the mass of the water channel structure agree very well with the missing 15 %. Since oxidation of Zircaloy is a major contributor to the hydrogen generation and heat production in the core during meltdown, the difference is substantial. An increase should therefore contribute to oxidation causing more hydrogen to be produced and possible accelerate the melt progression further, assuming there are no limited amount of steam and oxygen in core.

Table A.3. Comparison of initial core masses in MELCOR BWR 75 model,
the original MELCOR input [56] and MAAP

Initial core masses	MELCOR BWR 75	MELCOR Nilsson	MAAP
UO_2 (Normalized)	1.05	0.99	1
Total Zircaloy mass (Normalized)	0.85	0.85	1
Stainless steel core support plate (Normalized)	1.70 (#6)	1.70	1 (#1)
Zircaloy in cladding	28 730.5	28 731	-
Zircaloy in canisters	22 050	22 050	-
Inconel in spacers	604.6	604.6	-
B_4C in control rods	1706.9	1706.9	-
Stainless steel in fuel assembly inlet part	10 115.9	7700.0	-
Stainless steel in control rods	22 262.4	18 303.3	-

Core power distribution

A comparison of the axial and radial power profiles are presented in Figure A.4 respective Figure A.5. Axially, MAAP predict higher burnup in the top of the active core while the maximum power peaking factor is in the bottom half of the core in MELCOR. In MAAP data the area fraction of each radial ring were given but the radii unknown. Therefore the same outer radius of ring 5 as in MELCOR (3.2 m) was assumed to determine the radial power profile. Radially, MAAP has a flat profile in the center of the core at a lower power level compared to MELCOR.
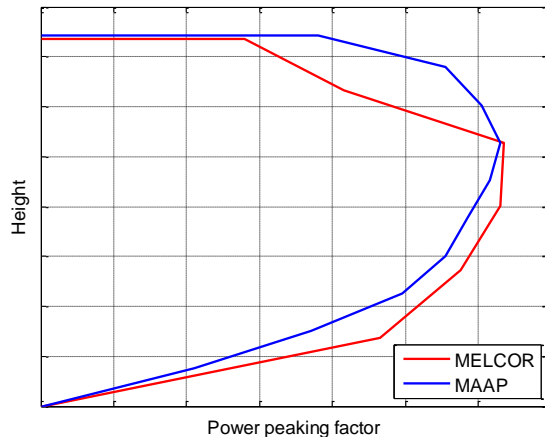
Figure A.4. Axial power profiles
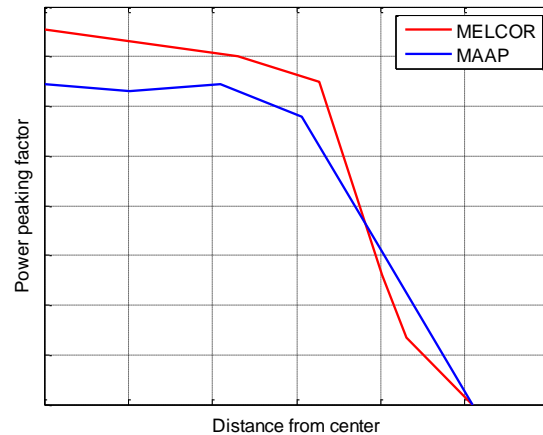
Figure A.5. Radial power profiles

Discrepancies in input parameters

Besides differences in nodalization and initial core masses e.g. 5 % more fuel in MELCOR, some major discrepancies in modeling parameters were discovered, summarized in Table A.4. The particle size of the particle comprising the particulate debris used in MELCOR BWR 75 is 4.77 times the size in MAAP. Since the diameter is used to determine the surface area applied in heat transfer calculations, the large difference of particle size is expected to have an effect on the hydrogen generation. Moreover, the velocity of the debris entering the lower plenum after core support plate failure is set to a value much lower in MELCOR BWR 75 input compared to MAAP. Somehow the default velocity in MELCOR differs between the manuals of 1 m/s [58] and 5 m/s [57], but the applied value is significant smaller than the default. First guess for the choice of such a small velocity was to enhance the debris/steam interaction by increasing the duration of the fall. However it was found out, the reason for this huge difference was due to a misinterpretation of MAAP data made by Nilsson [56] when the original input was created. The correct value is 98% larger than the one applied in the current model. Other differences were the irradiation time and the cladding failure temperature which was assumed 87 % respective 17% larger in MELCOR model compared to MAAP. In addition, a debris porosity of 25 % was applied in the MELCOR BWR 75 model, a value considerably less than the 40%. No value regarding porosity was available in the MAAP data so the MELCOR model was updated according to experimentally obtained results.

Table A.4. Normalized values of discrepancies in input parameters

Parameter	MELCOR
Initial UO$_2$ mass	1.05
Irradiation time	1.87
Particle size of particulate debris in lower plenum	4.77
Fuel cladding failure temperature	1.17
Debris falling velocity into lower plenum	0.02

Comparison SBO transient

By updating the MELCOR BWR 75 input in accordance to MAAP (power profiles and parameters specified in Table A.4) the inputs were made as similar as possible. However, no geometries were altered in MELCOR i.e. the nodalization and subsequently fuel distribution were kept unchanged. The known difference in prediction of decay heat was not taken into consideration. The missing Zircaloy mass (15 %) due to the presence of water channel structures was also not taken into consideration since no such input record is available in MELCOR. With inputs as similar as possible with respect to the discrepancies discovered, differences in results could be evaluated and uncertainties in modeling be addressed for the chosen SBO scenario.

In Table A.5, the timing of key events during the accident progression is compared. Low water level L4 (+0.5 m above TOAF) and activation of the ADS occur earlier in MAAP. A higher level of decay heat (9-10%) could be the reason for a more rapid boiling. On the other hand, the core is shifted upwards in MAAP relative MELCOR (section 1.1). Since similar initial water levels in the DC are observed, certain water levels are reached earlier in MAAP due to geometric differences of the defined control volumes. Hydrogen generation starts about 18 min earlier in MAAP, which indicates a more rapid core heat up and thus earlier steam/cladding interaction. However, start of relocation occurs after 50 minutes in MELCOR, approximately 20 minutes before MAAP. Thereafter the relocation progression is about 60 % faster in MAAP. Thus, the time required for reactor vessel failure to occur after a substantial mass of core debris relocated into the lower head is less in MAAP (4 h) compared to MELCOR (5.8 h). Most likely this arises from differences between the models for debris heat transfer within the reactor vessel lower head, and for structural failure model of the lower head segments. Opening of the CVS is predicted earlier in MAAP (4.6 h) compared to MELCOR (7.9 h). Hence, the containment pressure is higher in MAAP or different opening criteria are applied within each code. Modeling of the CVS is beyond the scope of this work and therefore not further analyzed.

Table A.5.Timing of key events

Event	MELCOR updated	MAAP
SBO	0 s	0 s
Reactor shutdown	3.5 s	4 s
Low water level L4 (+0.5 m)	900 s	736 s
ADS activation	1630 s	1153 s
Hydrogen production begins	2370 s	1273 s
Start of relocation to lower plenum	2970 s	4210 s
Core support plate failure	5127 s	4491 s
50% of debris relocated to lower plenum	5497 s	9366 s
90% of debris relocated to lower plenum	16 022 s	11 324 s
Vessel failure	21 039 s	14 498 s
Opening of CVS MVVS (via scrubber)	28 785 s	16 680 s

According to Figure A.6, a good agreement is seen between MELCOR and MAAP of the pressure in the primary system. The pressure drop after pressure relief is more rapid in MAAP, which is due to a higher flow rate according to Figure A.7. Further adjustment of the flow rate is needed in order to obtain the same pressure drop as in MAAP. A distinct pressure spike is seen in Figure A.6 after 6000 s in MAAP. This spike is caused by the first massive relocation to lower plenum followed by an increase in hydrogen generation. No rapid increase in hydrogen and consequently no pressure spike is predicted in MELCOR after core support plate failure. In Figure A.8, the maximum fuel temperature in MELCOR is compared to the maximum core temperature in MAAP. Initially the temperature is a bit higher in MELCOR but the temperature increase during core degradation until core support plate failure is in good agreement. Thereafter the temperature drops in MELCOR and at time of fuel rod failure which takes place approximately 300 s earlier in MAAP, the temperature is 1/3 compared to MAAP. Even though the fuel temperature is similar during core heat up, almost 50 % more molten debris is present in the core in MELCOR as seen in Figure A.9.

In Figure A.11, the debris mass in lower plenum is presented. In MELCOR, about six times more debris drips through the core support plate before failure. This indicates dissimilarities in modeling of plate/debris interaction. During the first massive relocation, almost 70 % of the total debris mass in MELCOR is instantly ejected into lower plenum, thereafter the relocation progression is significantly slower compared to MAAP. The reason is the initial fuel distribution in MELCOR where the majority of the fuel (about 75% compared to 36 % in MAAP) is distributed in the three innermost rings. Thus, a large amount of debris is formed and transferred to debris upon failure of the CRGT's. After failure of the center rings, heat up of the periphery of the core takes time. Because of this, the outer rings remain intact and the relocation progression is predicted to take almost 1.5 longer in MELCOR. Since more fuel is distributed in the outer rings in MAAP, large debris transition is also predicted in the end of the relocation progression. Moreover the debris in MAAP is accumulated in the lower head for approximately 50 minutes until vessel failure occurs. No similar behavior is seen in MELCOR.
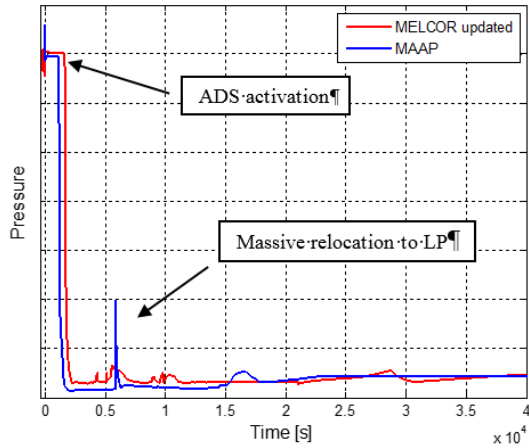
Figure A.6. Pressure in primary system
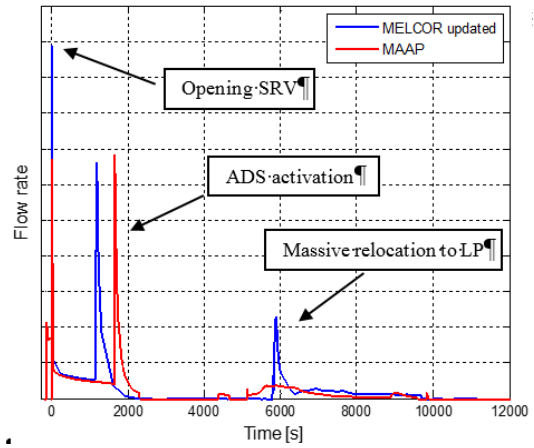
Figure A.7. Flow rate through SRV's and ADS
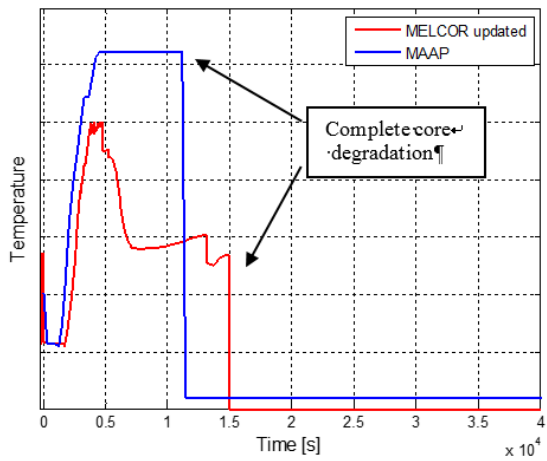
Figure A.8. Maximum core temperature
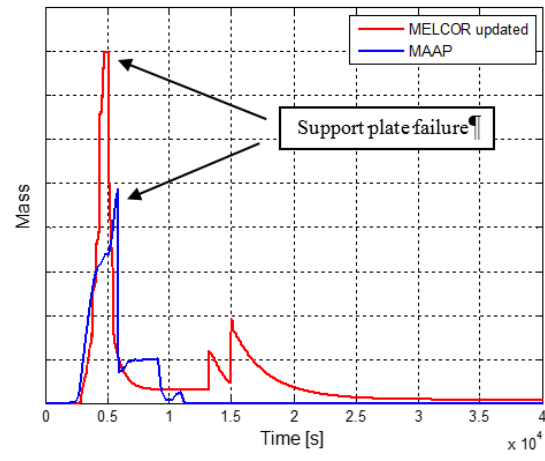
Figure A.9. Debris mass in core region
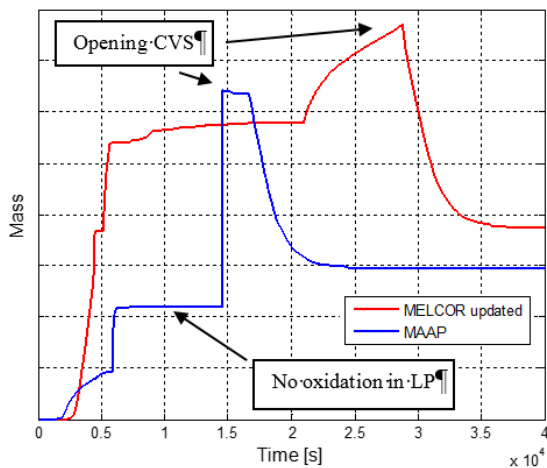
Figure A.10. Hydrogen mass in containment
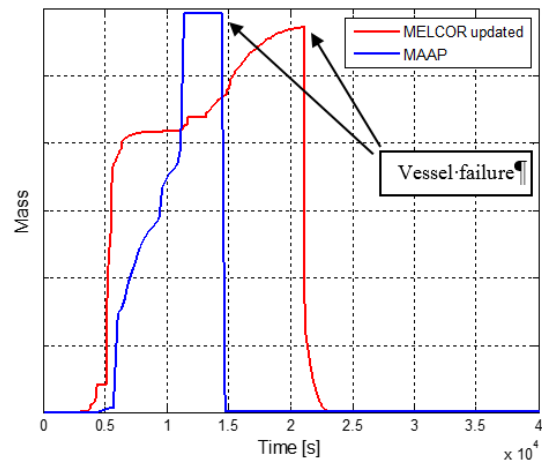
Figure A.11. Debris mass in lower plenum
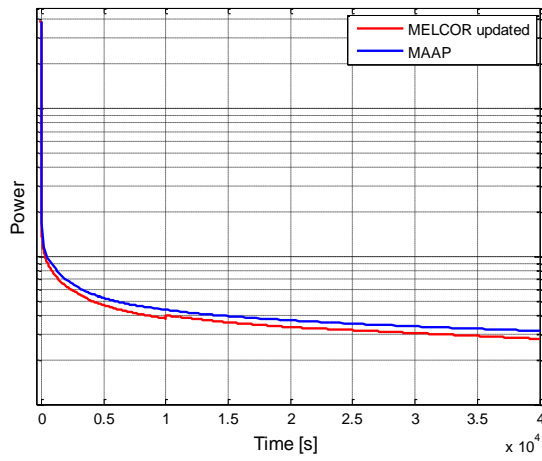
Figure A.12. Decay heat
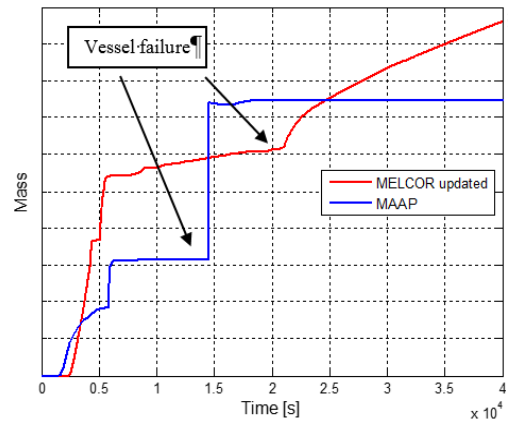
Figure A.13. Total hydrogen production
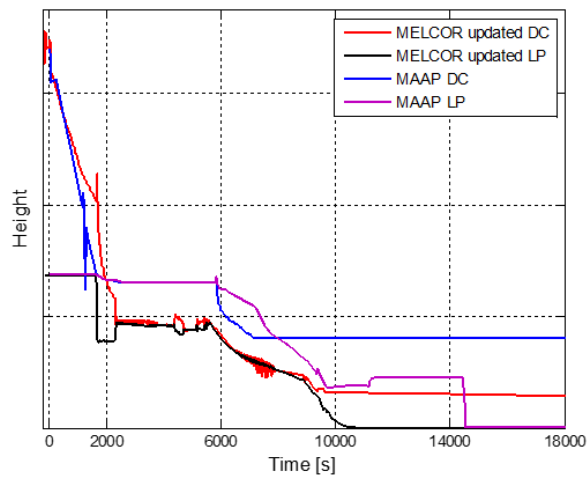
Figure A.14. Collapsed water level in
downcomer and lower plenum

Significant difference in modelling of oxidation can be seen in Figure A.10, which presents the hydrogen mass in the containment. In MAAP4, oxidation of debris particles is only considered during the entrainment and when falling from the lower plenum into the bottom of the cavity [55]. Thus, no oxidation is assumed to take place from the debris bed in lower plenum since the presences of crusts are supposed disable steam-debris interaction. This explains the stepwise hydrogen generation in Figure A.10. In contrast, MELCOR predicts a continuously hydrogen production over the whole degradation and relocation progression. After vessel failure at 14 498 s and 21 039 s in MAAP respective MELCOR, hydrogen is generated as ejected melt interacts with the water present in the cavity. The increase is not as significant in MELCOR as in MAAP where almost 50 % of the total hydrogen mass is produced instantly after vessel breach. In MELCOR, this phenomenon was not observed in previous comparison where no additional hydrogen was generated at the time of vessel failure [59]. By applying default values for a set of parameters responsible for the heat transfer in the cavity rather than the previous user-specified, a hydrogen increase is obtained. However, the continuous growth of hydrogen seems like a calculation error since the hydrogen level never stabilizes but no warning is obtained by MELCOR. Since this ex-vessel phenomenon is beyond the scope of this work, no further evaluation of the cavity input parameters is done but should be investigated in the future. In MELCOR it is possible to deduce the hydrogen production from oxidation of Zircaloy, steel and B_4C separately, which is not possible in MAAP. The total amount of hydrogen as a result of all oxidation processes can in MAAP be obtain in core region while it is given for the whole vessel in MELCOR. Thus, no comparison of the contribution of hydrogen from the different oxidation processes could be made.

The collapsed water level in the DC during the first 2000 s agrees well between the codes. Due to differences in elevation of the DC, the DC bottom is reached earlier in MAAP (at 7000 s) compared to MELCOR (around 11 000 s). After about 11 000 s no water is present to cool the debris in MELCOR, but the water levels stays constant on 1/3 of the initial level in MAAP until vessel breach. The reason for this behavior is unknown.

According to Figure A.12, MAAP predicts 9-10% higher decay heat compared to MELCOR. In previous comparison the difference was determined to 13 % [59], which means the deviation has decreased as a result of the updates made in MELCOR. However, 9-10 % difference is hard to explain since both codes use the ANS decay heat correlation (tabulated values of decay power with respect to time since scram). On the other hand, the formula applied in MELCOR consist of other correlations besides the tabulated values from ANS.

The decay power distributions of ^{235}U, ^{238}U, ^{239}Pu are also applied in MAAP but end-of-cycle values are used instead of averages over the whole cycle, which are applied in MELCOR.

Due to differences in radionuclide grouping, a complete comparison of the nuclides present in the core could be made. However, in some groups in MELCOR are identified with corresponding main contributor in MAAP (nuclides written in parentheses). As seen in Table A.6, MECLOR have smaller initial mass inventories for all nuclide groups identified. This is one possible reason why MAAP predicts a higher level of decay heat compared to MELCOR. Furthermore, it should be mentioned that a warning related to the decay heat was obtained in all simulations performed in MELCOR. Apparently, the decay heat deposited does not equal the calculated available total decay heat. The cause of this message has not been found and further investigation is needed.

Table A.6. Normalized initial radionuclide inventory

Radionuclide	MELCOR
Nobel gases	0.75
Alkaline Earths (SrO)	0.76
Chalcogens (TeO_2)	0.74
Transition Metals (MoO_2)	0.37
Tetravalents (CeO_2)	0.34
Trivalents (La_2O_3)	0.40

Debris characteristics in lower plenum

According to Figure A.16, two types of debris are considered in MAAP i.e. particulate debris bed and continuum pools. The metals and oxides are separated into two different pools, which are also modeled in MELCOR. In addition, MAAP models an oxide embedded curst as a result of the debris-to-wall heat transfer. By comparing the characteristics of the debris predicted by MELCOR and MAAP Figure A.17 respective Figure A.16, significant differences are seen in modeling. Since crusts in lower plenum are not modeled in MELCOR, the conglomerate debris has similar characteristics and prevents the molten material from further relocation, by occupying available space for downward relocation of molten materials (similar to flow blockage by conglomerate debris in core region, see Figure A.15). Moreover, MELCOR assumes that molten pools cannot penetrate into particulate debris beds in LP, which also leads to similar behavior as MAAP debris crusts.
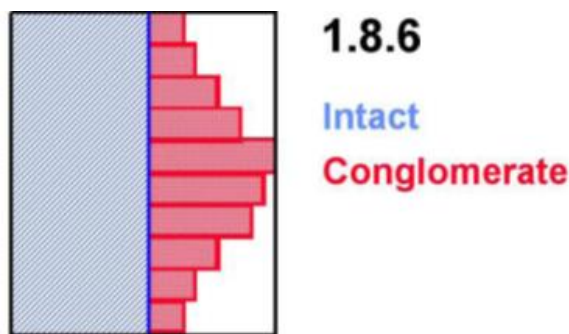
Figure A.15. Flow blockage for a cell, as predicted by the COR candling model of MELCOR.

In MAAP, molten pools are created from the start of relocation. Unlike MELCOR, the MAAP simulation estimates a significant fraction of the core liquefying prior to the initial slump to the lower plenum, this can be explained by the fact that in MELCOR simulations, debris formation in upper regions of the core usually results in relocation of particulate debris to the bottom of the core (on top of the core support plate) based on the leveling principle, in contrast, MAAP does not use such leveling principle for particulate debris idformed in the upper core region. The relocation of debris into originally open core regions result in debris blockages forming above core plate. This acts as crust preventing further downward relocation. Debris can relocate through these crusts once they fail, which typically requires high temperature conditions [60].

In MAAP crust is formed in the vicinity of the vessel wall in LP by debris-to-wall heat transfer. Right before vessel breach the mass of the oxide pool is almost half the total amount of debris present in the lower plenum, due to the different modeling of core degradation (within core region). In contrast, the presence of the molten pools MELCOR varies over time, often no pool is present at all. The amount of oxide pool is significantly less in MELCOR and exists only in the very end before vessel failure. For the major part of the relocation progression, MAAP predicts a constant amount of particulate debris i.e. no mass leaves the region by melting. Transition between the crusts and the continuous oxide pool is only seen at 11 000 s where all debris is accumulated in the lower head before vessel failure occurs. In MELCOR, properties of the materials are evaluated for each individual cell at each time step. Transition between solid and molten states is therefore calculated continuously and the amount of particulate, conglomerate and continuum pools varies over time. Differences in modeling of the characteristics of the debris in lower plenum is clear; MAAP seems to apply a set configuration where transitions between solid and molten states are not calculated to the same extend as in MELCOR.
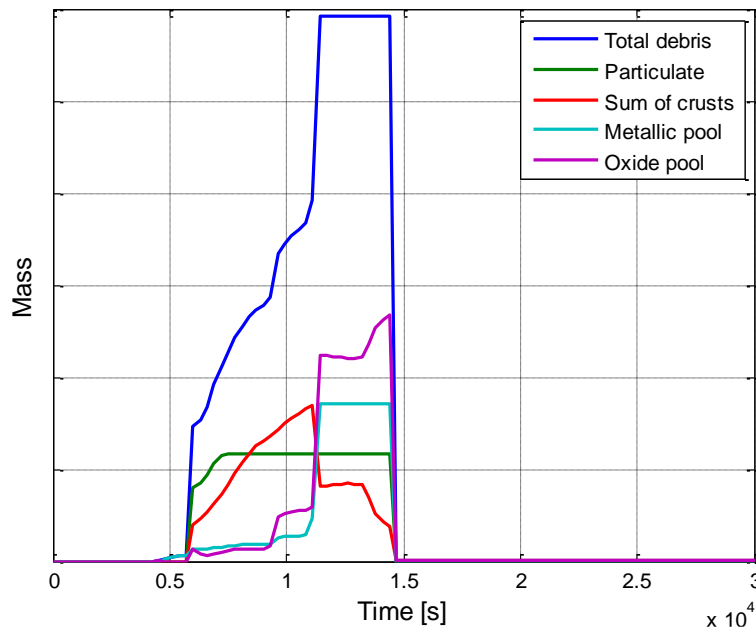
Figure A.16. Lower plenum debris characteristics in MAAP
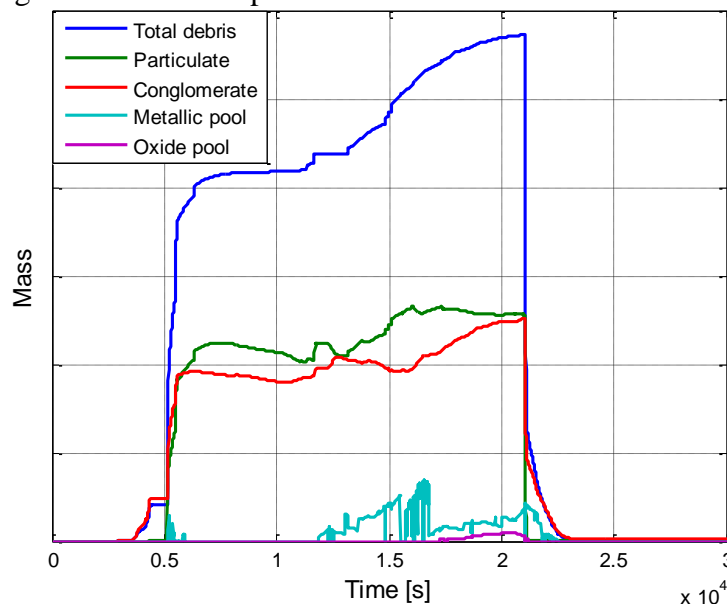
Figure A.17. Lower plenum debris characteristics in MELCOR

According to Figure A.18 , MELCOR predicts a higher temperature of the metallic pool, especially during the first relocation. For the oxide pool the temperature is higher in MAAP but the temperature profiles are more similar between the codes than for the metallic pool. Since the presences of the molten pools vary over time, the temperatures oscillate accordingly. In contrast to MAAP, MELCOR does not apply a lumped parameter approach to the whole region of the lower plenum. Instead the temperature is calculated independently in each of the 30 cell comprising the lower plenum. Therefore both the average and maximum temperature of the particulate debris is included in Figure A.20.
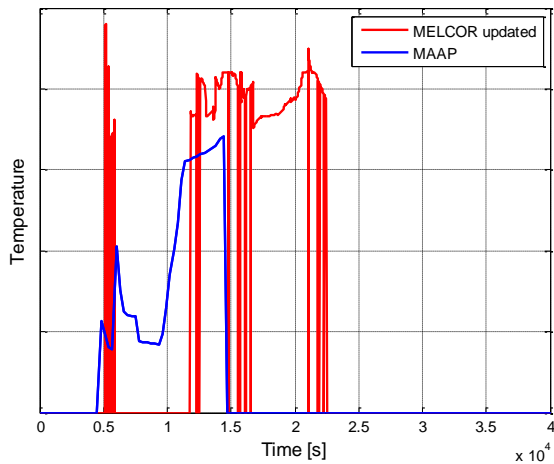
Figure A.18. Temperature of metallic pool in lower plenum
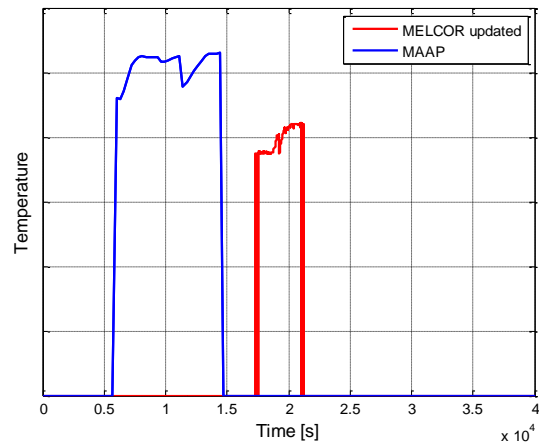
Figure A.19. Temperature of oxide pool in lower plenum
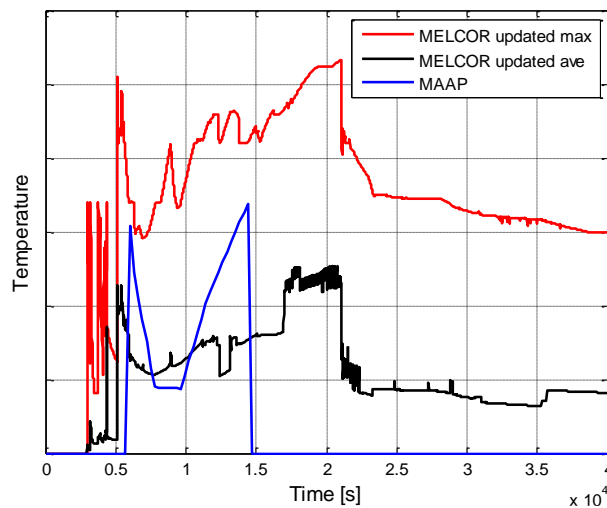
Figure A.20. Temperature of particulate debris in lower plenum, both maximum and average temperature in MELCOR are included

In Figure A.21 the composition of the total debris mass in the lower head is compared. Differences in composition and thermal conductivity is important for the time of vessel failure. In MELCOR, the composition of the oxide and metallic pool could not be specified and therefore not included. Since the pools contain only a small fraction of the total debris in MELCOR (Figure A.17), the pool mass has a minor impact in the result. Pool materials in MAAP are included in the diagram. In MAAP, data was only available

at 2, 4 and 6 hours after reactor shut down. A more frequent comparison was therefore not possible. Fortunately, vessel breach occurs after approximately 4 hours in MAAP. The resulting mass and composition of the debris in the lower head could therefore be compared to MELCOR, where the time of vessel failure occurs after 5.8 hours. After 2 hours, two times more debris has relocated in MELCOR compared to MAAP. The major difference in composition at this time is the quantity of steel, which corresponds to the collapsed CRGT's in MELCOR. A good agreement is seen for the resulting debris composition after 4 respective 5.8 hours. In MAAP the initial mass of Zircaloy was 15 % larger, which explains why more Zircaloy is present. Differences in ZrO_2 and steel oxides could be due to different modeling of oxidation and flow blockage i.e. prevents steam and debris to interact. After 6 hours, debris is still being ejected to the cavity in MELCOR. At all times, the amount of B_4C debris is almost identical between the codes.
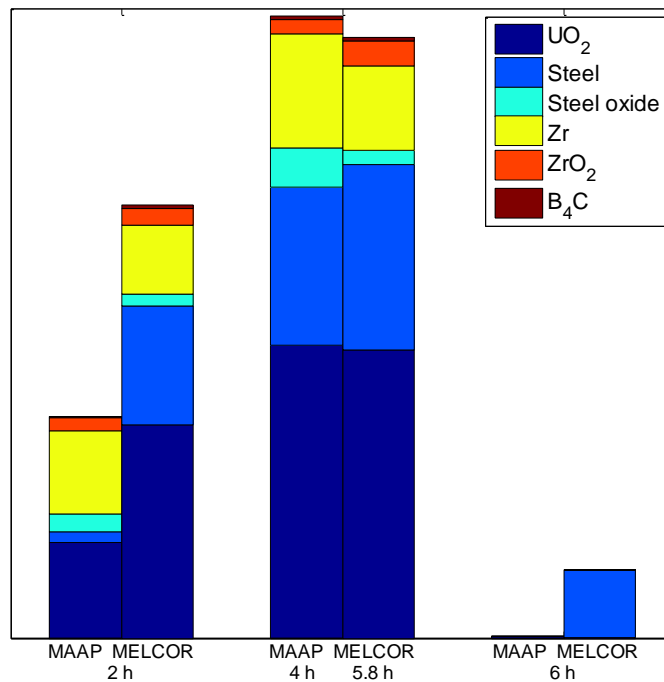
Figure A.21. Debris mass and composition in the lower head. Vessel breach occurs after 4 h and 5.8 h in MAAP respective MELCOR

Appendix B. GA-NPO – MELCOR Analysis

We employ the GA-NPO algorithm to search the parameter space for either a minimum or a maximum of the fitness function. The value of the fitness function can be any parameter or combination of parameters, which is producible using a Post Processing-Script, usually a bash-file, and which is available in the MELCOR Plot File. The result has to be a single value which is written into an external goal function, where it is read by GA-NPO and used to select the parameters of the next simulation.

MELCOR adjusts the time step of the simulation dynamically to reach convergence of the simulation. There is a limiting ratio between two consecutive time steps, resulting in a maximal allowable change between two time steps. The user input on this feature is essentially limited on the largest and smallest allowable time step. When several discontinuities happen in a relatively short time frame and the code "crashes" at this critical point in time, the times step can often not be automatically adjusted downward fast enough resulting in a premature crash of the simulation.

GA-NPO will automatically assign the parameter combination leading to a crash a very large negative value, causing future parameter selections to drift away from the "crash side". This is on the one hand logical as we want complete simulations for our analysis but can lead to a distortion of results.

To fix this problem the secondary purpose of the Post Processing-Script was introduced. In case of a crash, e.g. the actual end time is significantly smaller than the expected end time, the Post Processing-Script falls back to the closest MELCOR safe point, which are regularly distributed over the length of the simulation run, and restarts the MELCOR simulation from this point with a dynamically adjusted maximal time step. If the simulation fails again, the procedure is repeated with ever-smaller maximal time step. GA-NPO is paused during this process.

If successful the external goal function is computed as usual and the simulation is continued.

Fitness Function Selection

For the time being the work-horse of the GA-NPO software suite is the 1.8.6 MELCOR code. While further development in later versions of the MELCOR –code are underway, work will continue with the current 1.8.6 MELCOR version with which the proof of concept and the first practical experiments were conducted, part of the reasoning are legacy issues. Transformation of older input decks into newer versions are notoriously time intensive and error prone.

The fitness function can be chosen as any plot-able MELCOR variable or any combination of plot-able MELCOR variables that can be implemented using a bash script or any programming language (e.g. perl, AWK, or similar) installed on the Linux machine and callable from a bash script. The bash script is called the post-processing script and, if activated, will be called after the MELCOR run has been completed. It has to write its intended results in an external text-file, called the external goal function (or ext.goal) in the current implementation. The name of the post-processing script and the external goal

function have to be specified in the GA-NPO input file config.npo.mel.

Note that the criterion specified need not be identical to the input used to generate the external goal function. The former will override the later.

In the current implementation we use aptplot-script aptbatch to read out data vectors from the MELCOR Outputfiles, called MELC.PTF. The data vectors are than further processed by a combination of bash programming and AWK, an interpreted programming language designed for text processing, typically used for data extraction, and reporting.

The current fitness function is simply returning the absolute difference between the relocated mass to the lower plenum, defined as all cells below the lower core plate, and a user defined constant. This is useful, if we want to avoid unwanted concentration of the algorithm on the safe zone and are more interested in sounding out the critical edges of the "target area".

The external goal function is rather flexible and allows the superposition of various values, as long as we can combine it in final return value, weighted to user specifications, for the fitness function, that will either be maximized or minimized.

Appendix C. Pattern Analysis Approach

Pattern analysis and pattern recognition is a branch of machine learning that focuses on the recognition of patterns and regularities in data [44].

We use pattern analysis to identify possible core relocation patterns, and to find out if there is any typical behavior in the scenario space.

The main steps in approach used for pattern identification:
- Each scenario evolution in time is split into separate time frames with 30 min step.
    - In each time frame we analyze relocated mass compared to total relocated mass for this scenario according to Table C.1
        - e.g. in Figure C.1 the total relocated mass is around 250 tons, in the first time frame relocated mass is around 100tons, which gives Relocated Debris Ratio [25-50%] which belongs to cluster 2.
- Performing similar analysis for each time frame every scenario become represented by a set of numbers that characterize scenario behavior over time.
- Then, scenarios with identical behavior are grouped into patterns. The grouping algorithm is similar to the algorithm used in sequence pattern analysis [45].
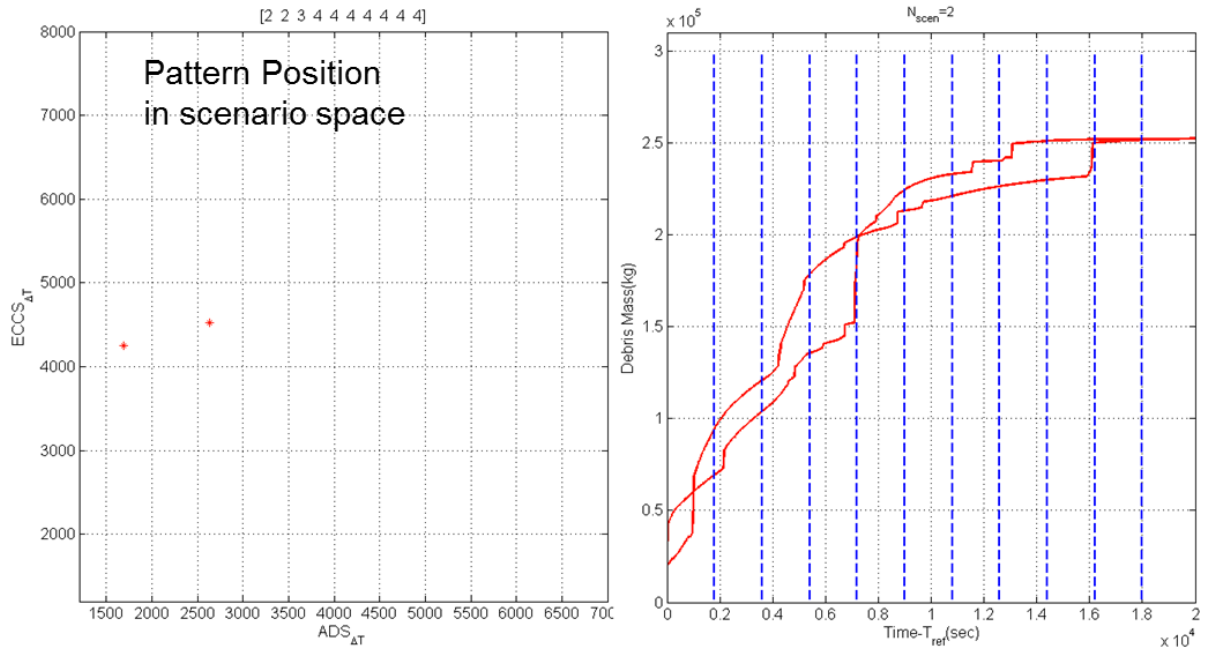
Figure C.1. Pattern Analysis Example

Table C.1. Clusters used in pattern analysis

Cluster N	Relocated Debris Ratio
[1]	[0%-25%]
[2]	[25%-50%]
[3]	[50%-75%]
[4]	[75%-100%]

Title	Deterministic-Probabilistic Safety Analysis Methodology for Analysis of Core Degradation, Ex-vessel Steam Explosion and Debris Coolability
Author(s)	Pavel Kudinov[1], Sergey Galushin[1], Dmitry Grishchenko[1], Sergey Yakush[1], Yvonne Adolfsson[2], Lisa Ranlöf[2], Ola Bäckström[2], Anders Enerholm[2], Pavel Krcal[2], Anna Tuvelid[2]
Affiliation(s)	[1]Division of Nuclear Power Safety (NPS), Royal Institute of Technology (KTH) [2]Lloyd's Register Consulting – Energy AB
ISBN	978-87-7893-427-7
Date	July 2015
Project	NKS-R / DPSA
No. of pages	88
No. of tables	12
No. of illustrations	63
No. of references	60

Abstract
max. 2000 characters

This reports summarizes the experience achieved within the NKS-DPSA project during 2014. The aim of the project is to develop the methodology for application of Integrated Deterministic-Probabilistic Safety Analysis (IDPSA) with PSA/DSA to the Nordic nuclear energy industry and regulatory needs. We further develop a Risk Oriented Accident Analysis Methodology (ROAAM) framework that demonstrates how dynamic behavior in NPPs can be better included in safety analyses. The methodology is developed and demonstrated through analysis of the relocation of the core melt to the lower plenum, as initial conditions for the melt-vessel structure interactions, melt release and ex-vessel steam explosion and debris bed coolability in Nordic BWRs. The influence of timing in PSA level 1 sequences and possible recovery actions on the amount and properties of the melt in the lower head are addressed. It is shown that IDPSA results can be used to refine and improve the PSA in several ways. One example is the analysis of recovery of core cooling, where IDPSA has provided usable information regarding the timing and possibility of core coolability (re-flooding). This information can be used as a basis material for the HRA, to re-define the binning of plant damage states as well as provide probabilities for failure of coolability. The analysis performed for phenomena such as steam explosion shows interesting results that are relevant for the PSA-modelling. The analysis provides insights regarding under which conditions each phenomenon should be modelled and can therefore influence the sequences for which the phenomena is modelled. The results may also be used as one input to the quantification of phenomena. The analysis can be developed to further facilitate the use in PSA. Experiences from performed studies are summarized in the report as well as suggestions of areas which need further investigations.

Key words	IDPSA, PSA, DSA, BWR, Severe accident, MELCOR, MAAP, core degradation, steam explosion.